Activation of Constitutive Androstane Receptor (CAR) in Primary Human Hepatocytes

Richard Alexander Maclennan BSc (Hons)

Thesis submitted to the University of Nottingham

for the degree of Doctor of Philosophy.

2015

Abstract

Human populations are at risk of exposure to constitutive androstane receptor (CAR) activators present in a range of substances, including pharmaceuticals, plasticizers and crop protection agents. What exposure to CAR activators means for human health is uncertain. Activation of CAR in rodents is associated with liver hyperplasia, increased proliferation and eventual hepatocarcinoma; however the effect in human hepatic cells is unclear. There are two methods by which a compound can achieve activation of CAR; directly or indirectly via cellular signalling pathways. Phenobarbital is a prototypical activator of CAR and does so in an indirect manner via suppression of epidermal growth factor receptor (EGFR) signalling. Direct activation of CAR in rodents also causes hepatocellular carcinoma but the human outcome is less clear. We have carried out microarray and miRNA analysis of CITCO (a potent and selective hCAR ligand) treated primary human hepatocytes. To mitigate the well documented effect of primary hepatocyte dedifferentiation primary hepatocytes were cultured in dynamic three dimensional culture *in vitro*. Gene expression changes indicate that direct activation of hCAR causes the promotion of a pro-proliferative and anti-apoptotic phenotype. The miRNA expression profile is crucially different to rodent data that is currently published. Despite the pro-proliferative phenotype shown there is no evidence that primary human hepatocytes proliferate in response to direct activation of CAR by CITCO. This leaves the possibility that a proliferative response may be observed *in vivo* or that the

changes in gene expression are solely a human physiological adaptation to direct hCAR activation by CITCO and no proliferation would occur. The effect on human health and liver toxicity is unclear but this body of work has provided data that may be used to further understand the mechanistic effects of direct hCAR activation in human hepatocytes. A more complete understanding of this will help to inform the toxic potential of direct hCAR activation *in vivo*.

Acknowledgements

Thanks for funding support must go to the Biotechnology and Biological Sciences Research Council (BBSRC) and Syngenta for a level of funding that allowed my research to progress using techniques that would otherwise have been out of reach. I'd like to recognise, and thank, FRAME for the general funding provided to the laboratory of Dr Andrew Bennett. It is important to recognise the people that also helped along the way. For the initial time spent assisting me with the first rat hepatocyte perfusions and tentative steps along the way I'd like to thank Dr Elke Gottschalg. Many evenings, nights and early mornings have been spent in the primary human tissue culture lab perfusing segments of liver or feeding isolated hepatocytes. This would have proved infinitely more challenging without the help of Monika Owen and Nikki De Vivo. As a member of Dr Andrew Bennett's lab I have been fortunate to be part of a lab group containing a diversity of projects and people. Andy has provided well directed supervision and always has ideas as to which direction my research is heading. On a personal level the PhD would have been much harder without the support of a number of people who also deserve my collective thanks.

1 Table of Contents

2 Abbreviations

CAR	Constitutive Androstane Receptor
hCAR	Human Constitutive Androstane Receptor
rCAR	Rat Constitutive Androstane Receptor
mCAR	Mouse Constitutive Androstane Receptor
PB	Phenobarbital
EGF	Epidermal Growth Factor
EGFR	Epidermal Growth Factor Receptor
LGF	Liver Growth Factor
HNF4α	Hepatocyte Nuclear Factor 4 alpha
PXR	Pregnane X Receptor
RXR	Retinoid X Receptor
DEN	Diethylnitrosmine
BrdU	Bromodeoxyuridine
LBD	Ligand Binding Domain
DBD	DNA Binding Domain
XRS	Xenobiotic Response Sequence
ZEB	Zinc-finger Enhance Binding protein

3 Figures

4 Tables

5 Introduction

The constitutive androstane receptor (CAR), a member of the nuclear receptor superfamily (subfamily 1, group I, member 3), is unique in its capacity as a nuclear receptor in that it can be active in the absence of ligand interaction but with the added ability of further regulation by activators and ligands. A large proportion of these activators (including the classic activator, phenobarbital) do not bind directly to the receptor but act through an indirect signalling system. A large range of molecules, chemicals and signals utilise CAR to alter transcriptional activity including numerous xenobiotics, a range of drugs, bile acids and hormones (Hernandez et al., 2009, Yamada et al., 2006). Central to the role of CAR is the alteration of the expression of genes responsible for the modification and detoxification of xenobiotics and steroids in response to these compounds and cellular metabolites. The mechanism of action of CAR is complex and involves translocation in the presence of activators from the cytoplasm to the nucleus followed by further activation and repression steps once inside the nucleus. Upon dimerization with retinoid-X receptor α (RXRα), CAR acts as a major regulator of phase I, phase II, phase III enzymes and transporters that are crucial for the efficient detoxification and elimination or removal of xenobiotics, bile acids and steroids. An example of this is the finding that CAR is a key regulator of the CYP2B gene family in response to phenobarbital shown by the generation of CAR null mice that do not show CYP2B responses to phenobarbital (Trottier et

al., 1995, Yamada et al., 2006). Phase II enzymes that CAR has been shown to induce include proteins such as Uridine diphospho-glucuronosyltransferases (UDPGT), sulfotransferases (SULTs) and Glutathione S-transferases along with phase III transporters such as multidrug resistant protein 1 (MDR1) and multidrug resistance-associated protein 2 (MRP2).

Data produced in the recent past have shown that activation of mammalian CAR can be caused by a diverse selection of chemicals from drugs, industrial chemicals and pesticides and crop protection agents (Stanley et al., 2006, di Masi et al., 2009, Zhang et al., 2006), however these effects are often species specific. Activation of rodent CAR leads towards proliferation and hepatocarcinoma, however the effect of direct activation in human hepatic cells remains unclear.

Chemical	**CAR**		**PXR**	
	Rodent	**Human**	**Rodent**	**Human**
Phenobarbital	+	+		
Androstanol	-	-		+
Androstenol	-			
Artemisinin		+		+
Bisphenol-A	+			+
CITCO		+		

Corticosterone	+		+	+
DDT	+		+	+
DEHP (phthalic acid)	+	+	+	+
Nonylphenol		+	+	+
Parathion	+			
TCPOBOP	+			

Table 5-1: Selection of rodent and human CAR and PXR activators showing cross reactivity between species and receptors. + indicates that the molecule is an activator for that receptor in the specific species. – indicates that the molecule is an inverse agonist for that receptor in the specific species.

5.1 Pesticide exposure and toxicity

Pesticide use worldwide is widespread and is a common method used to improve crop yields. Pesticides are not only used in large scale agriculture but also in small scale farming, garden and lawn maintenance. The term pesticide is a catch all term that includes chemical substances used to prevent, destroy or mitigate pests ranging from insects, rodents, and weeds to microorganisms. Human exposure to these compounds is widespread in the form of ingestion via food grown with the aid of pesticide use, via contamination of the water course and exposure as a direct result of pesticide application. Approximately 25 million agriculture workers are exposed whilst applying pesticides to crops

each year (Jeyaratnam, 1990). There are efforts to reduce pesticide use through the use of non-chemical pest control methods, however human exposure to pesticides is still common due to home and garden use, as an occupational hazard of agriculture work or indirectly via crop spraying and food consumption (Krieger, 2001). It is therefore of great importance to understand the potential effect on human health of exposure to compounds present in pesticides and crop protection agents.

The traditional method used in assessing the carcinogenic potential of pesticides in humans relies on animal based genotoxic studies and short term mutagenicity assays. This is the obvious route of carcinogenesis; however an increasingly important route to cancer progression is via non-genotoxic carcinogens. Many substances that have been investigated using epidemiology based studies (another important facet of human toxicity and health protection) found evidence of carcinogenesis in humans exposed to pesticides already passed as safe and non-genotoxic (Alavanja and Bonner, 2005). The discovery that pesticides found to be non-genotoxic or mutagenic were causing cancer in humans indicated that although current toxicity screening tests had prevented a number of genotoxic and carcinogenic compounds from human exposure there was a risk that non-genotoxic carcinogens were not highlighted in the current battery of tests (Alavanja and Bonner, 2005).

Many pesticides and crop protection agents contain compounds, either as the active ingredient or as part of the formulation mixture, that are able to bind and activate mammalian CAR (Stanley et al., 2006, di Masi et al., 2009, Zhang et al., 2006). Activation of CAR in rodents will invariably lead to liver hyperplasia and proliferation and eventual hepatocellular carcinoma (Huang et al., 2005a). Hepatocellular carcinoma in rodents as a consequence of CAR activation is a non-genotoxic process. The classic rat CAR (rCAR) activator, phenobarbital, is classed as a non-genotoxic rodent carcinogen for its ability to cause hepatocellular carcinoma in rodents without any mutagenic effect on DNA. This highlights the potential that non-genotoxic hCAR activators may play a role in hepatocellular carcinoma *in vivo*. There has been little published research into the effect that non-genotoxic hCAR activating compounds may have on the human liver. This is in part due to the difficulties and complexities associated with carrying out such research. A major issue is the paucity of reliable and representative *in vitro* models of human liver that retain the necessary phenotype required to evaluate the potential outcome of exposure to human CAR (hCAR) activators.

5.2 Current models of the liver

There are many different models of the human and rodent liver *in vitro*, each with their own set of advantages and disadvantages (Table 5-2). The primary reason for this abundance of different models and cell types is as a

consequence of the dedifferentiation that primary hepatocytes from all species undergo in traditional 2D static culture (Bissell et al., 1987b, Clayton and Darnell, 1983b, Godoy et al., 2009b, Koide et al., 1989b, Tong et al., 1994). Dedifferentiation of primary hepatocytes during the first 7 days in traditional static culture is well reported and the challenge of preventing it has given rise to a number of innovative solutions (Table 5-2) in an attempt to improve hepatic *in vitro* cultures.

Culture System or Cell Type	Advantages	Disadvantages
Isolated perfused liver	Functions close to that of *in vivo* organ. Lobular structure preserved. Functional bile canaliculi. Collection of bile possible. Short-term kinetic studies possible.	Short term viability (2-3hrs). Study of only a few compounds. Bile excretion decreased after 1-3hrs. Not possible in humans.
Liver slices	Lobular structure preserved. Functional bile canaliculi. Studies on human liver possible. Several compounds during one experiment.	Viability of 6hrs-2 days. No bile collection possible. Not all cells preserved similarly.
Immortalised hepatocyte cell lines	Some *in vivo* functions and phenotype preserved, unlimited in cell number and availability.	Drug metabolising and enzyme activities lost. Genotype instability over time.
Stem cell derived human	Some *in vivo* functions and	Always end in a “hepatocyte

hepatocytes	phenotype present, unlimited in cell number and availability.	like" cell that is similar but not the same as an *in vivo* hepatocyte.
Cryopreserved primary human hepatocytes	Ability to ship nationally. Uses primary human hepatocytes.	Low viability post thawing combined with rapid loss of *in vivo* functions.
Primary human hepatocytes	Upon isolation are as close to *in vivo* as possible (the gold standard).	De-differentiation occurs during the first 7 days *in vitro*.

Table 5-2: Hepatocyte cell types and their advantages and disadvantages currently used in molecular and toxicology research.

Traditional static conditions	Ease of use and economical to carry out.	Hepatocytes de-differentiate and die within a few days. Does not help to maintain phenotype.
Collagen sandwich cultures	Better maintenance of phenotype.	De-differentiation still an issue.
Hydrogel 3D spheroid	Prolongs certain hepatocyte function longer than collagen sandwich.	Necrotic and hypoxic centre. Cell retrieval for future study more difficult.
3D microfluidic physiologically relevant devices	Shown to enhance liver specific functions maintain phenotype better.	Can be expensive, low throughput. Relies on good quality primary cells.

Table 5-3: Culture conditions and their advantages and disadvantages currently used in molecular and toxicology research

5.2.1 Immortal cell lines (e.g. HepG2, HepaRG)

Cell lines have been used for decades to study mammalian cell biology and signalling. Cell lines, unlike primary cells, have an unlimited life span (assuming a stable genotype), a stable phenotype and are readily available and offer easy use. These attributes would seem to make cell lines ideal as tools to study biological functions *in vitro*. There are drawbacks to using hepatic cell lines that make them unsuitable for the study of certain cellular functions however. Many hepatic cell lines show very low or non-existent expression of certain drug and chemical metabolising enzymes, such as cytochrome P450 enzymes, when compared to primary hepatocytes or liver *in vivo* (Donato et al., 2008). The significant difference in expression of drug metabolising enzymes between hepatic cell lines and primary liver has been linked to the loss of expression of particular transcription factors and nuclear receptors (Rodriguez-Antona et al., 2002).

There is a wide array of cell lines readily available commercially and each one has specific advantages and disadvantages. For example a few cell lines have shown a more *in vivo* like phenotype when cultured in fully confluent conditions. HepaRG cells undergo further differentiation during several weeks of treatment with DMSO. Once differentiated, HepaRG cells show higher levels of drug and chemical metabolising compounds than other hepatic cell lines such as HepG2 (Kanebratt and Andersson, 2008). This was a promising development and the HepaRG cell line is perhaps the best equipped

commercial cell line to tackle drug and chemical metabolism studies, although it is by no means perfect. When HepaRG cells are compared to primary human hepatocytes, cytochrome P450 enzyme expression is lower with the exception of CYP3A4 (Kanebratt and Andersson, 2008, Lubberstedt et al., 2011). This is similar when comparing other hepatic cell lines such as HuH7. Culture of HuH7 cells at high confluency leads to lower expression of cytochrome enzymes compared to primary hepatocytes, with CYP3A4 the exception (Sivertsson et al., 2010).

These are just two well used examples of immortalised cell lines that aim to mimic primary human hepatocytes. The low basal level of cytochrome enzyme expression is a problem and major disadvantage when assessing drug and chemical toxicity. Many adverse reactions are as a result of detoxification and bioactivation processes that are carried out by these enzymes and the lack of well-maintained expression in these cell lines leaves them inadequate for the study of human toxicity.

5.2.2 Primary human hepatocytes in traditional static culture

Primary human hepatocytes are derived from the isolation of hepatocytes from pieces of healthy human liver resected as a consequence of hepatic carcinoma or from samples unfit for transplantation. They were first isolated in the 1970s using a two-step collagenase perfusion method (Seglen, 1976). As cells that are derived from *in vivo* tissue they represent a phenotype that closely resembles that of hepatocytes *in vivo*. It is common knowledge

however that primary hepatocytes cultured in traditional static conditions begin to dedifferentiate and die once isolated and cultured *in vitro* over the course of 48-72 hours. This is not necessarily a problem if the cellular event under study can be studied in that time frame. This highlights a second drawback using primary human hepatocytes has over other cell technologies, the limited number of cells available. Due to the fact that primary human hepatocytes do not readily proliferate the only way to generate more cells for study is through further perfusions and isolations. The availability of human tissue that can be used in this way is often limited and a close network of surgeons and researchers, along with appropriate ethics, is needed to maximise hepatocyte quality and availability.

5.2.3 Primary human hepatocytes in collagen sandwich culture

Collagen sandwich culture is an attempt to recreate the polarity normally observed in hepatocytes *in vivo* thereby maintaining hepatic phenotype for a longer period of time. The way this is achieved is by convincing hepatocytes that there are two extracellular surfaces present during *in vitro* culture. Hepatocytes are cultured between two layers of collagen, one on the bottom of the culture dish and one laid on top. Collagen sandwich cultures have been shown to help maintain hepatic phenotype better than those cultured in traditional single collagen layer culture (Kim et al., 2010, Dunn et al., 1991). The measures used to assess this improvement include prolonged secretion of liver specific proteins and chemicals compared to traditional culture over time

and improved gene expression profiles over the course of culture when compared to single collagen layer culture. The issue of dedifferentiation still exists when using collagen sandwich layer it is merely delayed. Cells *in vivo* are three dimensional in conformation whereas collagen sandwich is still a two dimensional system aiming to convince hepatocytes of the presence of a second extracellular matrix. Hepatocytes *in vivo* display a polarity that is a consequence of the expression of a distinct set of proteins on membranes (sinusoidal, basolateral and apical membranes) exposed to different environments of the liver and these proteins are often lost when cultured in 2D cultures (Berthiaume et al., 1996). Collagen sandwich culture helps to maintain hepatocyte polarity for a period of time *in vitro* allowing the study of polar hepatocytes (Berthiaume et al., 1996). In contrast traditional 2D culture techniques force hepatocytes to alter their structure and cytoskeleton to form a flattened hexagonal morphology. It follows that culture systems capable of supporting three dimensional culture of hepatocytes is a logical step to attempt to improve the characteristics of hepatocyte cells in culture.

5.2.4 Primary human hepatocytes in dynamic three dimensional culture

The dedifferentiation of primary hepatocytes *in vitro* when cultured under static conditions is well established and well reported (Bissell et al., 1987b, Clayton and Darnell, 1983b, Godoy et al., 2009b, Koide et al., 1989b, Tong et al., 1994). Hepatocytes *in vivo* exist in a three dimensional conformation that is lost when kept in traditional *in vitro* culture systems. There are three main

areas and encompassing technologies that constitute the current offering of three dimensional models; hepatospheres, hydrogels and synthetic three dimensional scaffolds.

5.2.4.1 *Hydrogel three dimensional scaffolds*

Hepatocyte spheroids can be produced and cultured in non-adhesive hydrogels such as Matrigel™ (Ringel et al., 2005, Koebe et al., 1994). Culturing hepatocytes in hydrogels such as Matrigel™ has been shown to help prolong the preservation of hepatic function and phenotype longer than collagen sandwich cultures (Moghe et al., 1997). There are other examples of hydrogels, generally based upon varying extra cellular matrix proteins, maintaining hepatocyte function better over longer time periods (Ranucci et al., 2000, Prestwich et al., 2007). As with many hepatocyte cultures that form spheroids or reside within small three dimensional architecture there are concerns about oxygen and nutrient diffusion throughout the culture. Once hepatocytes have been seeded into the hydrogel matrix it can be also tough to achieve efficient cell retrieval, an important step in post culture analysis. A variation on the aforementioned animal based hydrogel is Algimatrix™, a three dimensional gel based on alginate sponge (Rowley et al., 1999). When hepatocytes are cultured in this gel the interaction with the actual gel structure is low and are therefore able to form multiple hepatospheres (hepatospheres discussed in section 5.2.4.2) within the three dimensional space. This limits the dimension of the hepatospheres, allowing better

nutrient and oxygen diffusion; however this does not represent the *in vivo* structural organisation of hepatocytes in the liver and makes cell retrieval equally as challenging.

5.2.4.2 *Hepatospheres*

Hepatospheres rely on the ability of hepatocytes to re-aggregate by self-assembly to try and re-form a three dimensional structure *in vitro*. The premise is that hepatocytes are able to form three dimensional tissue architecture if the adhesion to a collagen like substrate is prevented (Kelm and Fussenegger, 2004, Kelm et al., 2003, Kelm et al., 2006). The phenotype of hepatocytes cultured in this way changes from that of a monolayer to a more spheroid type. Stress fibres formed by the cytoskeleton are not present (Chang and Hughes-Fulford, 2009, Tzanakakis et al., 2001), there are three dimensional cell-cell contacts and hepatocytes have shown polarity in membrane associated proteins (Peshwa et al., 1996). Cells used to form hepatospheres can be sourced directly from tissue as primary hepatocytes or from hepatocyte like cell lines. A plentiful supply of oxygen is crucial for hepatocyte cultures due to their high metabolic activity and oxygen consumption (Cho et al., 2007). A high up take of oxygen has been found to correlate with the level of albumin and urea production (Cho et al., 2007). Utilising better oxygen supply to improve hepatocyte cultures was attempted in simple liver sections where it was discovered that using a higher partial pressure of nutrient perfusion improved the phenotype of cells cultured

deeper inside the liver section (MacDougall and McCabe, 1967). This highlights a potential flaw when using hepatospheres and spheroids as three dimensional culture systems for hepatocytes. The diameter of the spheroid must not be so big as to prevent the efficient supply of oxygen and nutrients to the hepatocytes cultured in the core, thus allowing hepatocytes to retain functionality and a more *in vivo* like phenotype (Funatsu et al., 2001). It is therefore important to balance the increasing diameter of the spheroid with maintaining a good oxygen supply. Increasing the oxygen concentration is possible but there is a potential drawback to this in the production of reactive oxygen species that are damaging to cell health and viability (Lillegard et al., 2011). By including dynamic perfusion of culture medium through the cultured hepatocytes the oxygen and nutrient diffusion can be improved (Lee et al., 2007).

5.2.4.3 *Three dimensional dynamic culture (Bioreactors)*

Three dimensional dynamic culture is a broad term for all synthetic three dimensional scaffold based cultures that enable medium flow through the system and over hepatocytes. Whilst collagen sandwich culture enhances hepatocyte polarity and a number of biotransformation reactions useful in studying chemical metabolism, these changes are restricted to a few major overexpressed molecular entities (Kienhuis et al., 2007, Rowe et al., 2010) and do not seem to impact dedifferentiation in the long term. As discussed previously hepatospheres, spheroids and hydrogel matrices all present their

own individual advantages and disadvantages, the main one being oxygen and nutrient depletion. The aim of using three dimensional culture under dynamic flow is to mimic the *in vivo* conditions to which hepatocytes are exposed and to improve the supply of oxygen to hepatocytes cultured in three dimensional conformation. The basic components of almost all three dimensional bioreactors are a three dimensional scaffold into which hepatocytes can be seeded and a pump of varying design that enables medium flow through the seeded tissue. The aim of this approach is to allow hepatocytes to experience a three dimensional environment that has been shown to be beneficial to hepatic phenotype *in vitro* whilst improving the oxygen and nutrient supply to the seeded hepatocytes. LiverChip™ (CNBio Innovations) is one such three dimensional culture system.

5.2.5 LiverChip™

LiverChip™ is a three dimensional dynamic culture system that aims to mimic the sinusoidal structure of the liver in a practical way to allow better maintenance of hepatocyte function *in vitro*. As mentioned previously, culturing cells in a three dimensional conformation helps to improve hepatic function and maintenance of hepatic phenotype *in vitro*. With the addition of dynamic culture medium flowing through perfused channels in which primary hepatocytes can attach, LiverChip™ is a system that mimics *in vivo* conditions practically (Figure 5-1). A bonus is that the culture of primary hepatocytes in LiverChip™ is straightforward; there is no departure from standard tissue

culture techniques such as the use of pipettes to seed the hepatocytes into the three dimensional scaffold. To improve throughput and integration of LiverChip^{TM} into existing laboratory space the plate design and size was modelled on a standard tissue culture plate (Figure 5-2). Each plate houses twelve individual culture wells containing a three dimensional scaffold seeded with 600,000 primary human hepatocytes. Each culture scaffold contains a large number of channels that are collagen coated to which hepatocytes can adhere and form tissue like structures subjected to continuous medium flow. One of the major issues arising from the study of three dimensional culture systems such as hepatospheres and spheroids is the efficient oxygen diffusion that is often lacking in these systems (Griffith and Swartz, 2006). The oxygen consumption of hepatocytes seeded into LiverChip^{TM} was measured over time and it was reported that the culture system supported physiologically relevant oxygen concentration gradients across the entire three dimensional scaffold in response to continuous medium flow through the tissue (Domansky et al., 2010). Gene expression analysis was also carried out on primary rat hepatocytes cultured in LiverChip^{TM}. This revealed that hepatocytes cultured in LiverChip^{TM} retained hepatic phenotype better than those cultured in collagen sandwich culture (Figure 5-3, Sivaraman et al., 2005) and compared favourably to *in vivo* conditions. In addition to this study a group also found strong correlation between measured clearance of certain compounds in cryopreserved human hepatocytes cultured in LiverChip^{TM} and clearance rates observed *in vivo* (Figure 5-4 (Dash et al., 2009)). Despite the difference in

magnitude of observed clearance rates between *in vitro* and *in vivo* conditions shown in Figure 5-4 there is a good correlation between each condition. Each characteristic of LiverChip™ previously discussed suggests that this three dimensional culture system is a promising addition to the *in vitro* hepatocyte culture field of study. The characteristics detailed previously lay behind the decision to use LiverChip™ as the culture system in the remainder of this body of work.

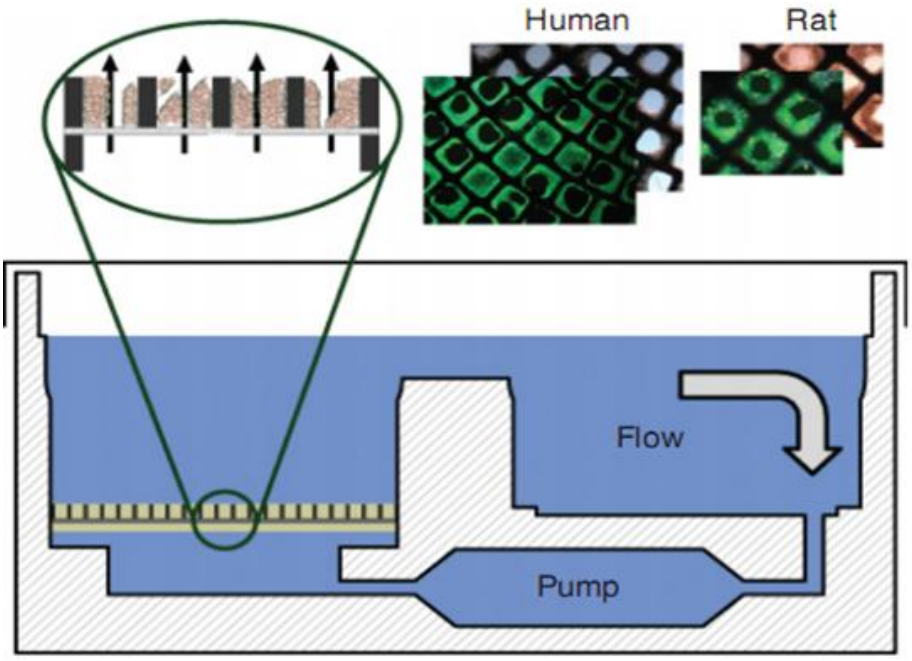

Figure 5-1: Schematic representation of the LiverChip™ three dimensional hepatocyte culture system. Multiple hepatocytes are seeded into each of the channels present in the three dimensional culture scaffold and culture medium is pumped through these channels and seeded hepatocytes. (Figure courtesy of CN Bio Innovations®)

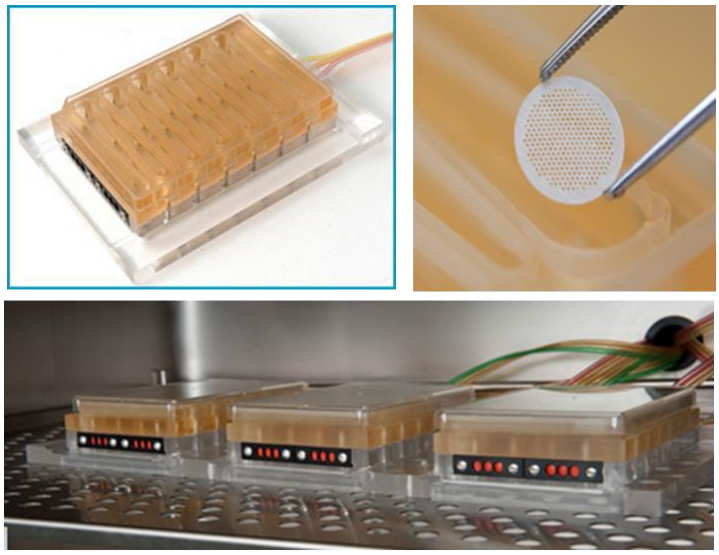

Figure 5-2: LiverChip™ perfusion plate and dock (top left). LiverChip™ three dimensional scaffold (top right). Three LiverChip™ perfusion plates and dock within a standard tissue culture incubator. (Figure courtesy of CN Bio Innovations®)

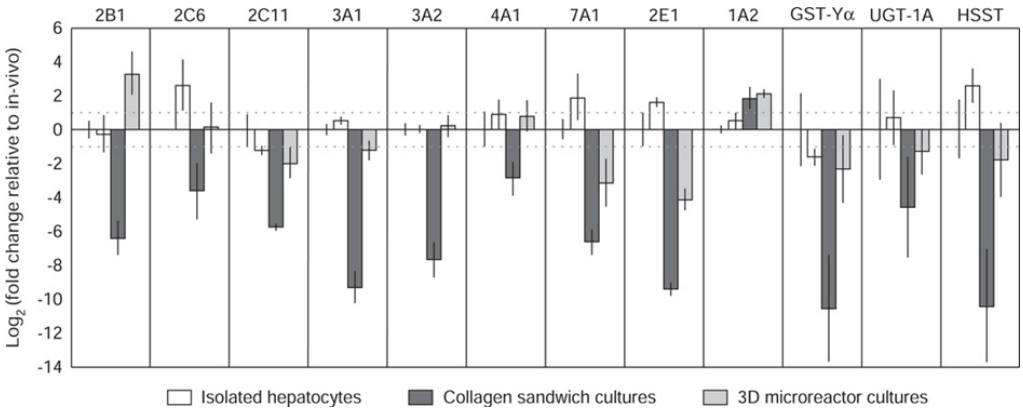

Figure 5-3: Expression of selected phase I and II genes in isolated primary rat hepatocytes cultured for a period of 5 days in LiverChip™, collagen sandwich and freshly isolated hepatocytes as fold change compared to rat liver *in vivo*. (Sivaraman et al., 2005). (HSST: heparan sulfate n-deacetylase/n-sulfotransferase)

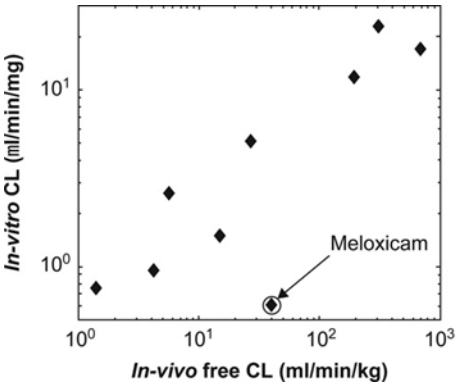

Drug	Enzyme	CL	Class
Tolbutamide	2C9	Low	Acid
Meloxicam	2C9 & 3A4	Mid	Acid
Diclofenac	2C9	High	Acid
Disopyramide	3A4	Low	Base
Metoprolol	2D6	Mid	Base
Verapamil	3A	High	Base
Theophylline	1A2	Low	Neutral
Methylprednisolone	3A	Mid	Neutral
Midazolam	3A	High	Neutral

Figure 5-4: Clearance rates of nine different compounds in cryopreserved human hepatocytes cultured in LiverChip™ compared to the clearance rates observed *in vivo* (Dash et al., 2009).

5.3 Liver nuclear receptors

Nuclear receptors expressed in the liver play an important role in the response to potentially toxic xenobiotics. They are responsible for the gene expression of a range of detoxification and metabolism enzymes, such as the cytochrome P450 family. Nuclear receptors not only recognise and metabolise exogenous chemicals, they are also able to respond to endogenous compounds such as lipids and cholesterol. There is a great deal of crosstalk between many nuclear receptors and the application of drugs or environmental compounds and many physiological functions such as bile acid homeostasis. This is shown by the fact that nuclear receptors are under the influence of drugs and environmental compounds but also sensitive to many endogenous compounds, therefore controlling target genes that range from drug and bile acid transport to those involved in energy and lipid metabolism (Pascussi et al., 2004).

Nuclear receptors are characterised by several structural characteristics and contain (with exceptions) six functional domains, A-F (Figure 5-5). Each domain shows varying degrees of sequence conservation across the family of receptors, forty-nine in total (Bain et al., 2007). The AF-1 domain, also known as the transactivation domain, is in the proximity of the N-terminal amongst the A/B domains. Each receptor is able to bind DNA and alter transcription; therefore a DNA binding domain (DBD) is also present within a highly conserved C region made up of two zinc finger domains. Ligand binding is an important step in transactivation of many nuclear receptors and to this end each contains a ligand binding domain (LBD) within the E region. The final two domains, D and F, consist of linker peptide sequences that join the DBD to the LBD and a C-terminal extension of the LBD (Bain et al., 2007). Nuclear receptors are able to bind both agonistic and antagonistic ligands at the LBD leading to the dimerisation of the nuclear receptor. This can be in the form of either homo- or heterodimerisation. Upon activation the nuclear receptor translocates to the nucleus where it binds to specific consensus DNA sequences amongst target gene promoter regions and modulates gene transcription (Bain et al., 2007). Ligand binding is not the sole method of regulation that affects gene expression in response to nuclear receptor activation. Ligand binding to the receptors, or via indirect mechanisms, is undoubtedly important however the interplay between nuclear receptors and co-regulatory proteins in the nucleus also has a significant role to play (Pascussi et al., 2008). Co-regulators are divided into classes depending on

their effect on nuclear receptor action. Those that cause chromatin relaxation and facilitation of further transcription factor recruitment are known as co-activators. Whereas those that lead to recruitment of histone de-acetylases (HDACs), supporting chromatin condensation and suppression of gene expression, are termed co-repressors.

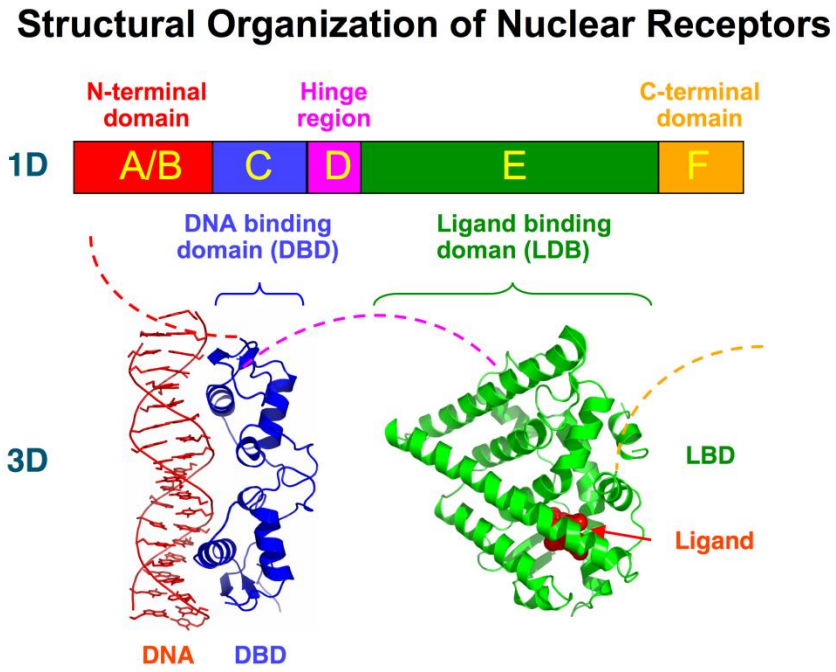

Figure 5-5: Top - Schematic 1D amino acid sequence of a nuclear receptor. Bottom - 3D structures of the DBD (bound to DNA) and LBD (bound to hormone) regions of the nuclear receptor. The structures shown are of the estrogen receptor. Experimental structures of N-terminal domain (A/B), hinge region (D), and C-terminal domain (F) have not been determined therefore are represented by red, purple, and orange dashed lines, respectively (This work has been released into the public domain by its author, Boghog2. Boghog2 grants anyone the right to use this work for any purpose, without any conditions, unless such conditions are required by law)

These structures, functions and shared similarities between nuclear receptors betray the wide ranging and sometime significant differences between

members of this family. For example pregnane-X receptor (PXR) has a wide ranging ligand profile of varying structures and low specificity compared to the constitutively active CAR which lacks the variety of ligands able to bind directly. What is common to both of these nuclear receptors is the ability and preference to bind in a heterodimer with retinoid-X receptor to modulate transcription upon activation or translocation to the nucleus.

5.3.1 Pregnane X receptor (PXR)

Whilst the focus of this thesis is centred on CAR it is important to note the other xenobiotic sensing nuclear receptor PXR. PXR is a master regulator of metabolic enzymes expressed in response to xenobiotic exposure. In contrast to CAR, PXR shows high ligand promiscuity and is able to bind many structurally distinct compounds (Kliewer et al., 2002). Structural x-ray crystallography studies found that PXR also contained a flexible ligand binding domain (LBD) that contributes to the diverse range of ligands able to bind to PXR (Watkins et al., 2001). The ligand promiscuity shown by PXR creates a problem that until relatively recently made investigating CAR specific gene expression changes in human hepatic cells tough. Many direct hCAR ligands also show a level of affinity towards PXR thereby making the changes in gene expression as a direct result of CAR activation tough to investigate.

The target genes regulated by PXR include a wide range of xenobiotic detoxification enzymes such as phase I, phase II and phase III enzymes (Synold et al., 2001, Xie et al., 2000, Goodwin et al., 2001). The CYP3A family of phase

I enzymes is directly regulated by PXR. In a mirror of the receptor that activates this family these enzymes show a wide ranging and diverse set of target substrates (Wrighton et al., 2000, Li et al., 1995). PXR is the nuclear receptor that is most closely related to CAR, sharing roughly 70% sequence identity in DBD and 50% identity in the LBD (Blumberg et al., 1998). CAR and PXR were originally shown to regulate differing cytochrome P450 families; CAR was shown to regulate CYP2B and PXR was shown to regulate the CYP3A family (Goodwin et al., 1999, Honkakoski et al., 1998). CAR and PXR signalling responses seemed to be separate due to the differing binding motifs exhibited by PXR and CAR specific cytochrome P450 families induced by each. It was subsequently discovered that PXR is able to bind to motifs within the phenobarbital response element (PBREM) upstream of CYP2B6 (Goodwin et al., 2001). There is further evidence to suggest that the overlap of target genes regulated by PXR and CAR extends beyond these specific cytochrome P450 enzymes and extends to other phase I and phase II enzymes along with a selection of drug transporters (Kast et al., 2002, Maglich et al., 2002, Gerbal-Chaloin et al., 2001). Despite the considerable overlap of CAR and PXR target genes each receptor targets a distinct set of genes responsible for a variety of cellular signalling pathways. The promiscuity of ligand binding that PXR shows also ensures that CAR, containing a smaller and less flexible LBD, is unable to bind a majority of PXR ligands.

5.3.2 Constitutive androstane receptor (CAR)

Constitutive androstane receptor (CAR) is similar to PXR as a fellow nuclear receptor responsible for the xenobiotic response in sequence and function. A large proportion of CAR ligands also show an affinity towards PXR. CAR is also unusual among nuclear receptors in that it demonstrates constitutive activity in the absence of ligand interaction (Forman et al., 1998). This constitutive activity is in part due to structural alterations associated with CAR compared to other nuclear receptors.

5.3.2.1 *Molecular structure*

Like other nuclear receptors CAR consists of functional domains organised into a specific structure. The domains present include; N-terminal domain, DNA binding domain which contains activation function 1 (AF1), ligand binding domain containing the activation function 2 (AF2) and the C-terminal domain (Kumar and Thompson, 1999). CAR is classified as NR1I3 (nuclear receptor family 1, sub-family I, number 3) and shares between 63-66% sequence identity of the DNA binding domain and between 37-45% identity of the ligand binding domain with PXR and VDR, other members of the NR1 family (Willson and Kliewer, 2002). A feature of CAR activity that distinguishes it from the other nuclear receptors in its family is its constitutive activity in the nucleus that seems ligand independent.

To date there have been a wide range of crystal structures produced of CAR as part of heterodimers and one of these has helped to provide a theory to

explain the constitutive activity of CAR (Xu et al., 2004). The constitutive activity arises due to the rigid AF2 domain helix that is one of the shortest among other nuclear receptors. The rigidity and reduced size of this helix allows it to form additional hydrogen bonds therefore allowing the AF2 domain to remain in an active conformation. This shorter linker region (AF2 helix) gives rise to a novel interaction with helix H10 of CAR. The interaction between these two regions is critical for the constitutive activity of CAR as shown in studies in which inserting three amino acids into the linker region disrupted the constitutive activity of CAR (Dussault et al., 2002).

The reduced ligand binding compared to PXR is explained by the existence of a barrier of four residues (F161, N165, F234 and Y326) which the helices, αAF and H-X, get pushed against. The barrier structure is strengthened by a hydrogen bond that forms between N165 and Y326. This barrier structure shields the ligand binding site from the αAF2 helix. The shielding of the αAF2 helix by the barrier structure makes ligand interactions with the αAF2 helix difficult. The αAF is stabilised in the active confirmation due to an interaction between a free carboxylate (the helix αAF contains no C-terminal extension leaving the free carboxylate) and K195 (Wu et al., 2013). When the structural features above are combined it they contribute to the structure of CAR favouring an active confirmation. When mouse CAR (mCAR) was investigated there were similar features to that of hCAR that seemed to contribute to the constitutive activity of mCAR (Suino et al., 2004).

Due to the barrier structure in hCAR it is hard for ligands to bind and interact with the αAF to promote activation. Due to this barrier (Xu et al., 2004) the role of ligands in CAR transcriptional activation was proposed to aid the passing of CAR from the cytosol into the nucleus rather than the classic conformational change of the C-terminal αAF to the active confirmation. Mouse CAR does not have the barrier structure that prevents a ligand from binding and causing a conformational change in the αAF helix suggesting that the role of ligand interactions in mCAR is more complex (Suino et al., 2004). As discussed the activation of CAR is not responsible for a conformational change, instead it is responsible for translocation from the cytoplasm into the nucleus where it is able to dimerise and affect transcription of target genes.

5.3.2.2 *Activation of constitutive androstane receptor*

Activation of the orphan nuclear receptor CAR is possible using a range of xenobiotic chemicals and steroids which is in contrast to many steroid receptors that respond mainly to endogenous substances (Giguere, 1999, Tzameli and Moore, 2001). Upon activation the DNA binding domain (DBD) contains structures unique to CAR that are able to bind to response elements on target genes, the xenobiotic response element (XREM) and phenobarbital response element (PBREM) (Makinen et al., 2002). Once translocated into the nucleus CAR binds to RXR forming a heterodimer and only then is able to bind specific response elements. As discussed previously the LBD of CAR contains a single turn helix, this prevents a change in AF2 domain conformation and

reduces the ligand binding pocket size (Xu et al., 2004). These features brought about by the additional helix allow CAR to maintain its constitutive activity once inside the nucleus by interacting with co-activators. It is therefore thought that translocation to the nucleus is the key step in activation of CAR, the control of which can be achieved via either indirect ligand activities or via direct ligand binding to CAR (Kawamoto et al., 1999 (Maglich et al., 2003).

The majority of CAR expression is centred on the cytoplasm (Kawamoto et al., 1999, Zelko et al., 2001) where it is kept in an inactive complex. The control of this nuclear translocation in other members of the nuclear receptor family is mediated using ligand binding and the activity of a nuclear localisation signal (NLS). The NLS is formed of a sequence of amino acids and is usually found in proximity or within the DNA binding domain (DBD). Human CAR seems to lack a functional NLS whereas rat CAR appears to contain two functional NLS domains (Kanno et al., 2005). However both human and mouse CAR possess a leucine rich region of amino acids in the C-terminal domain (Zelko et al., 2001). This sequence acts as a signal, in response to the presence of xenobiotics, to aid nuclear localisation and is termed the xenobiotic response signal (XRS). Upon ligand activation and translocation CAR is then able to enter the nucleus and form a heterodimer with RXR and bind to speicific DR4 motifs to alter transcription (Kawamoto et al., 1999, Sueyoshi and Negishi, 2001).

5.3.2.2.1 Indirect activation

Many CAR activators have been described ranging from endogenous metabolites to environmental contaminants and chemicals (Molnar et al., 2013, Qatanani and Moore, 2005). A large proportion of these activators do not act through a direct mechanism of ligand binding to CAR. Instead causing translocation of CAR from the cytoplasm to the nucleus (Li et al., 2009) where the constitutive activity allows it to recruit co-activators and heterodimerise to affect gene expression. The constitutive activity of CAR is not always of benefit due to unintended consequences that may present themselves upon continuous CAR mediated changes in gene expression. It is for this reason that CAR is mainly held in the cytoplasm in an inactive complex with heat shock protein 90 (HSP90), cytoplasmic CAR retention protein (CCRP) and protein phosphatase 1 regulatory subunit 16A (Kobayashi et al., 2003, Yoshinari et al., 2003, Sueyoshi et al., 2008). Indirect activation of CAR is the method utilised by phenobarbital and phenobarbital like activators (Yoshinari et al., 2003). Analogous to direct activation, treatment using phenobarbital like compounds stimulates the dissociation of CAR and the inactive complex in the cytoplasm and allows translocation to occur. The process of complex dissociation is caused by phosphorylation and dephosphorylation of various proteins and CAR; amino acid Thr-38 of CAR was found to be the crucial residue controlling nuclear entry via phosphorylation (Mutoh et al., 2009). Employing protein phosphatase 2A (PP2A) to dephosphorylate CAR and enable nuclear translocation phenobarbital acts through the suppression of epidermal

growth factor receptor (EGFR) signalling by providing competition for epidermal growth factor (EGF) in receptor binding (Mutoh et al., 2013). Lack of phenobarbital treatment allows EGF to bind to its receptor and activate Src kinase which is then able to phosphorylate receptor for activated kinase 1 (RACK1). Phosphorylated RACK1 is unable to interact with and allow PP2A to dephosphorylate and activate CAR. When phenobarbital is present and competing with EGF to prevent binding of EGF to its receptor the Src kinase is no longer able to phosphorylate RACK1 leaving it free to interact with PP2A and activate CAR translocation to the nucleus by de-phosphorylation of Thr-38. An overview of the translocation of CAR in response to phenobarbital treatment via RACK1/PP2A is shown in Figure 5-6.

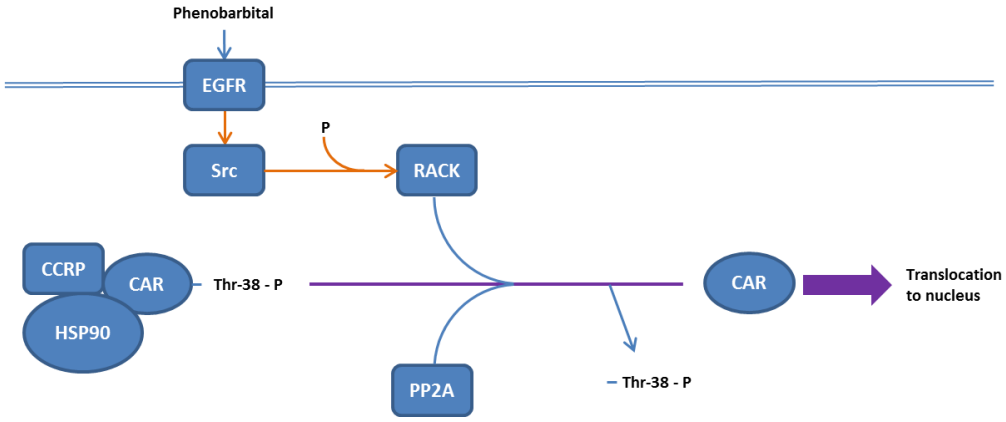

Figure 5-6: Overview of signalling pathways involved in translocation of CAR in response to phenobarbital treatment. Orange indicates a down-regulation in the pathway in response to phenobarbital treatment and blue represents and up-regulation in the pathway. Adapted from (Yang and Wang, 2014).

There is mounting evidence to suggest that various cytochrome P450 enzymes are repressed during liver infection, inflammation and regeneration. This

suggests a role for cellular signalling molecules in the control of expression of cytochrome P450 enzymes (Bauer et al., 2004, Koike et al., 2007a). Further study identified that the MEK-ERK signalling pathway was involved in phenobarbital dependant induction of CYP2B1. The suppression of MEK-ERK signalling (by treatment with U0126) led to an increase in CYP2B1 induction by phenobarbital (Joannard et al., 2006). This evidence was backed up by the finding that an endogenous ERK signal was able to regulate CAR phosphorylation and nuclear translocation. Using an ERK1/2 inhibitor (U0126) the induction of CYP2B10 via ERK1/2 de-activation was found to be completely removed when using a CAR knockout mouse model (Koike et al., 2007b). Enhancing the view that ERK1/2 signalling is important in the regulation of CAR translocation was the fact that ERK1/2 would only co-precipitate with Thr-38 phosphorylated CAR and that the C-terminal xenobiotic response sequence (XRS) is essential for this interaction (Osabe and Negishi, 2011). An overview of the regulatory effect that the MEK-ERK signalling pathway can have on CAR translocation is shown in Figure 5-7.

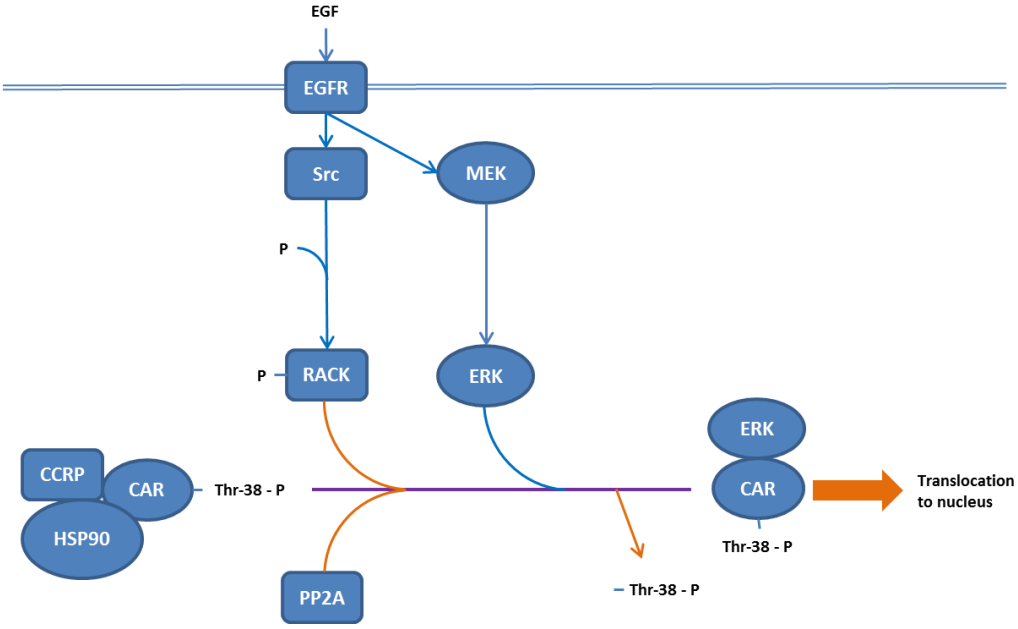

Figure 5-7: Overview of the effect MEK-ERK signalling has on nuclear translocation of CAR. Orange indicates a down-regulation in the pathway in response to endogenous EGF receptor signalling and blue represents an up-regulation in the pathway. Adapted from (Yang and Wang, 2014).

5.3.2.2.2 Direct activation

As a consequence of the constitutive activity shown by CAR, the inverse agonists androstanol and androstenol were the first direct ligands to be discovered (Forman et al., 1998). These chemicals act to disrupt the bonds holding CAR in a constitutively active conformation by disrupting the salt bridge locking H12 helix in the active form. This promotes co-activator release from the LBD without affecting DNA binding or CAR/RXR heterodimers (Shan et al., 2004). Species differences shown in direct ligand specificities of CAR ensure that extrapolating data from rodent experiments to humans is fraught with issues. For example the classical and potent mCAR activator TCPOBOP

has been shown to activate mCAR by interaction with the binding pocket (Tzameli et al., 2000) but does not bind to or activate hCAR. A further discrepancy highlighting the difference between mCAR and hCAR direct activation and suppression is that androstanol, progesterone and testosterone are able to repress mCAR but not hCAR (Handschin and Meyer, 2003, Maglich et al., 2003). To date the most promising direct agonist of hCAR is the imidazothiazole derivative CITCO. CITCO is able to bind hCAR directly and induce expression of CAR target genes in human hepatocytes *in vitro* (Maglich et al., 2003 (Faucette et al., 2006). Further evidence produced since suggests that CITCO is able to aid the recruitment of co-activators to the LBD of hCAR by competition with antagonists such as PK11195 (Li et al., 2008) and metformin (Yang et al., 2014). Despite the affinity CITCO shows towards hCAR it is also able to activate PXR at higher concentrations however CITCO shows a 100 fold preference for hCAR binding over PXR (Maglich et al., 2003). Other direct hCAR ligands reported to date also show potent activation of PXR rendering the comparison of direct hCAR and PXR genes challenging. Direct ligand dependant activation of hCAR is still, similar to indirect activation, likely to rely on the translocation of hCAR from the cytoplasm to the nucleus and the recruitment of co-activators that aid the constitutive activity rather than by the conformational change seen in other nuclear receptor activation.

5.3.2.3 *Xenobiotic gene expression changes*

As a nuclear receptor that is activated in response to many drugs and environmental chemicals it is unsurprising that the majority of genes induced are involved in drug metabolism and transport (Ueda et al., 2002). CAR and PXR share many xenobiotic activators and are responsible for inducing gene expression of a range of overlapping genes responsible for xenobiotic metabolism (Goodwin et al., 2001, Sueyoshi et al., 1999b, Sugatani et al., 2001, Xie et al., 2003). The genes induced by CAR activation include many cytochrome P450 enzymes (CYP2B6, CYP2A6, CYP3A4 and the CYP2C family), glucuronosylltransferases (UGT1A1, UGT1A6 and UGT1A9), sulfotransferases, glutathione S-transferases, and transporters such as multidrug resistance protein 1 (MDR1) and organic anion transporting peptides (OATPS) (Burk et al., 2005, Stanley et al., 2006). What is clear from this data is that CAR is central to the response of the liver to xenobiotic and environmental compounds. Of concern to many is the fact that some of these compounds have been shown to cause a hepatotoxic response in rodents.

5.3.2.4 *Constitutive androstane receptor mediated toxicity*

Data available to support liver toxicity in response to CAR activation mainly relies on the indirect activator phenobarbital and the response in rodent. This indirect, non-genotoxic compound activates CAR and induces the transcription of a panel of cytochrome P450 enzymes. As a result of repeated dosing phenobarbital causes hepatocellular proliferation and

hepatocarcinoma in rats and most mouse strains (Whysner et al., 1996). This is where one of the largest divergences between human and rodent CAR mediated toxicity exists. Humans have been ingesting phenobarbital deliberately as a sedative and anti-epileptic drug for decades. Phenobarbital treatment induces a similar panel of cytochrome P450 enzymes as in rodent (Pelkonen et al., 2008) however there has so far been no report of hepatocellular carcinoma formation as a result of phenobarbital indirect activation of hCAR *in vivo*. The reason for this species difference remains to be reported.

Phenobarbital activates CAR via an indirect mechanism; the consequence of activating hCAR directly with ligand binding is unclear however. Activation of rCAR is a critical initial step in tumour formation in response to phenobarbital treatment as show in rCAR knockout studies (Huang et al., 2005b). In addition to this, studies of CAR activation in mice in response to the treatment of known genotoxic carcinogen diethylnitrosmine (DEN) in conjunction with phenobarbital found that mCAR knockout mice did not show tumour development in response to DEN and phenobarbital treatment. Therefore showing that CAR activation was a necessary step in tumour formation (Yamamoto et al., 2004b). When a potent direct mCAR activator (TCPOBOP) was investigated it was discovered that CAR knockout mice did not show tumour formation in response to treatment. Interestingly mice showed tumour formation in response to solely TCPOBOP treatment or in conjunction

with DEN highlighting the role direct activation of mCAR plays in tumour development (Huang et al., 2005b). Due to the potential species differences associated with direct CAR activation and diversity of ligands across species the extrapolation of data from rodent activation studies to human is not possible. The effect of direct activation of hCAR on liver toxicity and potential hepatocellular carcinoma is therefore unclear and not reported.

5.3.2.5 *MicroRNAs in CAR mediated hepatocellular proliferation*

MicroRNAs (miRNA) are short, single stranded (roughly 20-25 nucleotides), endogenous RNA molecules that are able to regulate gene expression (Bartel, 2004). Mature miRNAs are kept in a complex called the RNA-induced silencing complex (RISC). This ribonucleoprotein complex mediates the post-transcriptional gene silencing associated with miRNAs (Hutvagner and Zamore, 2002). The RISC complex is targeted towards mRNA transcripts by way of complimentary base pairing between miRNA and mRNA molecules. The targeted mRNA is then degraded, destabilised or prevented from taking part in translation (Eulalio et al., 2008, Filipowicz et al., 2008). There is a weight of evidence which suggests that individual miRNAs can have an impact upon a large number of target mRNAs (Baek et al., 2008, Selbach et al., 2008).

There are many routes and ways in which the production of a mature miRNA can be achieved. The canonical pathway or miRNA processing is shown in Figure 5-8. Many cellular pathways are affected by miRNA activity however the most prominent of these pathways are involved in development and

oncogenic processes (Lu et al., 2005, Calin and Croce, 2006, He et al., 2007, Johnson et al., 2005).

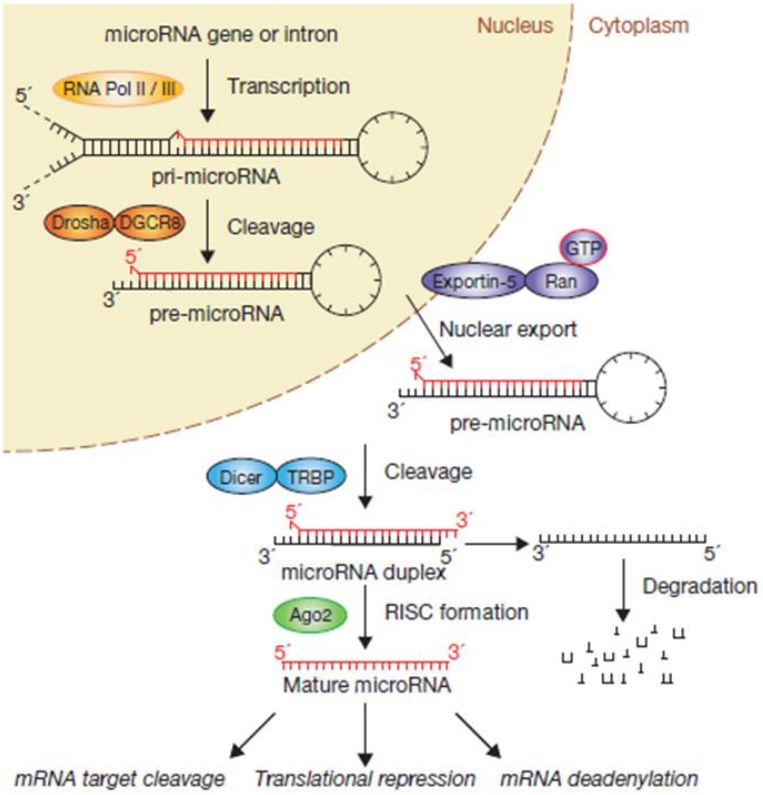

Figure 5-8: Canonical production of functional miRNA molecules. miRNA maturation includes the production of the primary miRNA transcript (pri-miRNA) by RNA polymerase II or III and cleavage of the pri-miRNA by the microprocessor complex Drosha–DGCR8 (Pasha) in the nucleus. The resulting precursor hairpin, the pre-miRNA, is exported from the nucleus by Exportin-5–Ran-GTP. In the cytoplasm, the RNase Dicer in complex with the double-stranded RNA-binding protein TRBP cleaves the pre-miRNA hairpin to its mature length. The functional strand of the mature miRNA is loaded together with Argonaute (Ago2) proteins into the RNA-induced silencing complex (RISC), where it guides RISC to silence target mRNAs through mRNA cleavage, translational repression or deadenylation, whereas the passenger strand (black) is degraded ((Winter et al., 2009).

MicroRNAs (miRNA) introduce an extra layer of complexity and intrigue to the overall control of physiological processes such as cancer progression and

tissue development in the cell. Proteomic studies have identified the ability of a single miRNA to impact hundreds of target genes (Baek et al., 2008, Selbach et al., 2008). MicroRNAs are short endogenous strands of RNA that are able to modulate and control gene expression (Bartel, 2004). Many cellular signalling pathways are affected by miRNAs with a particular focus on cell development and oncogenesis (Johnson et al., 2005, Lu et al., 2005, Calin and Croce, 2006). Initially it was thought that miRNA processing was facilitated by a single biogenesis pathway common to all mature miRNAs. This was added to when a variety of differing biogenesis pathways specific to a range of miRNAs and able to be regulated in a variety of ways was discovered (Winter et al., 2009).

Differential expression of certain miRNA transcripts in response to treatment with the prototypical CAR activator phenobarbital have been seen in rodent studies *in vivo*. A study in which rats were treated with phenobarbital for a period of three months and miRNA profiles investigated showed that a distinct set of miRNAs were induced in response to phenobarbital treatment (Koufaris et al., 2012). The miRNA clusters up-regulated were the miR-200a/200b/429 and miR-96/182 clusters. A follow up study was performed in which a time course of phenobarbital treatment was followed (Koufaris et al., 2013). During the initial phase of dosing (1-7 days) the typical changes in mRNA expression in response to phenobarbital and associated liver phenotype changes were observed. Despite this the change in miRNA expression was limited. Changes in miRNA expression did occur after 14 days

of phenobarbital treatment though. The main effect of phenobarbital dosing was the induction of miR-200a/200b/429 expression. An association between the differential expression of miR-200a/200b and global DNA methylation via zeb2 protein was also seen. Overall the data presented suggested that the differential expression of miRNA was unlikely to be the main driver of hepatocellular proliferation in response to phenobarbital treatment. A further point of interest lay in the observation that greater changes in miRNA expression coincided with the termination of proliferation and the achievement of maximum hepatomegaly. This response to longer term phenobarbital exposure led to the hypothesis that miRNA changes were attempting to maintain liver homeostasis in response to xenobiotic potentiated changes.

These initial studies and data highlight the growing understanding that changes in miRNA expression can have wide ranging effects or can be used as markers of hepatic phenotype. All current data centred on miRNAome changes associated with CAR activation were gathered in rodent based studies. Inter-species variability as mentioned previously is a well-known, if poorly understood, phenomenon. It is currently unknown what the species differences between rodent and human changes in miRNA expression in response to CAR activation are.

6 Summary and Aims

It is widely accepted that the activation of CAR in rodents is a known cause of hepatocellular proliferation and eventual carcinoma. The effect in human hepatocytes is less clear. There is a worldwide risk of exposure to crop protection agents via accidental ingestion. Many of these agents may contain direct human CAR activators as the active ingredient or as a mixing agent. Therefore it is crucial to understand the effect that CAR activation has upon the human population. Phenobarbital acts in an indirect (there has been no direct interaction between CAR and phenobarbital shown) manner to activate CAR and cause downstream gene expression changes. The effect direct activation of human CAR has upon gene expression is unknown. This is in part due to the paucity of direct ligands that show a high specificity to human CAR. CITCO is a recently published direct ligand that has shown preferential affinity towards human CAR. In rodents, as is the case with indirect activation, direct activation causes hepatocellular proliferation and hepatocarcinoma. It is the aim of this body of work to determine what gene expression changes occur in response to direct activation of human CAR by CITCO in primary human hepatocytes.

As discussed previously primary hepatocytes undergo dedifferentiation within 72 hours in traditional static culture. To help prevent this a three dimensional culture system that employs dynamic medium flow will be assessed before any study of CAR activation takes place. Characterisation of hepatocytes

cultured in this system is crucial to determine whether an *in vivo* like phenotype has been maintained so as to ensure that the gene expression changes observed are as close to the response that would be seen *in vivo* as possible. To this aim the expression of a range of hepatic specific genes will be investigated along with a suite of metabolic assays to ensure that the hepatocytes are as close to the *in vivo* phenotype as possible.

Recent data suggests that the *in vivo* gene expression changes due to CAR activation is more complex than previously thought. The involvement of miRNAs in the transition to hepatocellular proliferation and hepatocarcinoma has been demonstrated in rodent studies. For this reason the changes in miRNA expression in response to direct activation of human CAR will also be investigated.

It is the aim that by combining the mRNA gene expression data with miRNA expression data the potential cellular outcome of direct activation of CAR in humans will begin to become clear. Does direct activation of human CAR cause changes in mRNA and miRNA expression that could lead to hepatocellular proliferation, hepatocellular carcinoma or associated liver toxicity?

7 Materials and Methods

Unless otherwise stated all chemicals and reagents were obtained from Sigma-Aldrich®.

7.1 Rat liver perfusion and hepatocyte isolation

7.1.1 Solutions:

- 10X Hanks-Hepes buffer, pH7.4 (10XHH)
    - 80g NaCl
    - 4.0g KCl
    - 0.6g KH_2PO_4
    - 1.2g Na_2HPO_4 $12H_2O$
    - 47.6g HEPES
    - 0.1g Phenol Red
    - Approx. 3.5g NaOH

Components were dissolved in 1L of HPLC Grade water. The solution was then sterilised by autoclaving and stored at 4^{o}C.

- 1X HH
    - 10X HH was diluted 1:10 with HPLC grade water in 500mL quantities as required, sterilised by autoclaving and stored at 4^{o}C.
- Ethylene Glycol Tetraacetic Acid (EGTA)

- 0.48g EGTA in 25mL 1M NaOH and made up to 50mL with 1X HH. This solution was sterilised by filtration through a 0.2µm filter unit and stored at 4^{o}C.

- Calcium Chloride, 250mM
  - 1.84g calcium chloride (dihydrate) dissolved in 50mL HPLC grade H_2O, filter sterilised and stored at 4^{o}C.
- MBG Solution
  - Dissolved 3.1g sodium bicarbonate, 2.5g glucose and 0.75g methionine in 50mL HPLC grade water. Filter sterilised, divided into 10mL aliquots and stored at -20^{o}C.
- 90% Percoll
  - Percoll (Amersham Biosciences 17-0891-01, 1.131g/mL) was diluted 9:1 with 10X Hanks' Balanced Salt Solution (HBSS) and stored in 10mL aliquots at 4^{o}C.

7.1.2 Procedure

The water bath was heated to 40^{o}C and perfusion tubing set up and sterilised by circulation of industrial methylated spirits (IMS). The pump was set at approximately 10-15mL/cannula/min. The perfusion buffer was made up to give a final concentration of 2mM methionine, 5.56mM glucose and 14.76mM sodium bicarbonate. The perfusion buffer was split into three 100mL solutions. To two of these solutions 2.0mL EGTA solution was added. To the final 100mL solution 2.0mL calcium chloride and 50mg collagenase were

added. Approximately 250mL of distilled sterile water was used to flush the perfusion tubing to remove residual IMS. Once cleansed, one of the EGTA containing solutions was recirculated continuously.

All rats were humanely euthanased by dislocation of the neck and liver lobes removed individually and placed into perfusion buffer. Perfusion was established by cannulating the lobes with EGTA solution. Once the perfusion was established the recirculating solution was changed to the second EGTA containing solution. Recirculation of this solution continued for 15 minutes after which the recirculating solution was changed to the 100mL perfusion solution (digestion solution containing 50mg collagenase and 5mM calcium chloride). The digestion solution was recirculated for 10-15 minutes until the lobes were soft and beginning to disintegrate. After this the lobes were removed from the perfusion, placed in fresh perfusion buffer and minced using scissors. This solution was filtered through gauze which was rinsed with perfusion buffer. The filtered solution was centrifuged at 70g for 2 minutes at room temperature and the supernatant removed. The hepatocyte pellet was resuspended in serum containing culture solution and centrifuged at 70g for 2 minutes at room temperature. The remaining hepatocyte pellet was re-suspended in 9mL serum containing culture medium and added to 10mL Percoll. The Percoll/hepatocyte solution underwent centrifugation at 80g for 10 minutes at room temperature. As an estimate there was a loss of less than 10-15% pellet volume post Percoll centrifugation This demonstrated that the

hepatocytes were of generally high viability before Percoll centrifugation. The supernatant was removed and hepatocyte pellet resuspended in serum containing medium and centrifuged at 70g for 2 minutes at room temperature. This spin was repeated once more before finally re-suspending the hepatocyte pellet in 20-50mL serum containing culture medium and estimating the hepatocyte number and concentration using a haemocytometer.

7.2 Human liver perfusion and hepatocyte isolation

Primary human hepatocytes were isolated from donated liver tissue arising from liver resections carried out at Queens Medical Centre Nottingham. Consent for use of tissue was given via the QMC BioBank tissue collection initiative. The donor tissue was collected from resected tissue that was not required for further analysis and was free of tumour or disease. Unfortunately the drug and treatment history of each patient is not known.

7.2.1 Solutions:

Solutions used during the isolation of primary human hepatocytes were identical to those used during the isolation of primary rat hepatocytes with the exception of the initial buffer into which tissue samples are placed before perfusion.

- Soltran Solution

- Dilute Soltran Buffer (Baxter) to 330mOsmol/L with sterile HPLC water and store at 4^{o}C.

7.2.2 Procedure

The perfusion tubing was sterilised and cleansed using the same method as the rat perfusion. The water bath was set to 43^{o}C to allow for heat loss in the perfusion tubing. The following solutions were made up in appropriate Duran bottles of 1XHH:

- 500mL 1XHH + 10mL MBG + 10mL EGTA solution
- 1L 1XHH + 20mL MBG + 20mL EGTA solution
- 500mL 1XHH + 10mL MBG
- 500mL 1XHH + 10mL MBG + 10mL calcium chloride + 100mg collagenase + 80mg trypsin inhibitor

Once the liver tissue was received from surgery it was flushed by hand using a syringe and cold Soltran buffer to remove excess blood from the liver. The first 500mL EGTA containing buffer was used to establish a successful perfusion (shown in Figure 7-1). Once successful perfusion was established

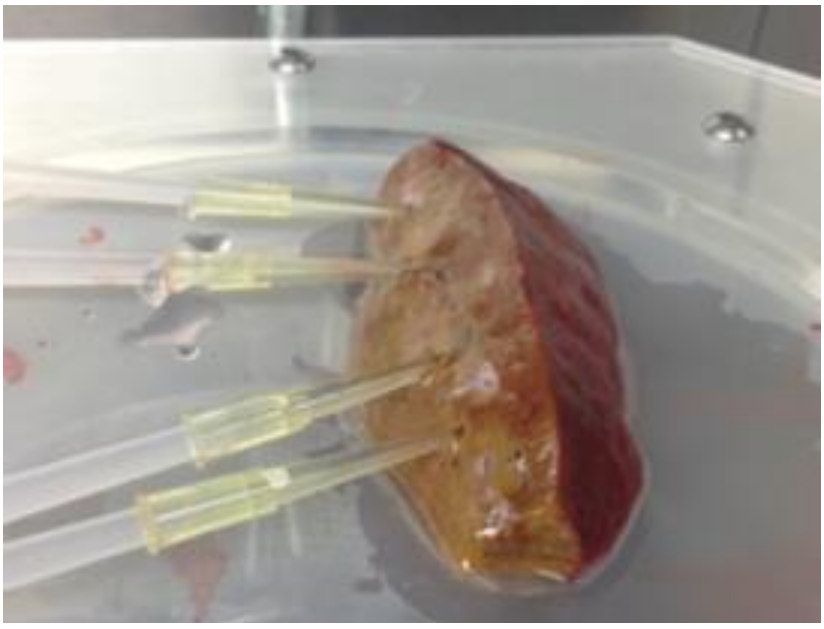

Figure 7-1: An excised piece of human liver received from a partial hepatectomy. Shown during the initial perfusion procedure.

the 1L EGTA containing buffer was used to continue the perfusion for 15-20 minutes. Some of the waste solution was sometimes used to recirculate in the perfusion (depending on the speed with which the initial solution was exhausted); the first 800mL of waste buffer was not used. The next solution used in the perfusion was the 500mL perfusion buffer without EGTA. This solution was used until it had run to waste. The final perfusion solution used was the perfusion buffer containing collagenase which was recirculated for approximately 20 minutes depending on tissue marbling and digestion efficiency. After digestion the tissue was removed and placed into perfusion buffer without EGTA and minced carefully with blunt ended scissors. The minced tissue was filtered through a 250µm and then a 100µm nylon mesh; each mesh was rinsed with HBSS after filtration. Hepatocytes were pelleted by centrifugation at 50g for 4 minutes at room temperature. The supernatant was removed and hepatocyte pellet re-suspended in serum containing culture medium. The cell suspension underwent a further centrifugation at 50g for 3 minutes at room temperature. After the supernatant was removed and the pellet re-suspended the cell suspension was filtered through a fresh 100µm mesh and centrifuged again at 50g for 3 minutes at room temperature. The removal of supernatant, re-suspension of cell pellet and centrifugation was repeated twice more. Depending on pellet size after the last centrifugation the cells were resuspended in 20-50mL serum containing culture medium and cell concentration estimated using a haemocytometer.

7.3 Hepatocyte culture conditions

Primary human and rat hepatocytes were cultured at 37°C and 5% CO_2 on collagen coated 12 or 6 well plates. Rat hepatocytes were seeded at a density of $4x10^5$ cells per well of a 12-well plate and $1x10^6$ cells per well of a 6-well plate. Human hepatocytes were seeded at $4.8x10^5$ cells per well of a 12-well plate and $1.2x10^6$ cells per well of a 6-well plate. Both were seeded in serum containing (10% Foetal Bovine Serum, PAA) Williams Medium E (US Biological Sciences, cat: W1105-05) for two hours before growth medium was changed to serum-free Williams Medium E; if the static cultures were to be compared to cultures grown in LiverChip™ they were left in serum containing medium for twelve hours so as to generate a useful comparison. All cultures were grown in 4mM glucose (Sigma, G7021), 1mM carnitine (Sigma, C0158), 5mM nicotinamide (Sigma, N3376), 8mM zinc sulphate (Sigma, Z4750), 3.8mM copper (II) sulphate (Sigma, 451657), 760nM dexamethasone (Sigma, D1756), 30nM sodium selenite (Sigma, S9133), $1.67x10^{-3}$ mg/mL transferrin (Sigma, T1428), 0.028mg/mL insulin (Sigma, I9278).

7.4 LiverChip™ hepatocyte culture

Primary human and rat hepatocytes were cultured at 37°C and 5% CO_2 in collagen coated three-dimensional scaffolds in the LiverChip™ device. They were subjected to a medium flow rate of 1µL/second. Hepatocytes were seeded at a density of $6x10^5$ cells per well in serum containing medium for a

period of twelve hours to allow attachment of the hepatocytes onto the scaffold. During the first eight hours of culture the flow direction was set to flow in the downward direction, helping to pull hepatocytes into the scaffold wells. After the initial eight hour seeding period the flow rate automatically switched to the upward direction for the remaining culture time.

7.5 Staining of primary hepatocytes with DAPI

Before staining hepatocyte nuclei with DAPI the cells need to be fixed using 4% paraformaldehyde (PFA). 4g of paraformaldehyde (P6148, Sigma) was added to 100mL phosphate buffered saline. This was then heated to approximately 70^{o}C whilst stirring until all the PFA had dissolved. Once dissolved the solution was left to cool and filtered using filter paper and stored at -20^{0}C or chilled on ice for use immediately.

To fix the hepatocytes cultured in LiverChip^{TM} the scaffold were removed from each well and placed in a fresh 24-well culture plate. To each well 500µL ice cold 4% PFA was added and incubated at room temperature for 15 minutes. After incubation the PFA solution was removed and the cells washed three times with ice cold PBS. After washing 500µL DAPI, final concentration of 0.2mg/100mL, was added and the cells incubated at room temperature for 15 minutes. Once the incubation was complete the cells were washed once more in PBS and then viewed under a fluorescent microscope (Leica DMIRB microscope with Hamamatsu ORCA-ER camera). Once staining was complete

the scaffolds containing stained primary hepatocytes were stored in PBS in a cell culture dish with a bottom formed of optical grade coverslips (ibidi, 81156).

7.6 Bromodeoxyuridine (BrdU) incorporation assay

BrdU incorporation is a technique used to investigate the proliferation that occurs over a prescribed time period by measuring the incorporation of a thymidine analogue (BrdU) into the cellular DNA of diving cells. An antibody directed towards BrdU can then be used in an enzyme-linked immunosorbent assay (ELISA) and a measure of proliferation gathered by comparison with negative and positive controls. To investigate proliferation a BrdU detection kit from Roche (catalogue no: 11 585 860 001) was used. The kit was used as described in the literature supplied with the kit. For clarity the basic steps of the BrdU assay are as follows. Incubation of the cultures to be studied with BrdU over a set period of time (24 hours unless otherwise stated) to allow incorporation. The cultures must be fixed and the DNA denatured to allow the antibody access to any incorporated BrdU. Once the cultures are fixed and denatured the BrdU is labelled with a peroxidase conjugated anti-BrdU antibody. Once labelled the peroxidase substrate solution can be added and incubated for 10 minutes. To stop the reaction 1M sulphuric acid is added to each well. The absorbance of the resulting sample solution was then read at 450nm.

7.7 Lactate production assay

The lactate production assay is based on LDH-mediated conversion of lactate to pyruvate which in the process converts NAD to NADH. The enzyme rate is quantified by following the increase in NADH at 340nm. Lactate concentrations are interpolated from a standard curve using known concentrations.

7.7.1 Reagents

Lactate Dehydrogenase, LDH (Sigma L2500, 25,000U/mL)

NAD (Sigma N7004)

80% Hydrazine hydrate (Sigma 225819)

Aqueous Glycine-EDTA-Hydrazine buffer pH 9.0

- Glycine (200mM)
- EDTA (2mM)
- 80% Hydrazine hydrate (250mM)

7.7.2 Reaction mix:

20mL glycine-EDTA-hydrazine buffer

20 U/mL LDH

3mM NAD

The absorbance at 340nm was measured immediately and again after 30 minutes. The values at 30 minutes were subtracted from the initial readings and the lactate concentration determined using the standard curve.

7.8 Urea production assay

Urea synthesis and secretion by hepatocytes is a function vital to the overall homeostasis of the body during which neurotoxic ammonia is converted to relatively non-toxic urea which can then be easily excreted by the kidneys. Urea synthesis from ammonia relies on functional mitochondria, requiring ATP and mitochondrial enzyme activity to occur successfully. The sample urea concentration was determined by interpolating the urea concentration from the OD using a set of known standards (1:2 serial dilution) ranging from 5mM to 0.3125mM.

7.8.1 Reagents

Solution 1:

120mg o-phalaldehyde (Fluoraldehyde, Pierce, 26015)

100mL 1M hydrochloric acid

Solution 2:

60mg N-Napthylethylenediamine di hydrochloride (Sigma, 2248)

0.5g tetraborate

100mL hydrochloric acid

7.8.2 Method

Immediately prior to use the reaction mix, consisting of two parts solution 2 and one part solution 1, was made up. 150µL of reaction mix was added to each well containing 25µL of culture supernatant or standard sample. After 30 minutes the absorbance was read at 550nm.

7.9 Glucose determination assay

The principle of this glucose determination assay is based on the oxidation of glucose by glucose oxidase to glucoronic acid and hydrogen peroxide. The hydrogen peroxide can then be quantified using horse radish peroxidase-linked oxidation of an acceptor to a chromogen (tetra-amino benzidine to a blue/yellow product measured at 540nm). (Neverova et al., 1994, Scaman et al., 1996)

7.9.1 Reagents

TrisHCl buffer, 1M pH 7.4

Glucose Oxidase (0.5 U/mL, Sigma G6125). Soluble in 50mM sodium acetate pH 5.1.

Horse Radish Peroxidase (HRP). (Sigma P8125 at 1 U/mL) Soluble at 0.1M PBS pH 6 or HPLC grade water.

Tetramethylbenzidine (TMB) (Sigma 860336 at 0.1mg/mL) Dissolve initially 1mg in 0.1mL DMSO.

Sulphuric acid 0.2M

Reaction mix: 5 units glucose oxidase + 10 units HRP in 10mL TrisHCl pH 7.4, then add 0.1mL TMB.

To each well of a 96 well plate 10µL of either test sample or known standard and 100µL reaction mix is added. After 30 minutes incubation at room temperature the reaction is stopped by the addition of 0.2M sulphuric acid and the absorbance read at 450nm. The glucose content of the samples is interpolated from a standard curve produced using known glucose concentrations.

7.10 RNA extraction

To isolate RNA from cells cultured in both traditional static culture and three-dimensional LiverChip™ a method using TRI Reagent (Sigma, T9424) was used. Firstly the culture medium was removed by aspiration and the cells washed briefly with PBS. To each well of a 12-well plate 350µL of TRI Reagent™ was used to lyse the cells attached to the plate. To harvest a substantial amount of RNA three wells were pooled together and the homogenates left at room temperature for five minutes to allow for complete dissociation of nucleoprotein complexes. For each millilitre of TRI-Reagent™ 0.2mL of 1-bromo-3-chloro-propane (BCP) was added to each homogenate and then mixed by vigorous shaking and overtaxing. To separate the homogenates into two phases so as to remove the protein and DNA from the

RNA phase the samples were centrifuged at 10,000g for 15 minutes at 4^{o}C, after which the upper aqueous phase (the RNA containing portion) was transferred to a fresh centrifuge tube. To precipitate the RNA from solution 0.7mL isopropanol per millilitre of TRI-Reagent^{TM} is added to each sample and either left at room temperature for 10-15 minutes or stored at -20^{o}C for processing later. To collect the RNA after precipitation the samples are centrifuges at maximum speed (17,000g) for 10 minutes at 4^{o}C. The supernatant has to be removed carefully and the pellet washed twice in absolute ethanol diluted to 75% with diethylpyrocarbonate (DEPC) treated HPLC grade water. After removing the supernatant from the final wash the residual ethanol needs to be evaporated by leaving the open tube on the bench for a few minutes. The pellet can then be dissolved in DEPC treated water and heated at 65^{o}C for 5 minutes. The next steps are to ensure that no DNA is present in the RNA samples. To do this each sample is treated with DNase to destroy any remnants of DNA that may remain in the samples. DNase (Qiagen, 79254) is added to each sample along with RDD buffer according to instructions provided with the DNase. Once the DNase step has been completed the enzyme and buffer need to be removed from solution using phenol/chloroform/isoamyl alcohol. An equal volume of this solution is added to each sample and then mixed well. The resulting mixture is then centrifuged at 10,000g for 10 minutes at 4^{o}C. AS before the upper aqueous phase (RNA containing phase) is removed into a fresh centrifuge tube. Pure RNA is precipitated by the addition of a 1/10 volume of 3M sodium acetate

(pH 5.2) and two volumes of 100% absolute ethanol. This solution is then left at room temperature for 10 minutes or stored at -20^{o}C for further processing. The precipitated RNA was then centrifuged at 17,000g at 4^{o}C for 10 minutes and the supernatant removed. Two further washes with 75% absolute ethanol dissolved in DEPC treated HPLC water follow before finally leaving the open tube on the bench to allow the remaining ethanol to evaporate before dissolving the RNA pellet in an appropriate volume of DEPC treated HPLC grade water.

7.11 Reverse transcription synthesis of cDNA from RNA

RNA was reverse transcribed to cDNA using the AffinityScript Multiple Temperature cDNA Synthesis Kit (Agilent, 200436) according to the manufacturer's instructions. A starting quantity of 500ng total RNA went into each reaction. Random Primers (Promega, C1181) were used in the reaction. Temperature and time conditions are shown in Table 7-1.

Temperature, °C	Time, minutes
65	5
Cooled to room temperature	
25	10
50	60
70	15
4	Hold

Table 7-1: Temperature and time conditions used during the rtPCR process using AffinityScript Multiple Temperature cDNA Synthesis Kit (Agilent, 200436).

7.12 Reverse transcription synthesis of DNA from miRNA

Due to the short length of mature miRNA and lack of random primer binding sites in miRNA a different method of reverse transcription to standard RNA is required. To be able to reverse transcribe all miRNAs present in the sample a polyadenylation step is required in order to add a string of adenosine bases to the 3' end of the mature miRNA; this allows a generic primer that is targeted towards the poly-A tail to bind during the next step in the process. The primer used during the reverse transcription is targeted towards the poly-A tail but also contains a unique DNA base sequence at the 5' end that is incorporated into the reverse transcribed DNA. This extra sequence allows one of the primers used during the qPCR reaction to bind to the 5' end of the DNA, the other primer is able to bind to the 3' end of the reverse transcribed DNA therefore allowing the PCR reaction to take place (Figure 7-2). An miRNA

reverse transcription and polyadenylation kit from GeneCopoeia™ (cat: AOMD-Q060) was used to synthesise DNA from miRNA according to manufacturer's instructions. 500ng of total RNA was used in each reaction.

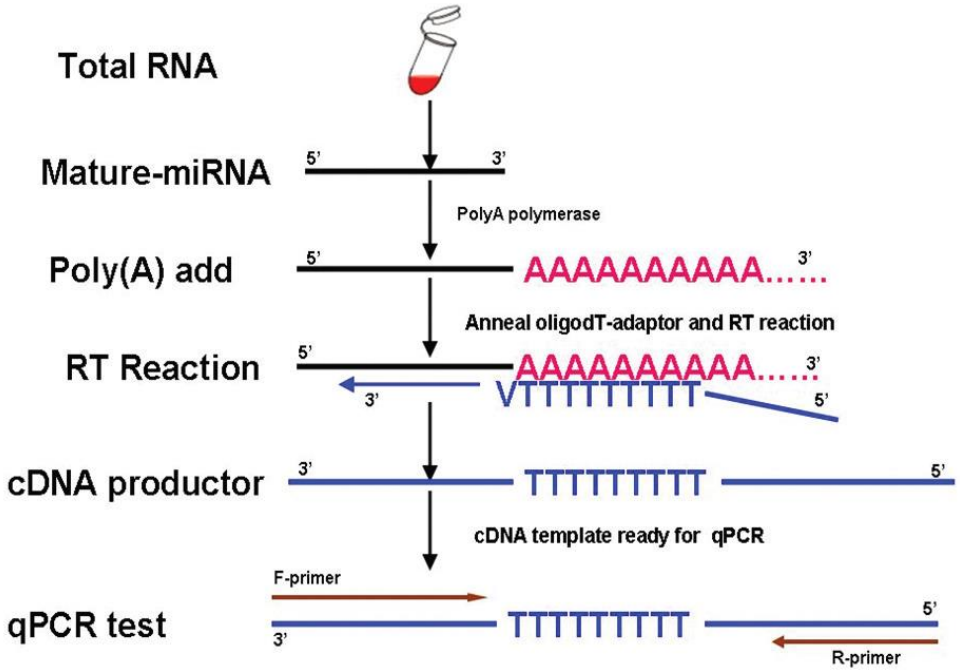

Figure 7-2: An overview of the steps involved in the 3' polyadenylation and reverse transcription of miRNA into DNA using the All-in-One™ miRNA qRT-PCR detection kit. Image taken from the GeneCopoeia™ MicroRNA Solutions brochure and application guide (http://www.genecopoeia.com/product/qpcr-mirna/).

7.13 Analysis of mRNA expression using Taqman™ semi-quantitative PCR

Expression levels of certain genes were quantified using the StepOnePlus™ real-time PCR (RT-PCR) system (Applied Biosystems). The Taqman standard curve method was used to generate reliable and repeatable mRNA expression data for each gene. The Taqman RT-PCR system uses a primer pair and probe

specific to each gene of interest; the probe is labelled with a fluorophore and quencher on each end and is designed to bind in between the forward and reverse primer pair. The fluorescent signal of the fluorophore is negated by the action of the quencher that is bound to the opposite end of the probe sequence. During the RT-PCR polymerisation/elongation step the probe is displaced from the DNA sequence and digested, releasing the fluorophore from the quencher and generating a fluorescent signal that can be detected by the system. The fluorescent intensity in each sample is measured in real-time after each round of polymerisation/elongation to generate a measure of expression levels in each sample.

To ensure accuracy and lack of contamination a non-template control (NTC), in which the cDNA template was replaced with DEPC treated HPLC grade water, was included on each plate to check for contamination of reagents. All plates where the NTC showed amplification (a very rare occurrence) of any sort were scrapped and replicated to ensure accuracy. A non-reverse transcriptase (no-RT) control was also employed to check the specificity of the primer and probe set for each gene and the lack of genomic DNA contamination. The no-RT sample was a pool of diluted RNA that underwent identical treatment to the samples without the addition of reverse transcriptase during the reverse transcription reaction. Any samples in a batch in which the no-RT showed amplification were discarded and the RNA would have undergone a clean-up procedure and fresh reverse transcription. None

of the samples tested in this thesis showed amplification in the no-RT control so no addition clean-up protocol was used.

7.13.1 Method

The Taqman standard curve method was the method used throughout due to reproducibility and reliability of the results. The gene expression of each sample is measured as the quantity present in the sample relative to a basis sample. In this case a pool of cDNA from each sample to be compared acts as the basis sample. A five point standard curve is produced by a serial 1:4 dilution of the basis sample (which has an assumed quantity of one). The relative gene expression of the test samples is determined from the corresponding standard curve and all quantities are expressed as relative to the basis sample.

Each of the samples and standards are assayed in triplicate to ensure accuracy. The threshold cycle (Ct Value) is the point at which the fluorescent intensity of the released fluorophore in a sample reaches a level above baseline at which it is considered statistically significant. A standard curve of Ct Value versus the logarithm of standard sample quantity is constructed. The standard curve produced can be used to generate a range of attributes that pertain to a variety of different parameters that help to gauge the effectiveness and accuracy of the semi-quantitative RT-PCR. The slope of the standard curve with a PCR efficiency of 100% is equal to -3.32; a curve with slope of -3.8 demonstrates an efficiency of 83%. Figure 7-3 is an example of a

standard curve with an r^2 of 0.999 and a slope of -3.37. The aim for each standard curve was to be between -3.32 and -3.6 (90-100% efficient). Any curve that fell outside this range was discarded along with any samples or plates where the triplicates for each sample had a variance of greater than 0.5 Ct Value. Cycling conditions used in the qPCR reaction are detailed in Table 7-2. Primer and probe sequences used for all genes are shown in Table 7-3.

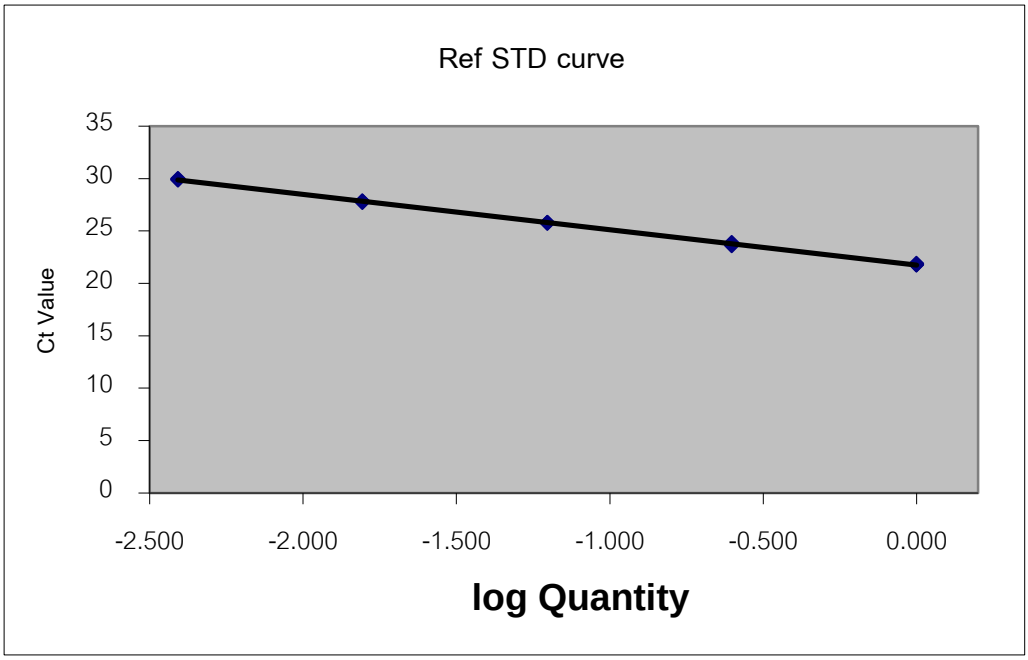

Figure 7-3: GAPDH Standard curve with slope of -3.37 and r^2 of -0.999.

Temperature, ^{O}C	Time, minutes:seconds	Instrument Detection	
95	00:20	No	
95	00.01	No	45X
60	00:20	Yes	

Table 7-2: Cycling conditions for qPCR using designed primers and probes. Blue coloured box indicates these conditions were repeated for 45 cycles to ensure amplification of target DNA.

7.13.2 Primer and probe sequences

Primer and probe sequences were designed using Primer Express 3 (Life Technologies) and checked for target gene specificity using NCBI Blast.

Gene ID	Fw Primer	Rv Primer	Probe
Rat HNF4a	AGATGAGCC-GTGTGTCCATTC	GGGTCAAAGA-AGATGATGGCTTT	CATCCTCGATGAGCTGGTCTTGCCC
Rat CAR	AGTATGGGCCA-AGGAACTGTGT	GTTCGTCTGAA-AAAGCCTTTGC	ACCGAGCCACGGGCTATCATTTCC
Rat GAPDH	TCTGCTCCTCC-CTGTTCTAGAGA	CGACCTTCACCA-TCTTGTCTATGA	ATCTTCTTGTGCAGTGCCAGCCTCGT
Hu GAPDH	CAACAGCCTC-AAGATCATCAGC	TGGCATGGACT-GTGGTCATGAG	CCTGGCCAAGGTCATCCATGACAAC
Hu HNF4a	CCCTTCCAGGAG-CTGCAGATCGATG	CTTGGCATCTG-GGTCAAAGAA	CCCTTCCAGGAGCTGCAGATCGATG
Hu CAR	TTGCTGGAAG-CTGTGAAGTCA	CGACAGTATCA-TGTCTTTCCTCATG	ACTCAGAGGCGCCACTGCCCA
Hu CYP2B6	AATACCCTCATG-TTGCAGAGAGAGT	TGCCTCTGTGT-ATGGCATTTTG	CACATCGCCCTCCAGAGCTTCATGA
Hu AJUBA	CACCGACTACCA-CAAAAATTATGC	CCATGGATATC-ACCCTCACGAT	TGTGCAGCCTGTGGCCAACCC
Hu AKR1B10	TTGCTGCAAA-GCACAAAAAAA	GACAATCACATT-CCTCTGGATATGG	CGCAGCCCAGGTTCTGATCCGTT
Hu PLOD2	GTAGATGTCCAT-CCAAACGTATCAA	TTAAGTGCTTCTT-TTGGGTAATCCA	AACCCCTTTTCTACCTCGGTTTCTGGACA
Hu ERN1	CAACATCGTTCA-CAGAGACCTAAAG	GGCCAAAGTC-GGAGATCATG	ACATCCTCATATCCATGCCCAATGCAC
Hu CYP1A1	CAAGAGGAGCT-AGACACAGTGATTG	CGGAAGGTCT-CCAGGATGAA	CGGCCCCGGCTCTCTGACAGAT
Hu PCK1	GCTGCAGAACA-TAAAGGCAAAAT	AGCCAGTGG-GCCAGGTATT	CCCTTTGCCATGCGGCCCT
Hu SLC2A2	GCTGCTCAACT-AATCACCATGCT	CATGGCTTTGAT-TCTTCCAAGTG	TGGTCCCTGTCTGTATCCAGCTTTGCAGT
Hu BHMT	CCGTGTCGA-CCACCTGTCT	GATGCCCTTC-TTGGCCTTTT	ACACCACGAAGATGCCACCCGTTG
Hu CYP7A1	GAGAAGGCAA-ACGGGTGAAC	CTCAAGAGGAT-TGGCACCAAA	ATTCCATACCTGGGCTGTGCTCTGCA
Hu GNMT	ATCATCGCAA-CTACGACCACAT	GTCCTTGGTCAAGTC-ACTCTTATAGTAGAT	CTCAGTACAGGCTGTGCACCCCCA
Hu HAO2	TGCCTTGTC-TGGCCTGATG	TGCTGGTGATGT-AGCAGATACCA	AAATGAGCACAGCAAGAGCTGCCCA
Hu PDK4 (MBG)	TCACATCGTGT-ATGTTCCTTCTCA	CCCGCATTGCAT-TCTTAAATAGT	CTCCATCATATGCTCTTT

Table 7-3: DNA sequences of primer and probes sets for specific genes used in the Taqman based qPCR reaction. Each probe was labelled with FAM fluorescent dye and TAMRA quencher.

7.14 Analysis of miRNA expression using SYBR® Green qPCR

Due to the short length of reverse transcribed miRNA sequences utilising a primer and probe set is not possible. During the reverse transcription process an extension to the 5' end of the DNA is added that contains a unique base sequence designed to complement a universal primer that is used during the PCR reaction in conjunction with a miRNA sequence specific primer. In this way it is possible to selectively amplify the target miRNA DNA sequence using only one specific primer sequence.

SYBR® Green is a dye that binds to the minor groove of double stranded DNA and fluoresces when bound and excited by a light source. It is these characteristics that make SYBR® Green quantitation less specific than using a primer pair and fluorescent probe set as SYBR® Green dye is able to bind to primer dimers and non-specific amplification. To overcome this, a melt curve analysis is required to analyse the length of amplicons produced and any other double stranded DNA present to ensure PCR specificity and a lack of primer dimers. During which the PCR products and any non-specific double stranded DNA are heated up from 65^{O}C to 95^{O}C incrementally with fluorescence measured at each temperature. Upon reaching the temperature at which the double stranded DNA product or contaminant denatures the SYBR® Green dye is released and no longer fluoresces. The major drop in fluorescence of the reaction mix should occur at the melting temperature of the specific product. If there is a large drop in fluorescence at a low melting

temperature this indicates that primer dimers may be present and any drop in fluorescence at temperatures other than the temperature of the specific product this suggests that non-specific amplification has occurred and the design of the primer pair needs to be revised.

The cycling conditions used during the SYBR® Green qPCR reaction are detailed in Table 7-4.

Temperature, ^{O}C	**Time, minutes:seconds**	**Instrument Detection**	
95	10:00	No	
95	00:10	No	X45
60	00:20	No	
72	00:15	Yes	
65-95	+0.3^{O}C/detection	Yes	Melt Curve
30	00:30	No	

Table 7-4: Amplification and melt curve cycling conditions used during SYBR® Green qPCR analysis of miRNA expression. A blue coloured box indicates the cycles were repeated 45 times to ensure amplification of target DNA sequence.

7.15 0 Affymetrix™ HTA2.0 Microarray and miRNA 4.0 Array

The Affymetrix™ HTA2.0 microarray and miRNA4.0 miRNA screen were both carried out at the Nottingham Arabidopsis Stock Centre (School of Biosciences, University of Nottingham, Sutton Bonington Campus,

Loughborough, LE12 5RD). Data analysis of the raw intensity files produced was performed in GeneSpring GX13 (Agilent Technologies Inc.).

N.B. "Log Ratio" values in all subsequent tables are taken directly from GeneSpring GX13 without any changes or manipulation. The software presents the log ratios as a positive or negative number to enable easier interpretation of the results despite the generation of negative log ratios being mathematically impossible.

8 Initial Evaluation of LiverChip™ in Culture of Primary Rat and Human Hepatocytes and direct CAR activation

8.1 Introduction

Before using the LiverChip™ system to explore direct CAR activation there was a need to ensure that the culture system supports primary rat and human hepatocyte culture. During isolation and the first 5-7 days in culture hepatocytes begin to dedifferentiate and die (Elaut et al., 2006). It is well established that under two dimensional culture conditions primary hepatocytes dedifferentiate and what follows is a substantial reduction in liver specific function (e.g. detoxification due to phase I and II enzymes and production and secretion of albumin). The loss of these functions can be seen in altered mRNA expression of phase I and II biotransformation enzymes and drug transporters (Baker et al., 2001, Elaut et al., 2006, Beigel et al., 2008). There is also significant evidence that suggests maintaining primary hepatocytes in three dimensional culture under dynamic medium flow helps to ensure cell viability and maintains a differentiated hepatic phenotype for longer (Bissell et al., 1987a, Clayton and Darnell, 1983a, Koide et al., 1989a, Matsushita et al., 1991, Tong et al., 1992, Godoy et al., 2009a, Clayton et al., 1985). Before using LiverChip™ to study direct human CAR activation the capability to support CAR mRNA expression during primary rat and human

hepatocyte culture has to be assessed. The main aim of this PhD is to study direct human CAR activation and any associated toxicological profile so the logical method uses primary human hepatocytes rather than rat hepatocytes which have been shown to illicit differing responses to nucelar receptor activation (Rusyn and Corton, 2012). Nuclear receptor sequence homology between vertebrate species is usually fairly high although CAR exhibits greater difference between species (Reschly and Krasowski, 2006, Suino et al., 2004, Xu et al., 2004) it is therefore of greater importance that a human based system is used. The system used has to be capable of culturing human hepatocytes *in vitro* that maintain an *in vivo* phenotype as closely as possible.

A hallmark of CAR activation in rodents is increased hepatocellular proliferation and eventual hepatocellular carcinoma (Yamamoto et al., 2004a, Huang et al., 2005b). To determine whether activation of hCAR is a potential cause of hepatocellular carcinoma, a culture system intended to investigate CAR activation should be capable of supporting hepatocellular proliferation. Therefore the capacity for LiverChip^{TM} to support proliferation of primary rat hepatocytes *in vitro* also needed to be verified.

Once the benefits and limitations of the culture system had been established the next step was to determine whether direct activation of CAR was possible in primary human hepatocytes cultured in LiverChip^{TM}. To determine whether CAR had been activated, the change in mRNA expression of CYP2B6 was studied. CYP2B6 expression was chosen as a marker of CAR activation as

direct and indirect activation of hCAR has been shown to upregulate the expression of CYP2B6 *in vitro* (Sueyoshi et al., 1999b). Although CYP2B6 induction has been shown *in vitro* it is unclear when the optimum activation of CAR occurs and whether this is altered in dynamic three dimensional culture. Do the gene expression changes happen immediately or over the course of a few days following repeated dosing of a CAR activator?

8.2 Aims

The main aim of this set of experiments was to isolate primary rat and human hepatocytes and seed them into LiverChip™ and static culture conditions. Once culture had been established it was important to ensure hepatic phenotype was maintained in culture so as to allow direct activation of hCAR. There was also a need to investigate the time period and interpatient variability of hCAR activation.

8.2.1 Objectives

- Isolate primary rat hepatocytes, seed into LiverChip™ and culture for seven days.
- Carry out a basic gene expression analysis of primary rat hepatocytes cultured in LiverChip™ to ascertain how well the system maintains hepatic phenotype *in vitro* (with attention to levels of CAR expression).
- Isolate primary human hepatocytes, seed into LiverChip™ and culture for seven days.

- Carry out a basic gene expression analysis to ascertain the ability of LiverChip™ to maintain hepatic phenotype *in vitro*.
- Further characterise LiverChip™ using a range of assays to check hepatic functions are supported and maintained in primary human hepatocytes cultured in LiverChip™.
- Investigate whether LiverChip™ is able to support primary rat hepatocyte proliferation.
- Determine the time-course during which CAR is activated and causes the greatest change in gene expression in primary human hepatocytes.
- Carry out a screen of patients to determine which samples to take forward to study full gene expression in response to direct CAR activation.

8.3 Experimental design and methods

The initial experiment to isolate primary rat hepatocytes and seed them into LiverChip™ was carried out according to the methods described in 7.1 (primary rat hepatocyte isolation) and 7.4 (LiverChip™ hepatocyte culture). RNA was extracted as described in 7.10 and reverse transcribed to cDNA as described in 7.11. Semi quantitative PCR (qPCR) was carried out on samples for individual genes as described in 7.13 and statistical analysis performed using Graphpad Prism 6 software. All BrdU incorporation assays were carried out according to manufacturer's instructions detailed in 7.6. HNF4α was used

as a measure of hepatic phenotype as it is a nuclear receptor implicated in the control of many liver specific genes (Eloranta et al., 2005, Tirona and Kim, 2005). Albumin gene expression was also used in human hepatocytes to give an indicator of the differentiation state of primary human hepatocytes cultured in LiverChip™ compared to static culture. Albumin expression was used as one function of hepatocytes *in vivo* is to synthesise and export albumin. It follows on from this that if the culture system is to be used to study CAR activation then the system needs to be able to maintain a level of CAR mRNA expression to allow activation. A range of metabolic assays were also employed to further characterise primary human hepatocytes in each system. Due to a lack of information regarding direct CAR activation *in vitro* the time period during which CAR is activated in response to daily repeated dosing needed to be investigated by measuring CYP2B6 induction in response to CAR agonists at different time points.

8.4 LiverChip™ maintains mRNA expression of liver specific genes in primary rat and human hepatocytes

8.4.1 Primary rat hepatocyte culture and mRNA expression in LiverChip™ compared to traditional two dimensional static culture

Primary rat hepatocytes were isolated and seeded into LiverChip™ and traditional 2D static culture in serum containing Williams E medium (see section 7.3 and 7.4) for 12 hours. After 12 hours, serum containing medium

was removed and the cells were cultured in serum free Williams E medium; this was replaced with fresh serum free medium after every 24 hours in culture and repeated for up to 7 days. Before carrying out any gene expression studies it was necessary to ensure that rat hepatocytes could actually be seeded into LiverChip™ successfully. Two scaffolds were removed and stained with DAPI (see section 7.5) 72 hours after removing serum free medium. The resulting image is shown in Figure 8-1. The fluorescent image shows two representative scaffolds, each seeded with primary rat hepatocytes for 72 hours, one of which shows a completely filled scaffold channel and the other showing a partially filled scaffold channel.

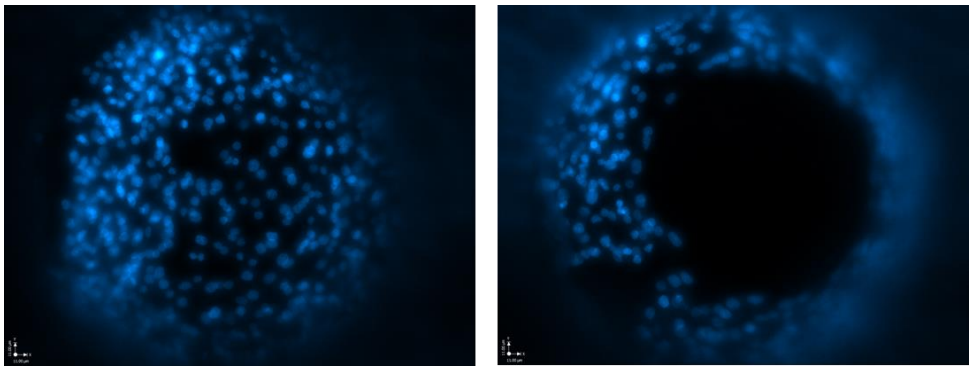

Figure 8-1: Primary rat hepatocytes cultured in two separate scaffolds in LiverChip™ after 72 hours, stained by incubation with DAPI post fixation with paraformaldehyde. Scale bar = 11μm.

These images are a representative example of the majority of channels in scaffolds seeded with primary rat hepatocytes. In each scaffold well the cells are able to grow in a three dimensional structure which can be seen in the images. These images give confidence in the seeding technique and enable

the meaningful study of gene expression profiles of primary rat and human hepatocytes.

Following the initial seeding and culture of primary rat hepatocytes the basic gene expression profile was investigated. The genes investigated were HNF4α and CAR for reasons discussed previously. Figure 8-2 is a graphical representation of the HNF4α and CAR expression profile of primary rat hepatocytes cultured in LiverChip™ and traditional 2D static conditions after 7 days in culture compared to fresh liver tissue pre-hepatocyte isolation normalised to glyceraldehyde 3-phosphate dehydrogenase (GAPDH). During the first seven days in culture it is clear that primary rat hepatocytes begin to lose expression of HNF4α. There is less reduction when culturing primary rat hepatocytes in LiverChip™, this indicates an *in vitro* cellular phenotype that more closely resembles the *in vivo* phenotype after seven days *in vitro*. The reduction in CAR expression compared to HNF4α is greater in both static and LiverChip™. However, the expression levels of CAR are marginally better in LiverChip™ than two dimensional static culture; potentially highlighting an advantage of using LiverChip™ over tradition two dimensional static culture.

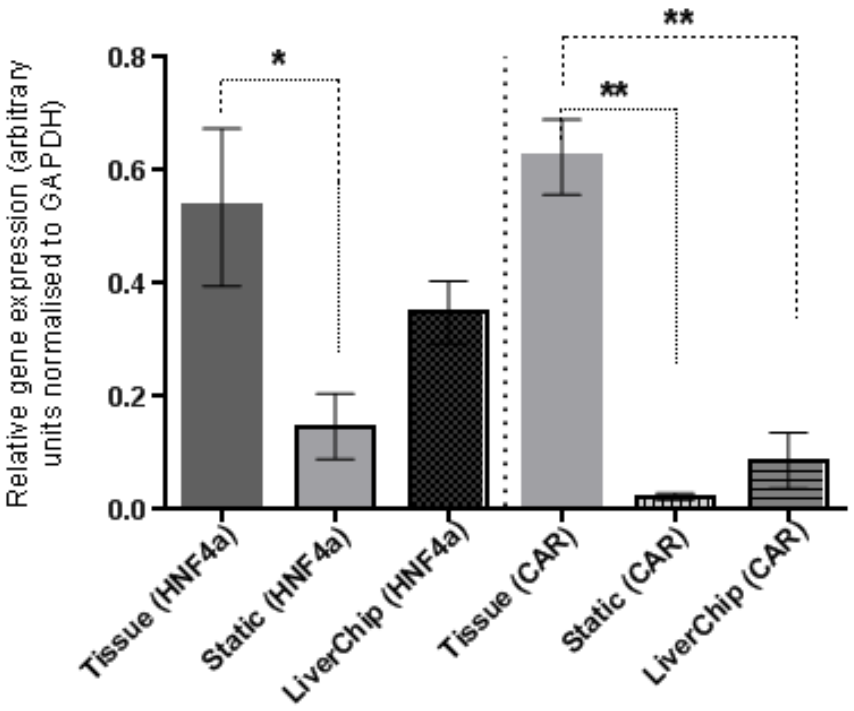

Figure 8-2: HNF4a and Constitutive Androstane Receptor (CAR) gene expression in rat tissue pre hepatocyte isolation compared to primary rat hepatocytes in traditional 2D culture and LiverChip™ after 7 days. Gene expression carried out using the StepOnePlus™- qPCR system. N=4 rats, one way ANOVA * = $p < 0.05$, ** = $p < 0.01$. Data are displayed as mean +/- SEM

After the brief initial study looking at primary rat hepatocytes cultured in LiverChip™ compared to static culture the next step was to study primary human hepatocytes under the same conditions.

8.4.2 Primary human hepatocyte culture, mRNA expression and metabolic assays in LiverChip™ compared to traditional two dimensional static culture

Primary human hepatocytes (obtained with full ethical approval from patients undergoing partial hepatectomy via Nottingham University Hospitals Trust NHS BioBank) were isolated and seeded into LiverChip™ and traditional 2D

static culture in serum containing Williams E medium (see sections 7.2, 7.3 and 7.4) for 12 hours. After 12 hours, serum containing medium was removed and the cells were cultured in serum free Williams E medium; this was replaced with fresh serum free medium after every 24 hours in culture and repeated for up to 7 days. RNA was extracted using TriReagent™ as detailed in section 7.10 at specific time points then reverse transcribed into DNA as specified in section 7.11. mRNA expression was quantified using Taqman™ qPCR (see section 7.13 for details). RNA was extracted from hepatocytes grown in two dimensional culture every 24 hours during the first 72 hours of culture and from both static and LiverChip™ after 7 days in culture. The aim here was to confirm that the results shown with primary rat hepatocytes were consistent in primary human hepatocytes. To investigate the ability of LiverChip™ to maintain primary human hepatic phenotype *in vitro* the expression of a selection of hepatic specific genes was investigated. CAR mRNA expression was also investigated for the reasons detailed in section 8.4.1. As an extra marker of hepatic function albumin expression was also investigated. Further investigation into the basic metabolic and hepatic phenotype was also carried out using a suite of biochemical assays to obtain a more detailed overview of primary human hepatocytes in LiverChip™.

The first hurdle to overcome when assessing gene expression in primary human hepatocytes was in finding a suitable reference gene that did not vary greatly in expression (≈2 CT) between samples. Finding a reference gene that

is consistent across all samples, including freshly isolated hepatocytes, is almost impossible due to the large stress induced by the isolation procedure. A common reference gene used to normalise gene expression data is β actin. A decision was made to avoid using this as the differences in cell structure and cytoskeleton between freshly isolated cells, hepatocytes cultured in traditional two dimensional culture and those cultured in LiverChip™ are likely to be large. It was for this reason that 18S RNA was chosen as a potential reference gene initially.

When 18S expression across all samples was investigated it was found that the CT values all fall between 13.5 and 14.6 cycles (Figure 8-3). The small differences in CT value between samples show that 18S is a reference gene that can be used to normalise future expression data for this study in primary human hepatocytes.

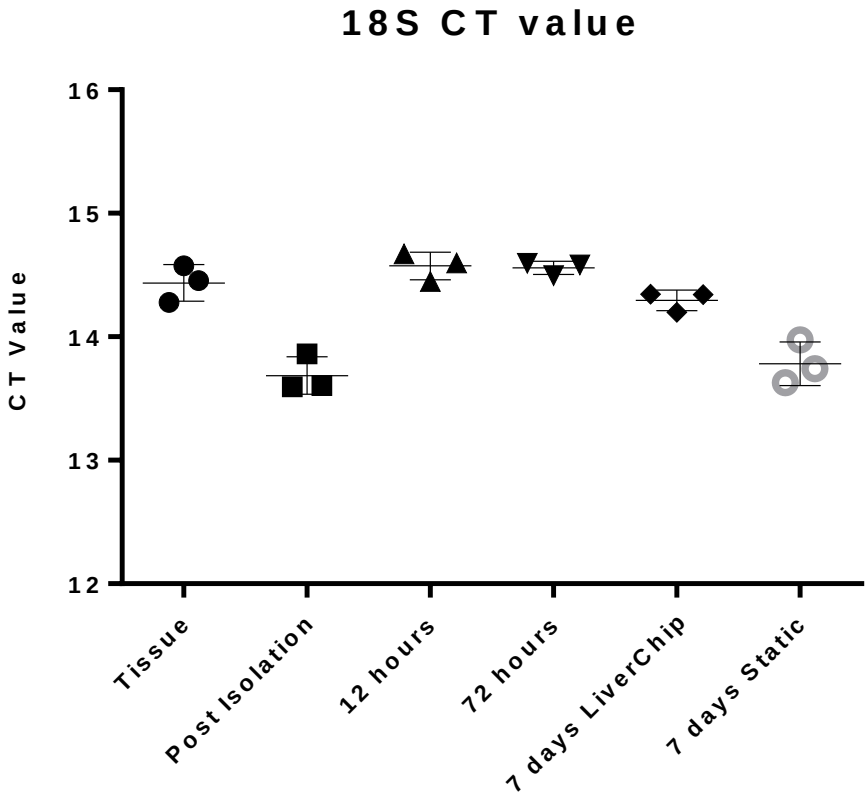

Figure 8-3: Cycle threshold (CT) values for 18S across samples of primary human hepatocytes cultured in traditional static culture and LiverChip^{TM} compared to post isolation hepatocytes and fresh tissue. N=3 technical repeat, Data are displayed as mean +/- SEM.

Having settled on using 18S as a reference gene the mRNA expression profiles of HNF4α, CAR and albumin were studied.

HNF4α gene expression as shown in Figure 8-4 indicates that upon isolation hepatocytes undergo a period of stress and readjustment to the new culture conditions over the first 72 hours. This is unsurprising given the large change in environment that the cells undergo. This finding is consistent with other experiments from our lab (data not shown) in both rat and human primary hepatocytes. During the isolation procedure gene expression of HNF4α drops but within 12 hours the expression level of HNF4α has returned to pre isolation levels. The expression profile then shows HNF4α expression as increasing to a maximum at 72 hours indicating that the hepatocytes are beginning to recover and maintain the hepatic phenotype. Between 72 hours and seven days the level of HNF4α expression begins to drop in both static and LiverChip^{TM}. Primary human hepatocytes cultured in LiverChip^{TM} maintain HNF4α expression marginally better than those cultured in traditional static culture although the difference does not reach significance.

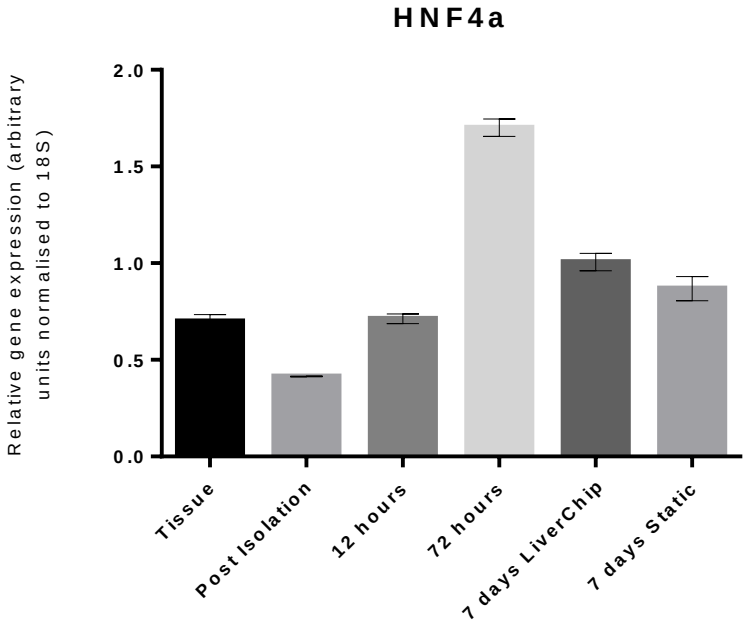

Figure 8-4: mRNA expression of HNF4α in primary human hepatocytes over the course of 7 days in static culture and LiverChip™. RNA was isolated from static cultures at specific time points in static culture and from both static and LiverChip™ at 7 days. N=3 patients. Data are displayed as mean +/- SEM.)

The expression pattern of CAR (Figure 8-5) in static culture and LiverChip™ follows a similar pattern to that of HNF4α. There are a few significant differences between the two gene expression profiles though. The initial loss of CAR mRNA expression during isolation is not as great as HNF4α; however the levels of CAR expression drop significantly over the course of the first 12 hours. After this initial drop the expression level Figure 8-5 begins to return to normal at 72 hours and then fall again when the cells are cultured in traditional static culture. This recovery after isolation and seeding and subsequent fall again is consistent, albeit with the initial fall slightly delayed, with the gene expression profile observed for HNF4α. During the period after

the initial drop in CAR expression, between 72 hours and 7 days, culturing primary human hepatocytes in LiverChip™ has a positive impact on the expression of CAR. The level of CAR expression is reduced from levels observed in fresh tissue but has not fallen as far as those hepatocytes cultured in static culture. This highlights a benefit that using LiverChip™ for the study of direct CAR activation has over using the traditional static two dimensional method of culturing primary hepatocytes.

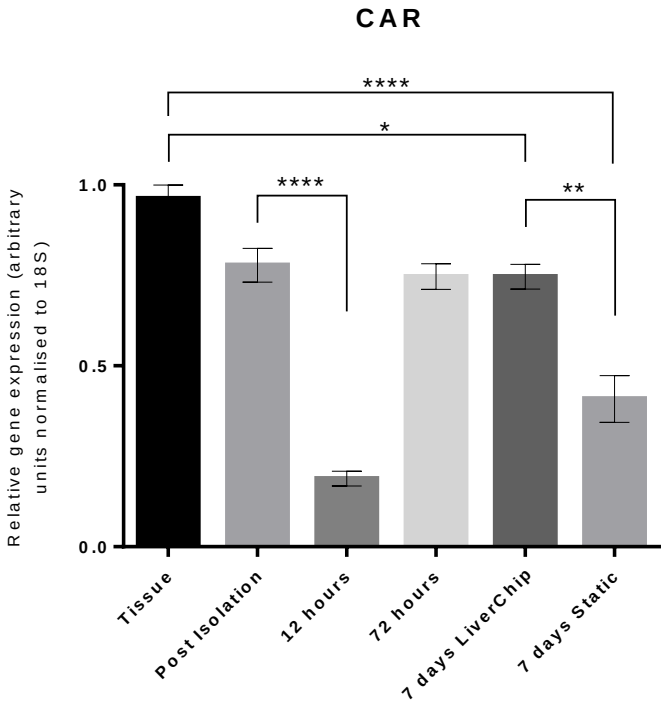

Figure 8-5: mRNA expression of constitutive androstane receptor in primary human hepatocytes over the course of 7 days in static culture and LiverChip™. RNA was isolated from static cultures at specific time points in static culture and from both static and LiverChip™ at 7 days. (**** = $p < 0.0001$, ** = $p < 0.01$, * = $p < 0.05$, one way ANOVA. N=3 patients). Data are displayed as mean =/- SEM.

The third gene expression profile investigated was that of albumin (Figure 8-6). Albumin expression in primary human hepatocytes cultured *in vitro* shows a differing gene expression pattern to both HNF4α and CAR. Rather than undergoing an initial dip in expression levels the expression of albumin mRNA remains at a level consistent with fresh tissue. Albumin expression undergoes a steady reduction between 12 hours and 72 hours. This drop in expression continues in static culture to 7 days. The primary human hepatocytes cultured in LiverChip™ do not show the same reduction in albumin expression at 7 days. This finding adds weight to the hypothesis that LiverChip™ helps to maintain primary human hepatocyte phenotype for longer.

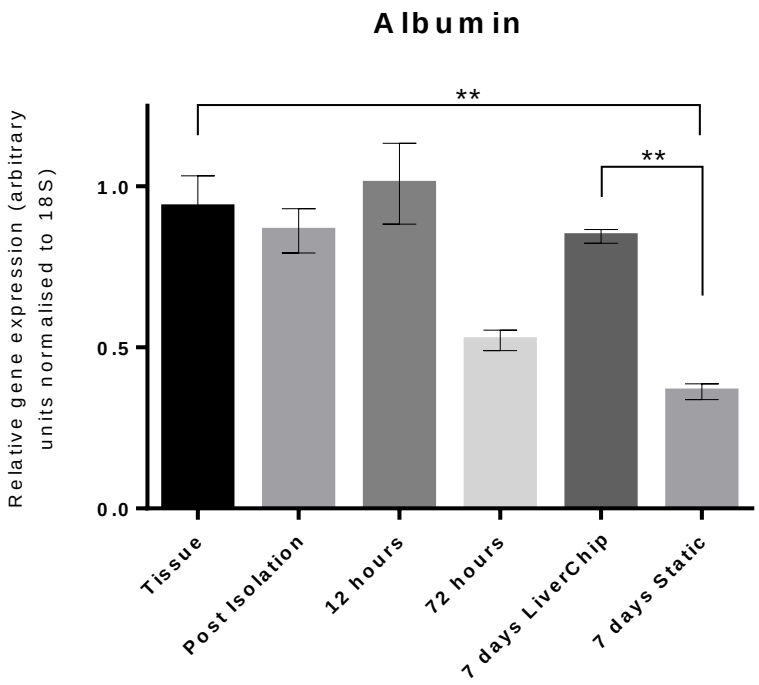

Figure 8-6: mRNA expression of albumin in primary human hepatocytes over the course of 7 days in static culture and LiverChip™. RNA was isolated from static cultures at specific time

points in static culture and from both static and LiverChip™ at 7 days. (** = $p < 0.01$, one way ANOVA. N=3 patients) Data are displayed as mean +/- SEM.

The evidence gained in these experiments indicates that primary human hepatocytes cultured in dynamic three dimensional conditions maintain a more hepatic like phenotype than those cultured in traditional static culture. To gain further insight as to the state of primary human hepatocytes cultured in LiverChip™ a range of assays were carried out. The assays carried out were urea production, as a marker of hepatocyte function, glucose uptake from medium and lactate production.

The data displayed in Figure 8-7 are the results gained from each assay on the same isolation of primary human hepatocytes. When examining the lactate concentration in the medium it is clear that primary human hepatocytes cultured in LiverChip™ produce less lactate than those in static culture. Lactate production is a product of anaerobic metabolism of glucose during glycolysis. This process does not require the use of the mitochondria and is often associated with immortalised cell lines (Mulukutla et al., 2010, Vazquez et al., 2010). During cell line culture a high concentration of glucose is often used as the growth medium due to the reliance of these cells on glycolysis rather than the full aerobic energy production cycle utilising mitochondrial proteins. For an *in vitro* system designed to test toxicity and direct activation of CAR it would be beneficial to have a system whereby the primary human cells to be studied underwent cellular metabolic processes as similar to the *in*

vivo environment as possible, e.g. utilising the full aerobic energy production pathway including the TCA cycle and therefore bypassing production of lactate. The lactate production shown in Figure 8-7 of primary human hepatocytes cultured in both LiverChip™ and static shows that when cultured in static the hepatocytes produce a larger amount of lactate per cell than those cultured in LiverChip™. This indicates that the hepatocytes grown in LiverChip™ are prioritising the mitochondrial TCA cycle as a method of producing energy as opposed to the incomplete metabolism of glucose during glycolysis.

Despite producing less lactate when cultured in LiverChip™ human hepatocytes also consume more glucose than those cultured in static culture. A probable reason for this could be that the hepatocytes cultured in LiverChip™ demand more energy to help maintain *in vivo* like hepatic phenotype in a system that, whilst mimicking the *in vivo* environment closer than static culture, doesn't represent an identical setting to that experienced *in vivo*. Having said that, it is clear from the results gained from sampling urea production in the medium that human hepatocytes cultured in LiverChip™ do not synthesise as much urea as those cultured in static culture. Urea synthesis and export is a process that hepatocytes are responsible for *in vivo*. During this process highly toxic ammonia is converted to relatively non-toxic urea which can then be excreted easily by the kidneys. Despite this the levels of

urea production do begin to rise after 72 hours in culture, suggesting that there is capacity to improve over a longer time period.

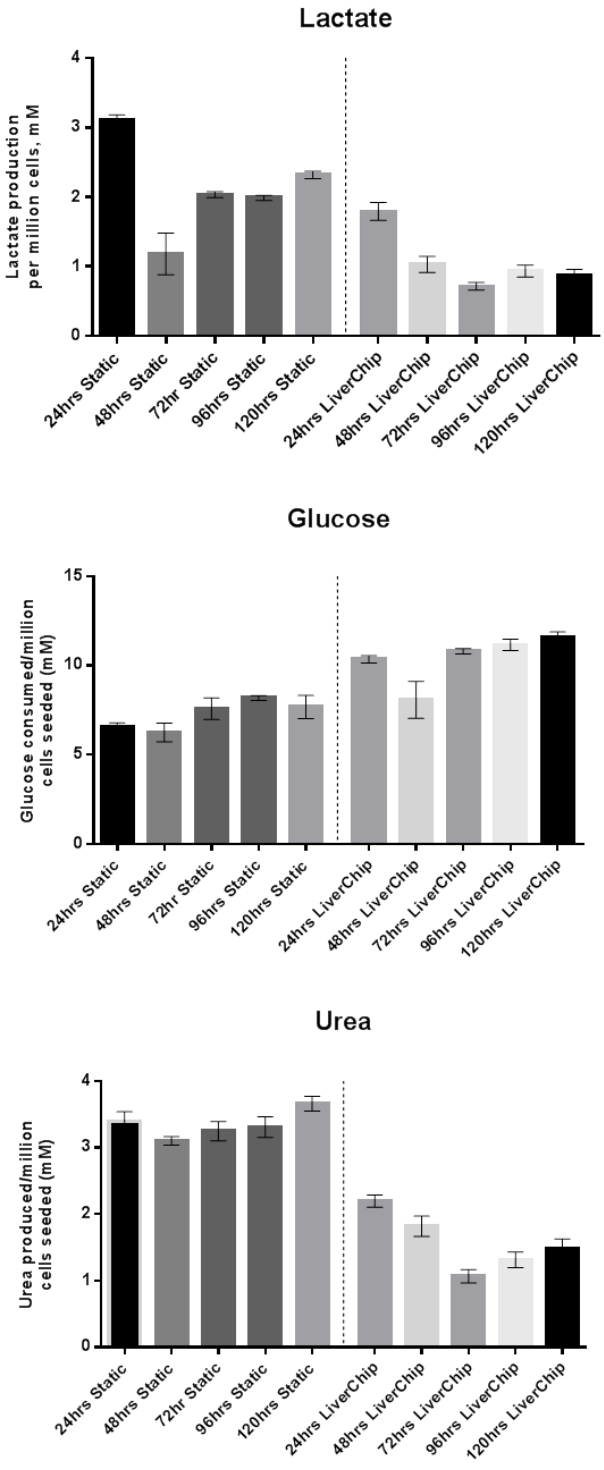

Figure 8-7: Primary human hepatocytes cultured in either LiverChip™ or static for up to 5 days. Lactate, glucose and urea content of medium supernatants was measured every 24 hours. Concentrations were normalised against cell seeding number and presented per million cells. N = 6 technical repeats. Data are displayed as mean +/- SEM

Activation of rodent CAR *in vivo* leads to hepatocellular proliferation and eventual hepatocarcinoma (Huang et al., 2005b, Yamamoto et al., 2004a). Whilst there is little evidence that this is the case in the human liver it is important that any culture system used to study the toxicological profile associated with direct activation of human CAR is able to support proliferation. The following section details an experiment used to evaluate the ability of LiverChip™ to support proliferation of primary rat hepatocytes *in vitro* in response to epidermal growth factor (EGF) and phenobarbital (PB) treatment.

8.5 LiverChip™ supports primary rat hepatocyte proliferation

It is important that any system used to study potential hepatotoxicity is capable of supporting proliferation. This experiment aimed to test whether LiverChip™ was capable of supporting hepatocyte proliferation; particularly proliferation of primary rat hepatocytes in response to dosing with phenobarbital (PB). PB is an indirect CAR activator that has been shown to be pro-proliferative in rodents *in vivo* (Whysner et al., 1996). Therefore it serves as a good test of whether the *in vitro* system of primary rat hepatocytes cultured in LiverChip™ coupled with a BrdU incorporation assay is able to detect proliferation when exposed to CAR activation. Treating primary rat hepatocytes with PB is a more realistic example of the proliferation that may occur in response to direct CAR activation in primary human hepatocytes

compared with using other pro-proliferative compounds such as epidermal growth factor (EGF) or liver growth factor (LGF). These compounds are likely to have a much larger proliferative effect than PB; therefore the sensitivity needed to detect proliferation is reduced when these compounds are used compared to PB induced proliferation.

Primary rat hepatocytes were isolated according to methods described in section 7.1 and cultured in static and LiverChip^{TM} (sections 7.3 and 7.4). Hepatocytes were dosed with EGF (50ng/mL) or 100µM PB. Medium was changed daily and BrdU was included for the final 24 hours of culture for each time point, e.g. BrdU was included between 24 and 48 hours for the 48 hour time point.

After treatment with EGF it is clear in Figure 8-8 that primary rat hepatocytes proliferate in both static and LiverChip^{TM} at 24, 48 and 72 hours demonstrating that the BrdU incorporation assay is possible in LiverChip^{TM} and that primary hepatocytes have the ability to proliferate in both static and LiverChip^{TM}. When looking at the proliferation data produced by treating with PB it is clear that any proliferative response to this treatment is small in comparison to that observed with EGF. An advantage of using LiverChip^{TM} to study CAR mediated proliferation is the ability for it to support proliferation due to CAR activation during the first 24 hours of culture. This allows LiverChip^{TM} to pick up any early stage and immediate proliferative responses that would be missed when using static culture. During the course of culture

and treatment there is consistently high EGF mediated proliferation and a low level of PB mediated proliferation in both static and LiverChip™, these data provide additional support for the use of LiverChip™ in the study of potentially hepatotoxic and hepatoproliferative direct human CAR activation.

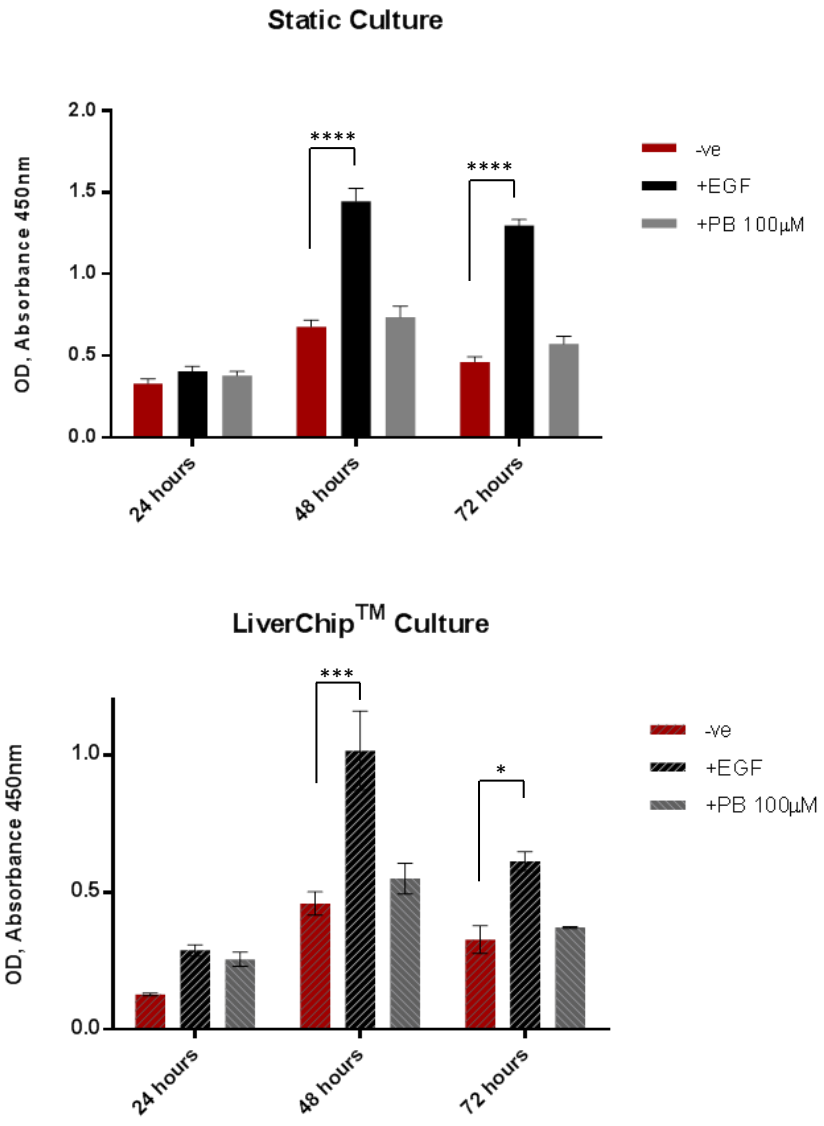

Figure 8-8: Primary rat hepatocytes cultured in static culture and LiverChip™ dosed with either 100µM phenobarbital (PB) or 50ng/mL epidermal growth factor (EGF). Proliferation measured using BrdU incorporation over the final 24 hours of culture at each time point. N = 4 rats. **** = $p < 0.001$, *** = $p < 0.005$, * = $p < 0.05$, one way ANOVA. Data are displayed as mean +/- SEM.

8.6 The optimum time-period for direct activation of hCAR

Despite the wide array of data available when investigating rat CAR activation there is little in the way of *in vitro* data detailing at what time point in culture direct human CAR activation affects gene expression. There was also a need to understand when direct hCAR activation occurs in LiverChip™ upon treatment with a direct activator as this culture system hadn't been used to study CAR activation. Until relatively recently a specific and direct hCAR activating ligand was unavailable. PB doesn't directly bind hCAR (Moore et al., 2000) but does cause translocation to the nucleus (Honkakoski et al., 1998, Kawamoto et al., 1999, Sueyoshi et al., 1999a) where the intrinsic activity of hCAR can cause a change in gene expression. Furthermore PB has also been shown to act on PXR (Moore et al., 2000) and may cause some gene expression changes due to changes in phosphorylation state of PXR inside the cell (Ueda et al., 2002). This background led to the need for a novel direct hCAR activator. Using a range of *in vitro* techniques Maglich et al (Maglich et al., 2003) were able to identify CITCO as a potent, selective hCAR activator. CITCO was found to be selective towards CAR over PXR and was found to bind directly to hCAR and induce the expression of the CAR dependent cytochrome p450 CYP2B6 *in vitro*. Despite this there was still a need to investigate the ideal time period for hCAR activation in our culture system.

Primary human hepatocytes were isolated according to the methods described in section 7.2 and cultured as described in sections 7.3 and 7.4.

Hepatocytes were treated with CITCO (100nM) and re-treated every 24 hours along with the medium change. The first attempt to activate hCAR in primary human hepatocytes was run over the course of 5 days with RNA extracted (see section 7.10) after every 24 hour period in static and LiverChip^{TM}. RNA was then reverse transcribed into cDNA and gene expression measured using Taqman qPCR (sections 7.11 and 7.13).

Initially the time points chosen to sample for CAR activation were 24 hours, 72 hours and 120 hours. The rationale being that it is possible hCAR direct activation could be rapid but sustained or it could a single event at some point in the culture period. By sampling in this way it was hoped that activation would be picked up during at least one 24 hour period.

At 24 hours there was significant ($p < 0.005$) hCAR activation according to CYP2B6 mRNA expression (Figure 8-9). The induction of CYP2B6 was smaller than that observed at both 72 hours in LiverChip^{TM} and 120 hours in both static and LiverChip^{TM}. CYP2B6 mRNA expression at 72 hours was significantly ($p < 0.001$) upregulated upon treatment with CITCO in LiverChip^{TM} but not static. The final time point investigated in this experiment was 120 hours. CYP2B6 mRNA expression at this point was significantly ($p < 0.001$) up-regulated in both static and LiverChip^{TM}, although the up-regulation in hepatocytes cultured in LiverChip^{TM} was more pronounced than that in static. On the evidence of Figure 8-9 it seemed that CYP2B6 up-regulation due to CITCO treatment was increasing between 24 hours and 120 hours; because of

this the culture time was be extended to 7 days to see whether the trend continued past 120 hours and CYP2B6 mRNA induction became more pronounced.

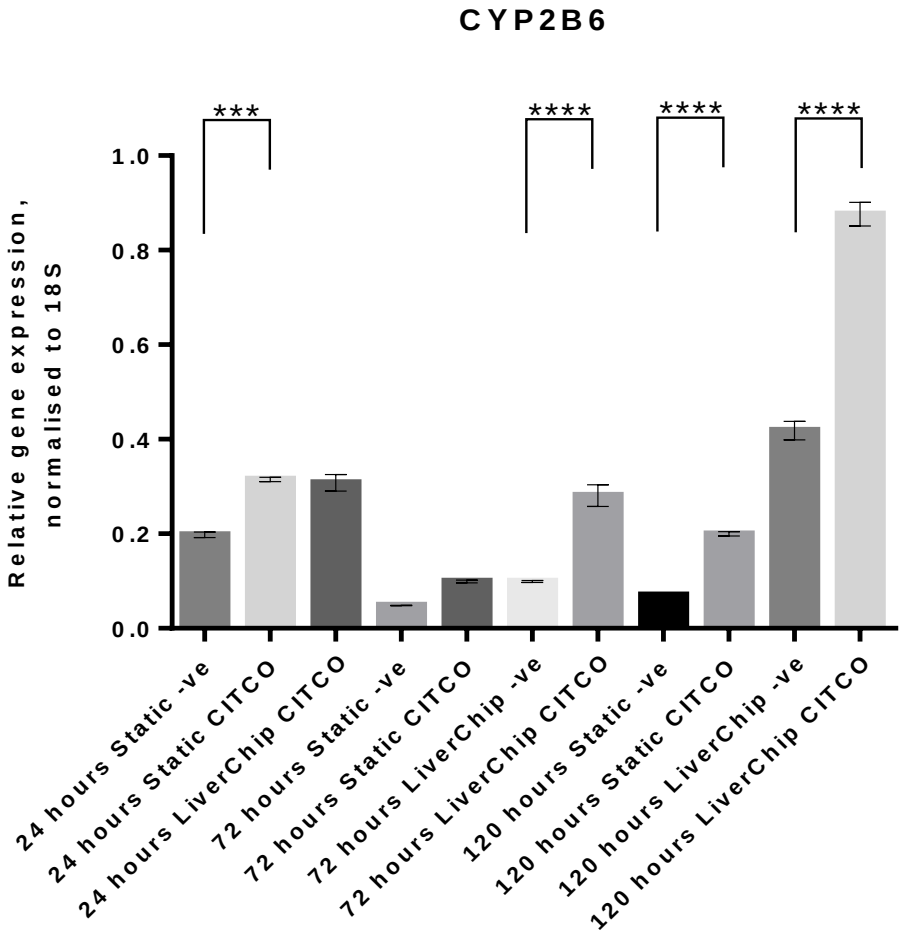

Figure 8-9: mRNA expression of CYP2B6 in primary human hepatocytes (patient L220) cultured in static and LiverChip^{TM} treated with CITCO. N = 4 technical repeats. *** = $p < 0.0001$, one way ANOVA with Bonferroni's multiple comparisons test. Data are displayed as mean +/- SEM

Data analysis showed that the trend of CYB2B6 induction upon treatment with CITCO (Figure 8-10) continued to 7 days when hepatocytes were cultured in

LiverChip™. Although this looked promising, when the fold change compared to DMSO control was examined (Figure 8-11) it became clear that the biggest change in CYP2B6 mRNA expression, and therefore induction due to CAR activation, was at 5 days. Hepatocytes cultured in static retained a similarly positive fold change in CYP2B6 mRNA expression when treated with CITCO; however this was relative to a low baseline level in the DMSO control as shown in Figure 8-10.

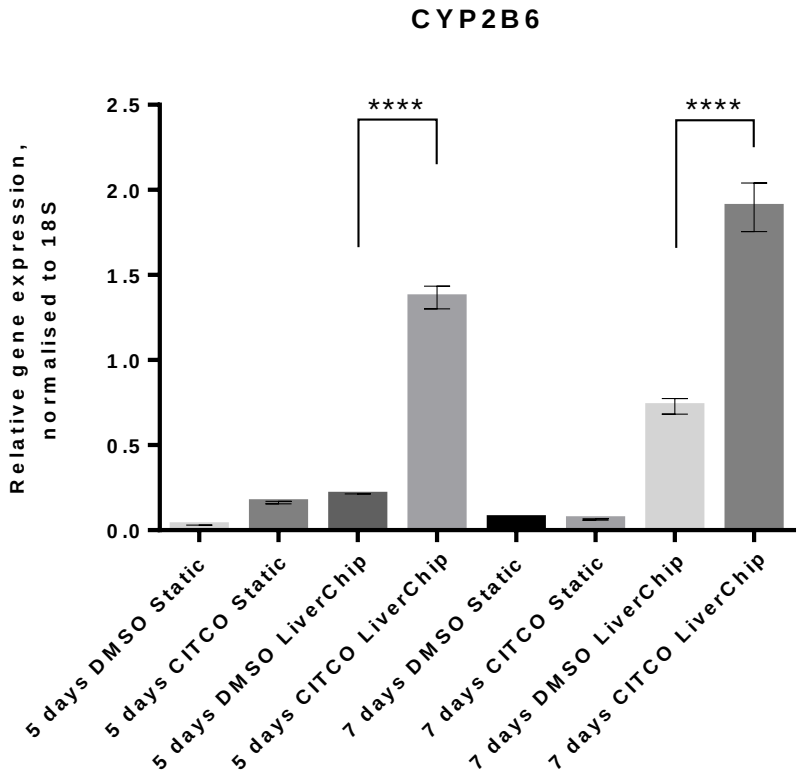

Figure 8-10: mRNA expression of CYP2B6 in primary human hepatocytes (patient L221) cultured in static and LiverChip™ treated with CITCO or DMSO control. **** = $p < 0.001$, one way ANOVA with Bonferroni's multiple comparisons test. N = 4 technical repeats. Data are displayed as mean +/- SEM.

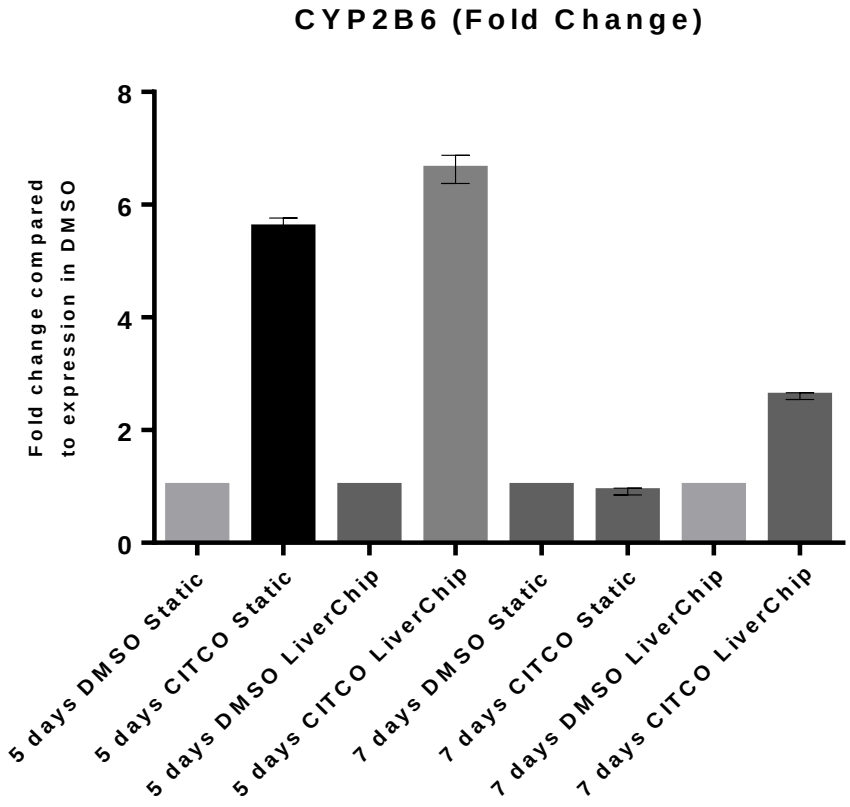

Figure 8-11: Fold change in CYP2B6 mRNA expression in primary human hepatocytes (patient L221) cultured in static and LiverChip™ treated with CITCO or DMSO control. N = 4 technical repeats. Data are displayed as mean +/- SEM.

From the results gained in this experiment it was clear that CYP2B6 induction was at its greatest at 5 days when compared to other time points. It is for this reason that treatment with CITCO was carried out up to 5 days and RNA sampled at the end of 5 days *in vitro* culture. When examining the data for CYP2B6 induction at 24 hours it became clear that there was a small increase in mRNA expression. For this reason the hypothesis that there may be important small scale gene expression changes occurring during the first 24 hours of direct hCAR activation was formed. The increase in CYP2B6 induction

upon repeated dosing and sustained direct hCAR activation up to 5 days suggests that there may be a more large scale change in gene expression during the repeated dosing of CITCO; either as a result of the initial changes caused by hCAR activation during the first 24 hours being sustained over a period of time or as a result of repeated dosing and activation of hCAR. The time points that became the focus of the remainder of this work were 24 hours and 5 days as these offered the chance to investigate the early onset changes in gene expression and what effect repeated dosing and activation of hCAR had on gene expression. Prior to carrying out microarray analysis to investigate wholescale gene expression at 24 hours and 5 days the samples to be studied needed to be generated. This involved a study to discover what the level of variance in hCAR activation and CYP2B6 induction due to individual donors was.

8.7 Patient screen to generate samples for further analysis

Before carrying out a whole genome microarray there is an added layer of complexity that cannot be ignored, inter-patient variability. It is an inevitable fact that when dealing with primary human hepatocytes, or many other primary cell/tissue types for that matter, from different donors there is potential for large inter-patient variability. When carrying out previous experimental work using human tissue as a starting material our lab has found that there can sometimes be large variations in response between patients.

As a study into the potential toxicological effects of hCAR activation the most interesting samples will derive from the donors that respond robustly to direct activation of CAR. Therefore there was a need to determine which patients responded in the most robust way to direct hCAR activation to allow any gene expression changes to be unmasked.

As discussed in the previous section two time points were studied to investigate direct hCAR activation, 24 hours and 5 days. The first patient sample tested consisted of hepatocytes isolated from patient L225 and treated with CITCO for 24 hours. CYP2B6 expression was examined as a marker of hCAR activation (Figure 8-12). Patient L225 responded to CITCO treatment with a significant (Static: $p < 0.05$, LiverChip^{TM}: $p < 0.01$) induction of CYP2B6 mRNA expression in both static and LiverChip^{TM} demonstrating that hCAR activation had taken place. These samples were taken forward to microarray and miRNA array.

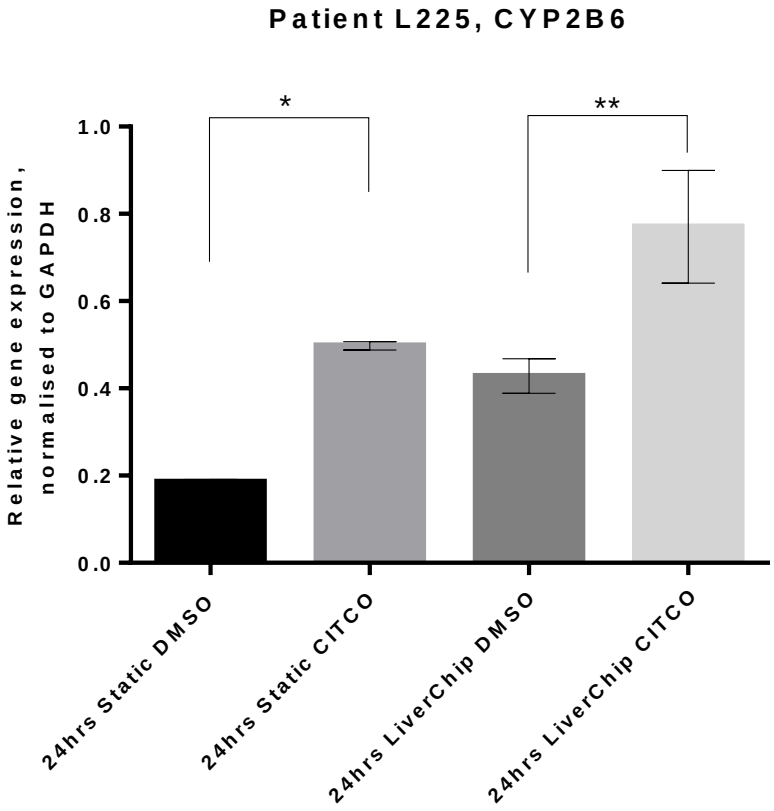

Figure 8-12: Primary human hepatocytes isolated from patient L225 treated with CITCO or DMSO control for 24 hours. RNA was extracted and CYP2B6 mRNA expression examined. N = 4 technical repeats. * = $p < 0.05$, ** = $p < 0.01$, one way ANOVA with Bonferroni's multiple comparison test. Data are displayed as mean +/- SEM.

The second patient, L233 shown in Figure 8-13, showed significant ($p < 0.001$) CYP2B6 induction upon treatment with CITCO when hepatocytes were cultured in LiverChip^{TM}. Whilst there did appear to be an increase in CYP2B6 mRNA expression when hepatocytes cultured in static were treated with CITCO it was not significant.

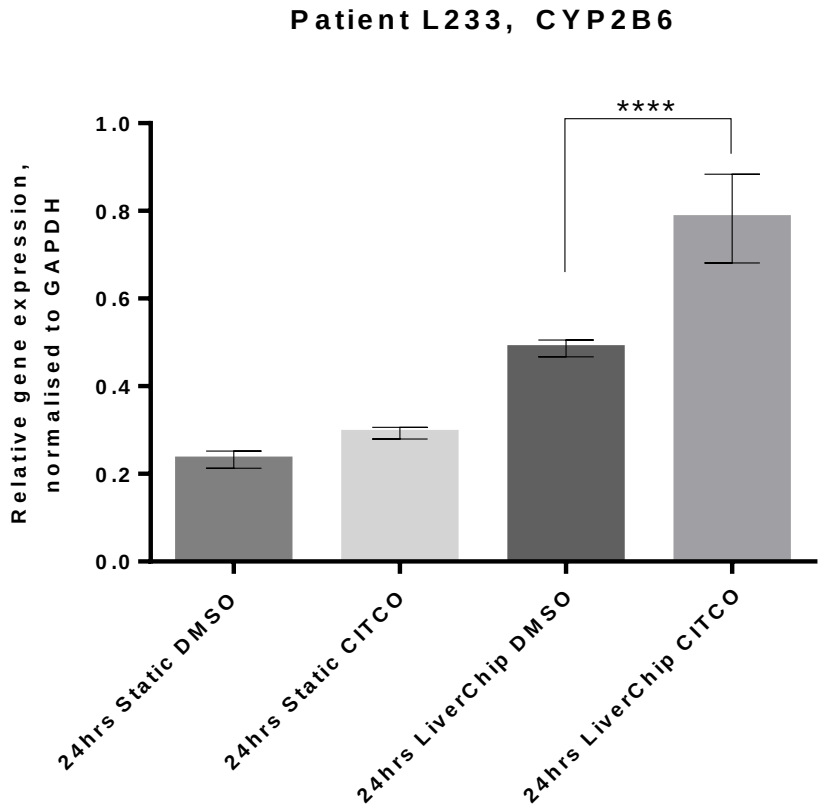

Figure 8-13: Primary human hepatocytes isolated from patient L233 treated with CITCO or DMSO control for 24 hours. RNA was extracted and CYP2B6 mRNA expression examined. N = 4 technical repeats. **** = $p < 0.001$, one way ANOVA with Bonferroni's multiple comparison test. Data are displayed as mean +/- SEM.

To determine whether this may have been as a result of lower expression levels of CAR in hepatocytes from L233 cultured in static the mRNA expression of CAR was investigated (Figure 8-14). There was a difference in CAR expression between hepatocytes cultured in LiverChip™ compared to those cultured in static. Hepatocytes cultured in LiverChip™ maintained a higher level of CAR gene expression compared to those cultured in static culture. This

could provide an explanation as to why there was no significant induction of CYP2B6 in hepatocytes from patient L233 cultured in static.

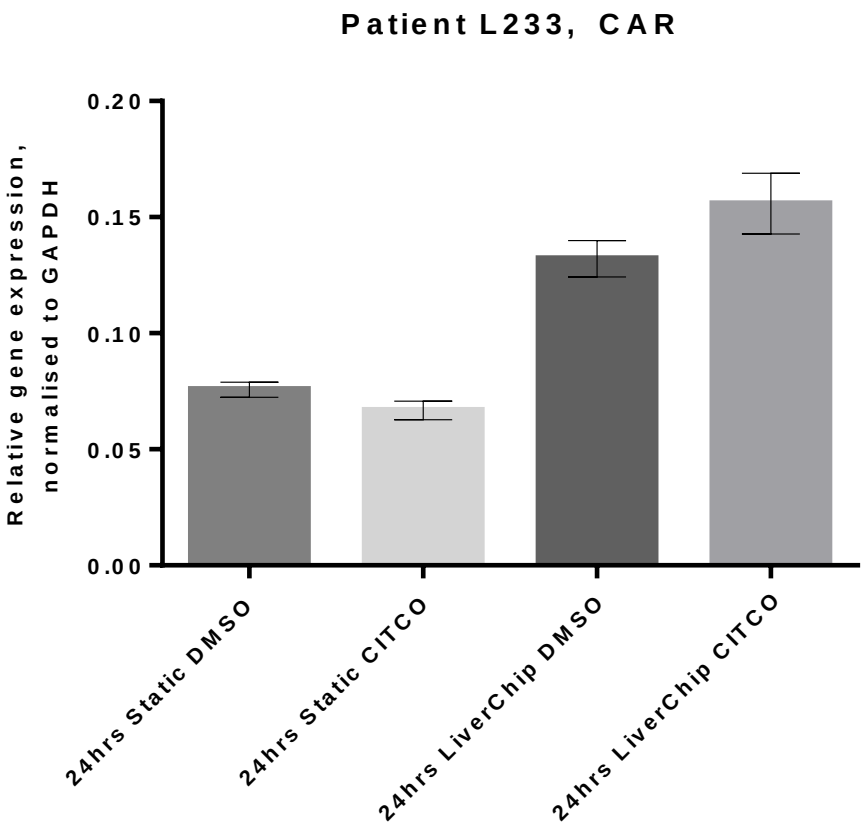

Figure 8-14: Primary human hepatocytes isolated from patient L233 treated with CITCO or DMSO control for 24 hours. RNA was extracted and CAR mRNA expression examined. N = 4 technical repeats. Data are shown as mean +/- SEM.

As a result of the lack of CYP2B6 induction in primary hepatocytes isolated from patient L233 when cultured in static, combined with the knowledge that hepatocytes cultured in LiverChip™ maintain hepatic phenotype better than those in static culture, a decision to send only those RNA samples isolated from hepatocytes cultured in LiverChip™ for full gene expression microarray and miRNA array was made.

The second time point chosen was 5 days as discussed in section 8.6. Further samples of primary hepatocytes derived from individual patients were screened in the same way as the 24 hours study. The first isolation of hepatocytes from patient L228 were seeded into LiverChip^{TM} and static culture and treated with CITCO for 5 days. Figure 8-15 clearly shows a significant (Static: $p < 0.005$, LiverChip^{TM}: $p < 0.001$) induction of CYP2B6 upon treatment with CITCO for 5 days in hepatocytes cultured in LiverChip^{TM} and static conditions. This data indicates that the samples generated from the hepatocytes isolated from patient L228 are ideal to use in the study of full mRNA expression and miRNA expression.

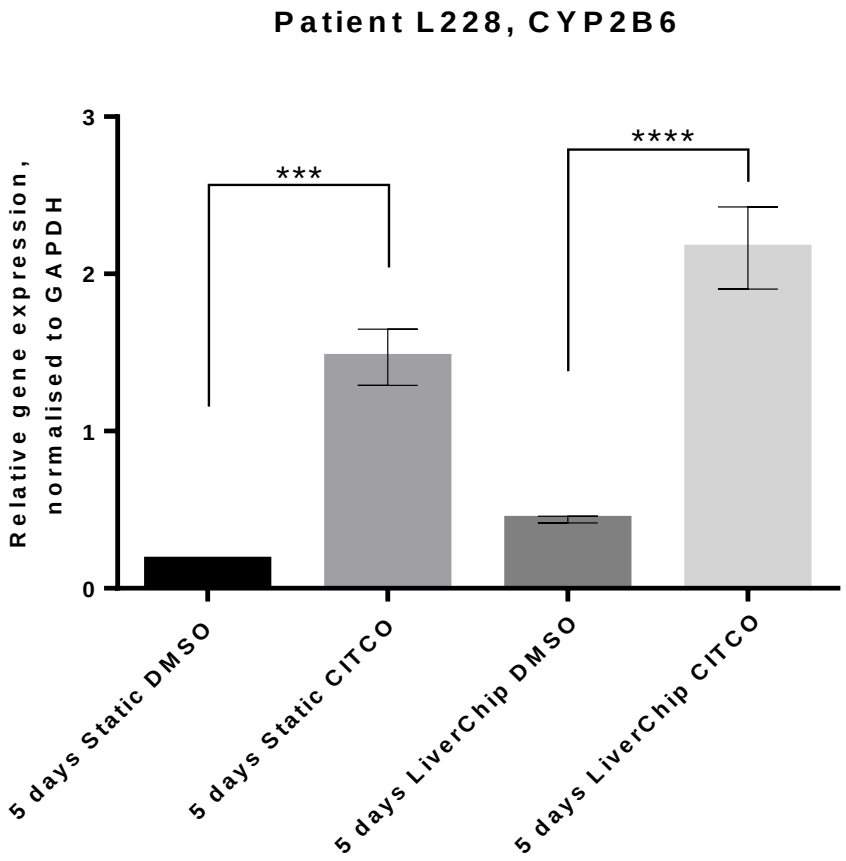

Figure 8-15: Primary human hepatocytes isolated from patient L228 treated with CITCO or DMSO control for 5 days. RNA was extracted and CYP2B6 mRNA expression examined. N = 4 technical repeats. *** = $p < 0.005$, **** = $p < 0.001$, one way ANOVA with Bonferroni's multiple comparison test. Data are displayed as mean +/- SEM.

Having produced one set of suitable samples, primary hepatocytes isolated from a fourth patient (L238) were tested in an identical way to those from patient L228. When the samples generated from L238 were analysed for CYP2B6 induction (Figure 8-16) it became clear that there was a significant ($p < 0.001$) induction in CYP2B6 expression in hepatocytes treated with CITCO and cultured in LiverChip^{TM} whereas there was no significant increase in

CYP2B6 induction in hepatocytes cultured in static conditions. This follows a similar pattern to that observed in hepatocytes isolated from patient L233.

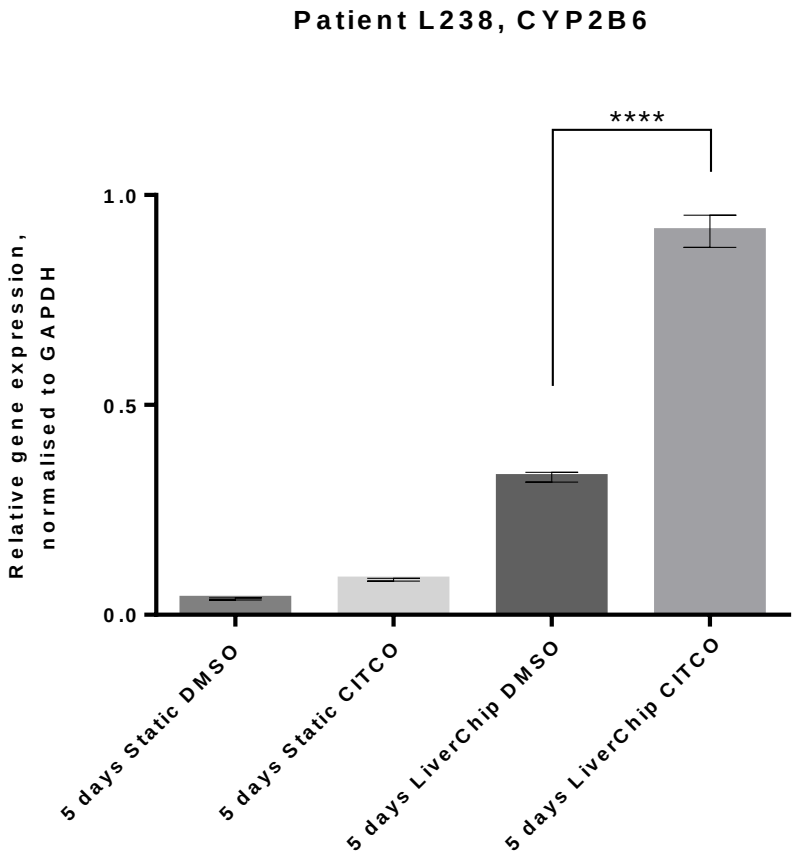

Figure 8-16: Primary human hepatocytes isolated from patient L238 treated with CITCO or DMSO control for 5 days. RNA was extracted and CYP2B6 mRNA expression examined. N = 4 technical repeats. **** = $p < 0.001$, one way ANOVA with Bonferroni's multiple comparison test. Data are displayed as mean +/- SEM.

As interest lies mainly with hepatocytes cultured in LiverChip^{TM} it was decided that samples generated by hepatocytes isolated from patients L225 and L233 and cultured in LiverChip^{TM} would be subjected to a full mRNA and miRNA array to better understand any gene expression changes associated with direct hCAR activation at 24 hours. Samples generated by hepatocytes

isolated from patients L228 and L238 and cultured in LiverChip™ were also subjected to a full mRNA and miRNA array analysis to investigate gene expression changes associated with direct hCAR activation in response to repeated dosing of a known hCAR activator over the course of 5 days.

9 Effect of Constitutive Androstane Receptor Activation on Gene Expression in Primary Human Hepatocytes

9.1 Introduction

Having established that LiverChip™ supports effective primary human hepatocyte culture, appears to maintain good hepatocyte differentiation and is also able to support CAR activation over the course of 1–5 days the large scale mRNA expression changes associated with direct CAR activation were studied.

9.2 Aims

- Generate full gene expression data from primary human hepatocytes cultured in LiverChip™ and treated with CITCO compared to DMSO control at 24 hours and 5 days using Affymetrix Human Transcriptome Array 2.0 (HTA 2.0. Affymetrix, 902310).
- Analyse the generated gene expression data using GeneSpring GX13 (Agilent).
- Import the analysed GeneSpring data into Ingenuity Pathway Analysis (IPA, Qiagen) and perform analysis of pathway activation/suppression.

9.3 Experimental design and methods

Having already generated the samples to be sent for microarray during the patient screen in section 8.7 the samples to be studied were transferred to the Nottingham Arabidopsis Stock Centre (NASC, School of Biosciences, University of Nottingham). The labelling, hybridisation and scanning was undertaken by members of the NASC team. The flow chart in Figure 9-1 highlights the major steps carried out when analysing microarray data generated by the Affymetrix HTA 2.0 microarray.

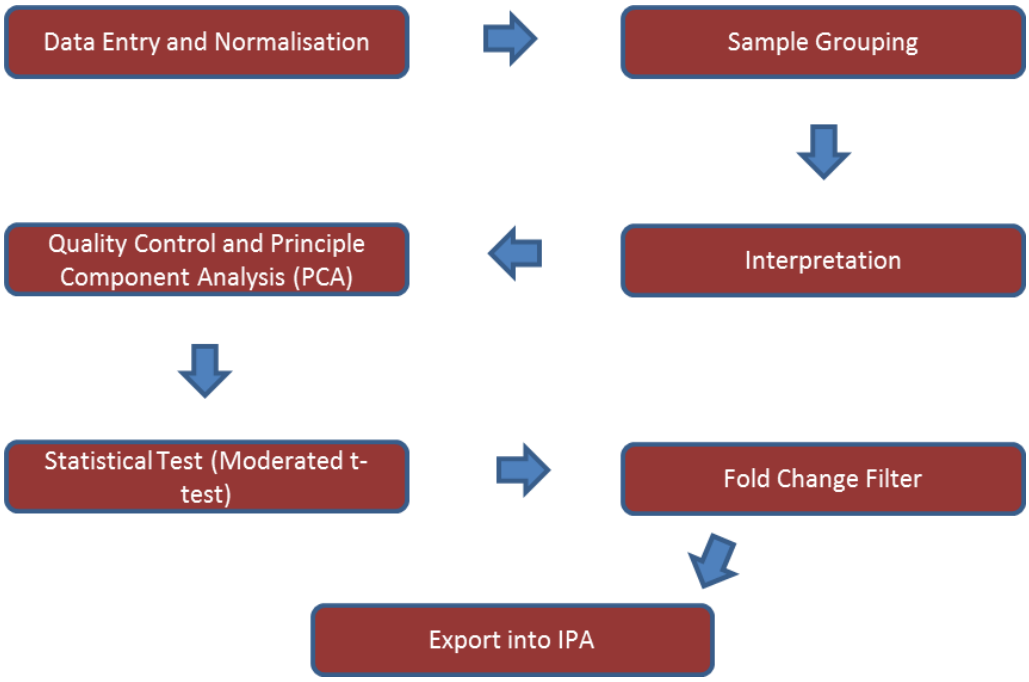

Figure 9-1: Basic overview of the steps required to perform the analysis of microarray data generated in the form of raw intensity files from Affymetrix HTA 2.0 using GeneSpring GX13.

Firstly the raw intensity files generated by the microarray process were uploaded into GeneSpring and normalised using the RMA-16 algorithm. They were then grouped by treatment, patient and time point. The interpretation

stage in GeneSpring allows comparison of samples from different groups to each other. For example it is possible to compare all the CITCO treated samples from one time point to the DMSO control samples of the same time point, whilst a second interpretation could look at a comparison of CITCO treated samples from one patient to the DMSO control samples of the same patient. By creating different interpretations of the data it increases the flexibility of the data analysis, allowing different experimental parameters to be investigated.

An important step is quality control and principle component analysis (PCA). Quality control ensures that the actual process of hybridisation and intensity recording of each sample is consistent. The PCA analysis details the particular variable (principle component) in the data set that accounts for the majority of the variation in that data set. This variable can be any of the variables that exist in the data set. The next step is to carry out a statistical test on the data set to determine which genes are significantly up or down regulated compared to the DMSO control. A fold change filter is applied which aims to remove the genes with a small change in expression. The final step involves importing the data into Ingenuity Pathway Analysis (IPA, Qiagen) where more detailed pathway analysis using the genes that are up or down regulated in response to hCAR activation can be undertaken. Before that however the PCA was carried out.

9.4 Inter patient variability at 24 hours and 5 days

Figure 9-2 shows the PCA plot that is produced when using all the samples generated during the 24 hour hCAR activation experiment (L225 and L233). In this plot the samples are coloured by patient. What becomes immediately obvious is that the principle component responsible for the variation between samples is the patient hepatocytes are isolated from. There is a clear separation between samples from different patients.

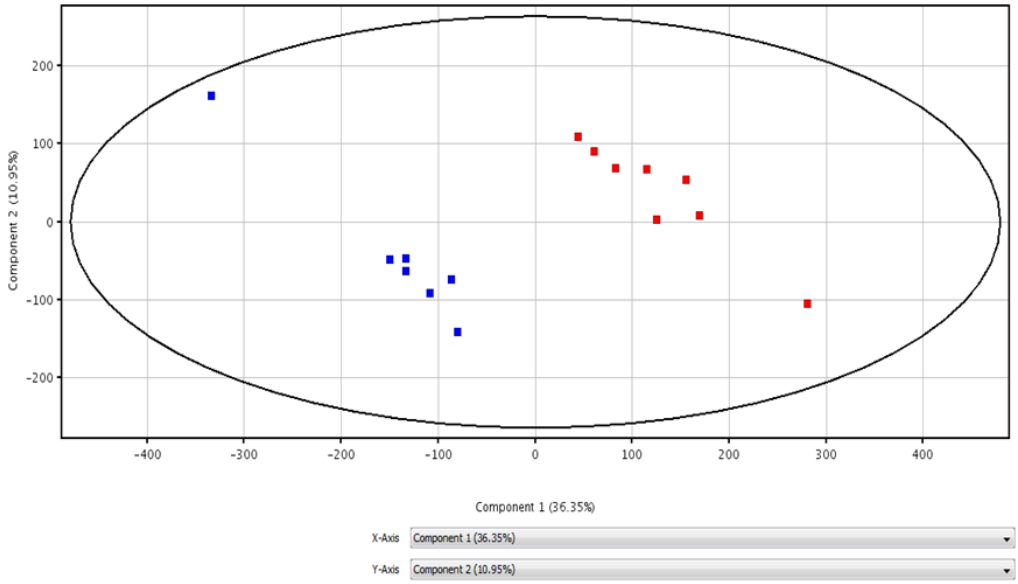

Figure 9-2: Principle component analysis of all samples at 24 hours; coloured by patient.

Colouring the data points by treatment rather than patient, as in Figure 9-3, leads to a less well defined separation between the samples of different colours. The samples do group together but the grouping is not as strong as between patients.

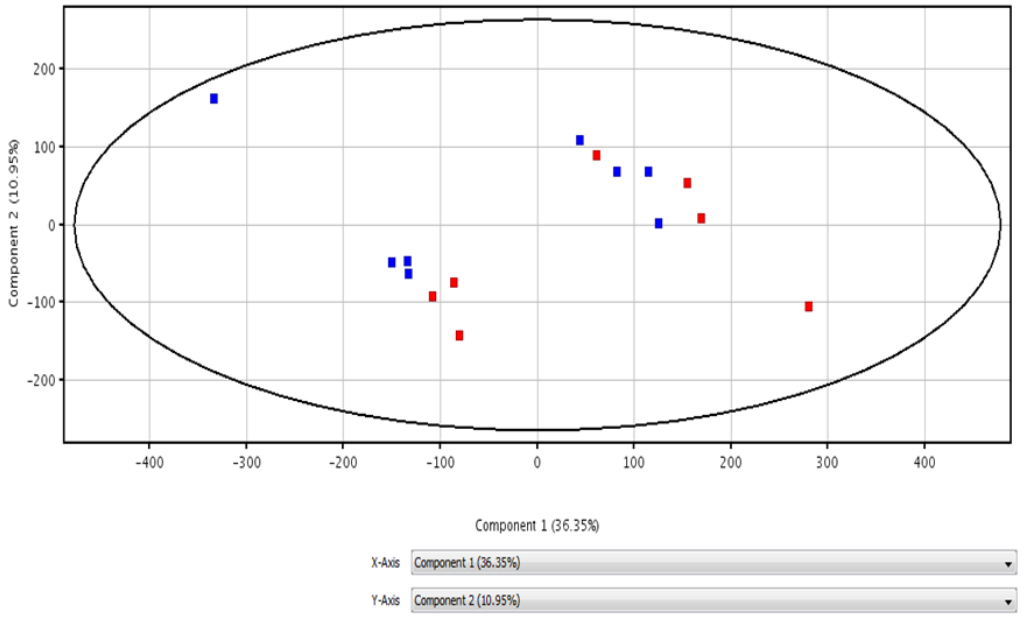

Figure 9-3: Principle component analysis of all samples at 24 hours; coloured by treatment.

The PCA plots for samples generated after 5 days of CITCO treatment (Figure 9-4 and Figure 9-5) show a similar pattern. That is, the samples separate and group by patient initially rather than by treatment.

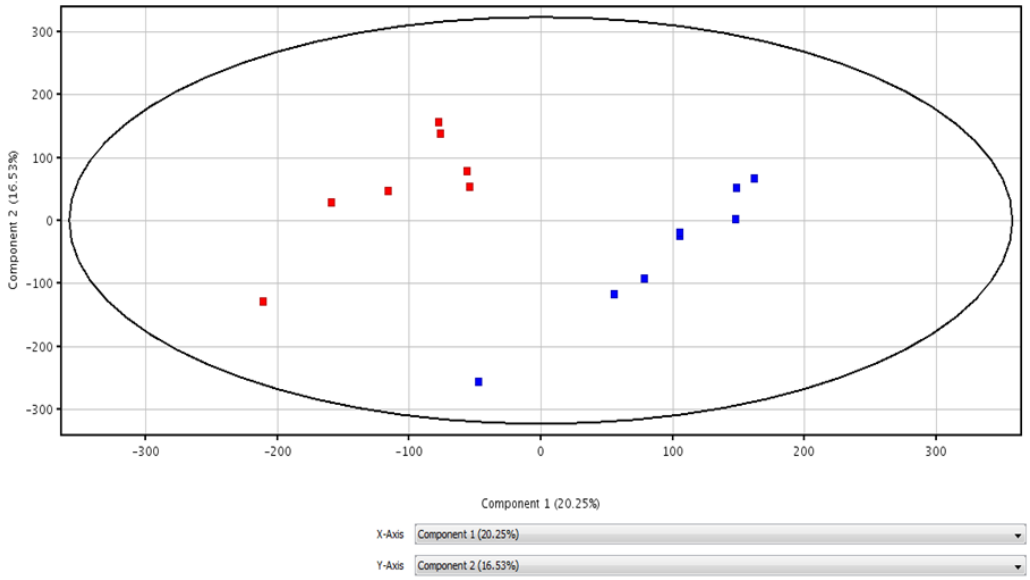

Figure 9-4: Principle component analysis of all samples at 5 days; coloured by patient.

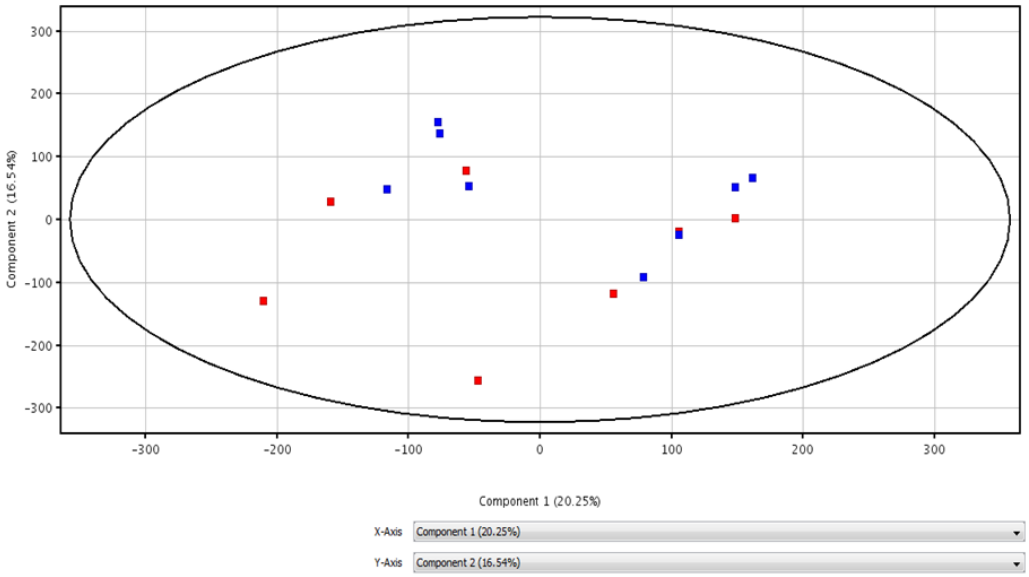

Figure 9-5: Principle component analysis of all samples at 5 days; coloured by treatment.

The observation that the data separates by patient rather than by treatment is unsurprising as the number of genes differentially expressed in two patients can be in the order of thousands, whereas the number of genes differentially regulated due to nuclear receptor activation is likely to be in the order of tens or hundreds as a maximum. For these reasons it was decided that analysing the data from each patient separately would ensure that no major or important gene expression changes would be omitted. Once each patient had been analysed and a list of up and down-regulated genes produced these would be combined together. Any genes appearing on the list of up or down-regulated genes for both patients at each time point were included in the subsequent analysis. In this way the effect of inter-patient variability was negated as much as possible.

9.5 Gene expression (mRNA) changes associated with CAR activation at 24 hours

Having established that each patient would be analysed individually and gene expression changes from each patient at the same time point combined to form a list of genes at each time point, the next step involves analysing the data using GeneSpring. As discussed previously the samples were divided by patient then by treatment and time point. For expression data generated from samples derived from the same patient the gene expression of CITCO treated samples was compared to untreated samples using a modified T-test. This produced a list of genes significantly ($p < 0.05$) up and down-regulated that could be filtered by fold change so that only those with a fold change above 1.25 were included in the pathway analysis. The initial results from this statistical test indicated that there were few changes in gene expression observed at 24 hours (Table 9-1). The list of significantly ($P < 0.05$) differentially regulated genes above 1.25 fold change is shown in Table 9-2 and Table 9-3. The genes up-regulated are limited to members of the CYP2B and CYP2A families and two non-coding RNAs. The induction of CYP2B6 and CYP2A6 in response to CITCO activation of hCAR has been reported previously (Maglich et al., 2003).

	P value (All)	P < 0.05	P < 0.02	P < 0.01	P < 0.0050	P < 0.0010
Fold Change (All)	67539	4373	1541	654	276	38
FC > 1.1	2643	796	408	204	110	25
FC > 1.5	12	5	4	3	2	2
FC > 2.0	0	0	0	0	0	0

Table 9-1: Number of genes with significantly altered expression at 24 hours observed in cells treated with CITCO.

Symbol	Fold Change	Entrez Gene Name	Location	Cell Function/Disease
SCARNA3	1.937	small Cajal body-specific RNA 3	Other	ncRNA
CYP2A6	1.780	cytochrome P450, family 2, subfamily A, polypeptide 6	Cytoplasm	Drug metabolism
CYP2B7P	1.729	cytochrome P450, family 2, subfamily B, polypeptide 7, pseudogene	Other	Drug metabolism
CYP2B6	1.613	cytochrome P450, family 2, subfamily B, polypeptide 6	Cytoplasm	Drug metabolism
SNORA2A	1.601	small nucleolar RNA, H/ACA box 2A	Other	ncRNA

Table 9-2: Significantly (P < 0.05) up-regulated genes with a fold change greater than 1.25 common to both patients (L225 and L233) after 24 hours of treatment with direct hCAR activator CITCO.

Symbol	Fold Change	Entrez Gene Name	Location	Cell Function/Disease
CYP1A2	-1.722	cytochrome P450, family 1, subfamily A, polypeptide 2	Cytoplasm	Xenobiotic Metabolism
CYP1A1	-1.702	cytochrome P450, family 1, subfamily A, polypeptide 1	Cytoplasm	Xenobiotic Metabolism

Table 9-3: Significantly ($P < 0.05$) down-regulated genes with a fold change greater than -1.25 common to both patients (L225 and L233) after 24 hours of treatment with direct hCAR activator CITCO.

Having examined the gene expression changes associated with direct activation of hCAR at 24 hours it was unnecessary to carry out a pathway analysis with such a small list of differentially expressed genes common to both patients as this was unlikely to produce any robust biological insight. Due to these small changes in gene expression profiles observed when both patients are taken into account the gene expression profile of patient L225 was further examined. The rationale for choosing to examine this patient in more detail is that L225 displays far more gene expression changes in response to CITCO treatment compared to L233. Appendix I (section 11.1) lists the change in gene expression profile of primary human hepatocytes derived from L225 and treated with CITCO for 24 hours. The changes in gene expression profile in hepatocytes isolated from patient L225 are more pronounced than that of L233. A more detailed analysis of the changes in gene expression profile of hepatocyte from L225 were carried out and described in section 9.8.

9.6 Gene expression (mRNA) changes associated with CAR activation at 5 days

An identical analysis was carried out on samples from primary hepatocytes isolated from patients L228 and L238 and treated with CITCO for 5 days. The samples from each patient were analysed separately and a list of genes altered during CITCO treatment produced. This list was then combined with that of the second patient to generate a list of genes differentially regulated due to direct hCAR activation common to both patients. Table 9-4 shows the number of genes differentially regulated after 5 days treatment with CITCO. What becomes immediately clear is that there are far more changes in gene expression after 5 days than 24 hours.

	P value (All)	P < 0.05	P < 0.02	P < 0.01	P < 0.0050	P < 0.0010
Fold Change (All)	67539	6646	3299	1988	1204	392
FC > 1.1	4357	2393	1618	1171	811	337
FC > 1.5	47	33	30	25	24	16
FC > 2.0	5	3	3	3	3	2
FC > 3.0	1	1	1	1	1	1

Table 9-4: Number of genes with significantly altered expression at 5 days due to treatment with CITCO in both patients L228 and L238.

There were 33 genes differentially expressed with a fold change above 1.5 when treated with CITCO after 5 days compared to only 5 after 24 hours. The full list of genes differentially regulated by repeated CITCO dosing over 5 days is presented in section 11.2. Having carried out the statistical analysis of gene expression changes associated with direct activation of hCAR at both 24 hours and 5 days the microarray results needed to be verified. When conducting a microarray study it is important to note that gene expression changes can occasionally be over or understated. To attempt to improve confidence in the results obtained from the microarray a follow up study using Taqman qPCR was undertaken.

9.7 Confirmation of mRNA gene expression changes using Taqman™ qPCR

To ensure that the gene expression changes seen as a result of the microarray are accurate it is important to confirm this using qPCR. Taqman is a more robust method of measuring gene expression than microarray. The limitation of this technique is that it is low throughput in terms of the number of genes that can be studied compared to a microarray. RNA was reverse transcribed according to section 7.11 and gene expression analysed by Taqman qPCR according to section 7.13.

9.7.1 Confirmation of mRNA gene expression at 24 hours

Gene expression profiles of specific genes differentially regulated at 24 hours were investigated. The choice of genes used as confirmation for the microarray data at 24 hours was limited due to the lack of gene expression changes observed at this time point (Table 9-2 and Table 9-3). Subsequently the decision to choose differentially regulated genes specific to patient L225 was made for the confirmation of microarray data. Figure 9-6 presents the expression patterns of three genes that were shown as up-regulated by treatment with CITCO in patient L225 with a fold change above 1.25 when microarray data was analysed. What becomes clear is that there is little change in the expression pattern of these genes when examined using Taqman qPCR, however the same is true when assessing the microarray data. As discussed previously the gene expression changes at 24 hours were small. The fold change observed for each up-regulated gene studied in Figure 9-6 from the microarray and the corresponding fold change of that gene when studied using qPCR is shown in Table 9-5. It is evident that the fold change observed when studied using qPCR varies compared to that observed in the microarray data. Despite this all three genes, albeit one with a very small fold change, have a positive fold change that mirrors that of the microarray data in terms of direction.

Confirmation of genes down-regulated was also carried out using the same methodology as that used to confirm the changes in up-regulated genes. The

gene expression profiles observed using Taqman qPCR are shown in Figure 9-7 and the fold changes of these genes when investigated using qPCR compared to microarray are detailed in Table 9-6. The fold change associated with down-regulated genes was more pronounced than those associated with up-regulated genes. This is reflected in the Taqman qPCR analysis which shows that the fold change is more pronounced than those of the up-regulated genes. Confirmation analysis of both up and down-regulated genes highlighted by the microarray study has shown that despite the differences in the fold change between microarray data and qPCR data the direction of the fold change is consistent. This lends confidence to the microarray process and data analysis performed using GeneSpring however it is abundantly clear that at 24 hours the gene expression changes are small scale and inter-patient variability is a major factor.

An interesting consequence of examining CYP1A1 via qPCR was the finding that the expression of this gene, in both treated and untreated hepatocytes, was only retained in primary human hepatocytes cultured in LiverChip^{TM} and not static.

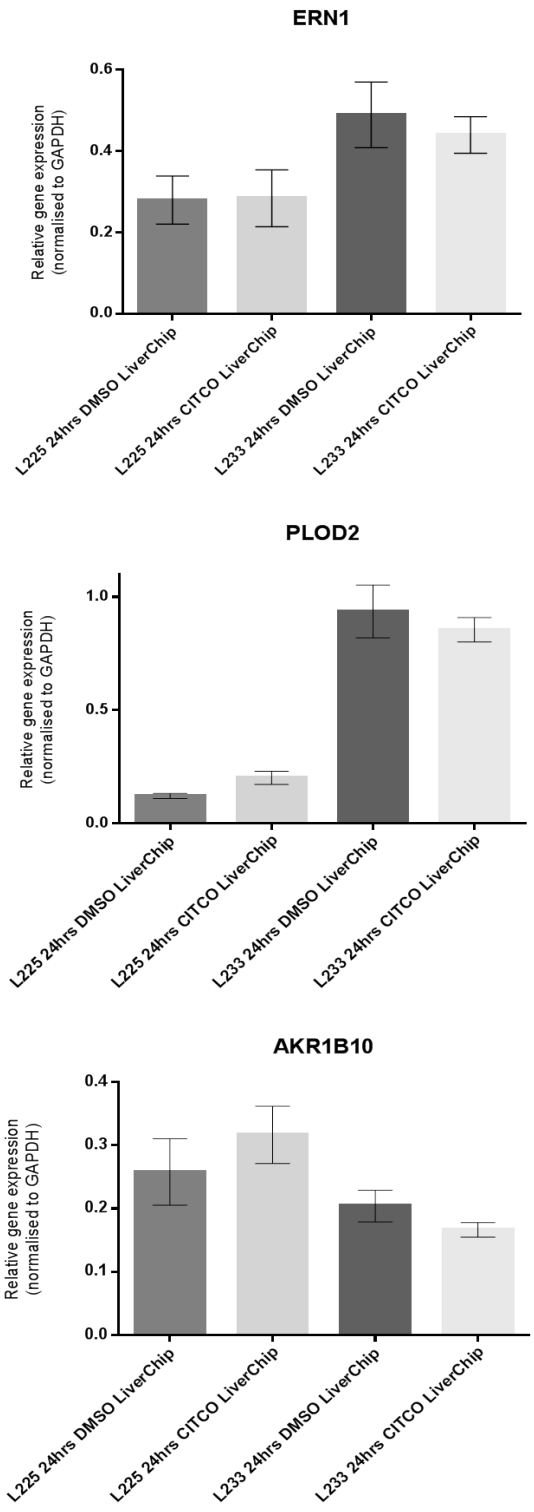

Figure 9-6: Expression pattern of genes shown as up-regulated when studied using microarray in primary human hepatocytes cultured in LiverChip™ after treatment with CITCO over the course of 24 hours. Gene expression determined using Taqman qPCR. Data are shown as mean +/- SEM. N = 4 technical repeats.

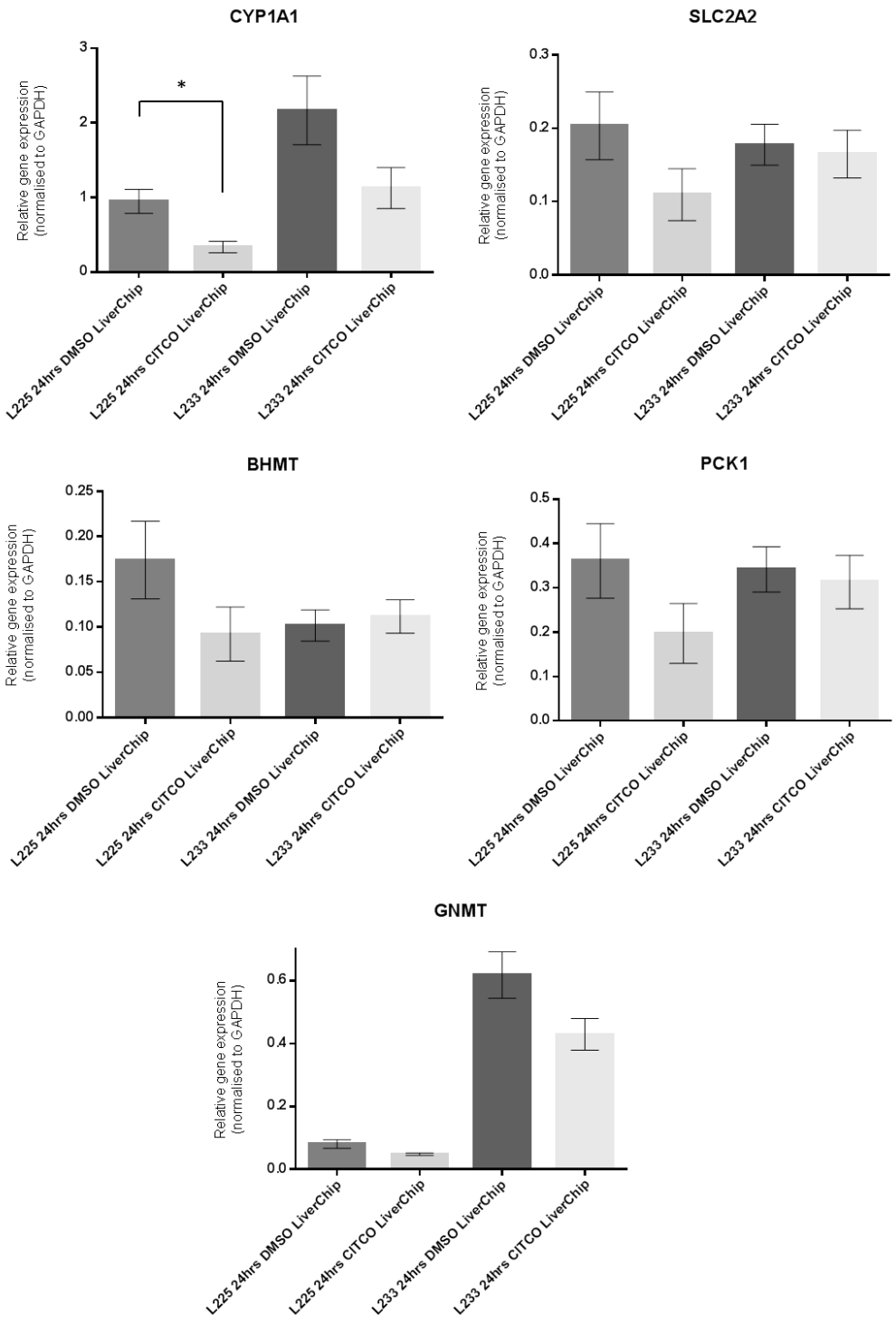

Figure 9-7: Expression pattern of genes shown as down-regulated when studied using microarray in primary human hepatocytes cultured in LiverChip™ after treatment with CITCO over the course of 24 hours. Gene expression determined using Taqman qPCR. Data are shown as mean +/- SEM. N = 4 technical repeats. Unpaired T-test, * = $P < 0.05$.

Gene	Microarray Fold Change	Taqman Fold Change
	L225	**L225**
ERN1	1.293	1.02
CYP2B6	1.613	1.89
PLOD2	1.344	1.65
AKR1B10	1.326	1.23

Table 9-5: Fold change values (L225) associated with genes up-regulated in the microarray study. Fold changes are shown as the expression when treated with CITCO compared to the control.

Gene	Microarray Fold Change	Taqman Fold Change
	L225	**L225**
CYP1A1	-1.702	-2.86
SLC2A2	-1.436	-1.85
BHMT	-1.394	-1.89
PCK1	-1.325	-1.82
GNMT	-1.296	-1.69

Table 9-6: Fold change values (L225) associated with genes down-regulated in the microarray study. Fold changes are shown as the expression when treated with CITCO compared to the control

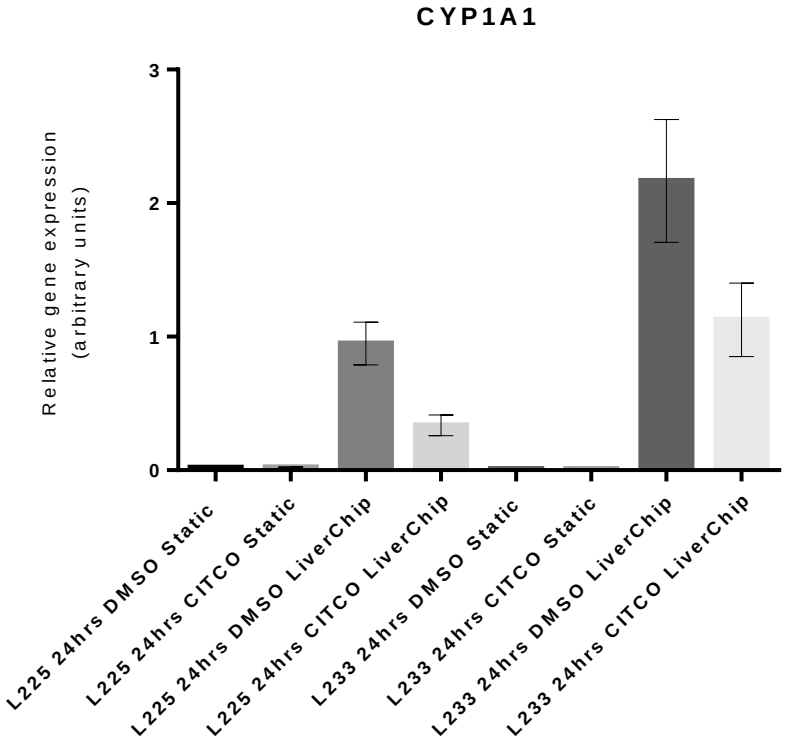

Figure 9-8: CYP1A1 gene expression profile in primary human hepatocytes cultured in both static conditions and LiverChip™. Hepatocytes derived from both patients show improved expression of this gene when cultured in LiverChip™. Data are shown as mean +/- SEM. N = 4 technical repeats.

9.7.2 Confirmation of mRNA gene expression at 5 days

Having examined the gene expression changes associated with CITCO treatment at 24 hours the gene expression changes associated with CITCO treatment were also investigated using Taqman qPCR.

What is clear when looking at Figure 9-9 and Table 9-7 is that the expression pattern of up-regulated genes is maintained between microarray analysis and qPCR confirmation. What is less consistent is the fold change of each gene when comparing the microarray data with qPCR data.

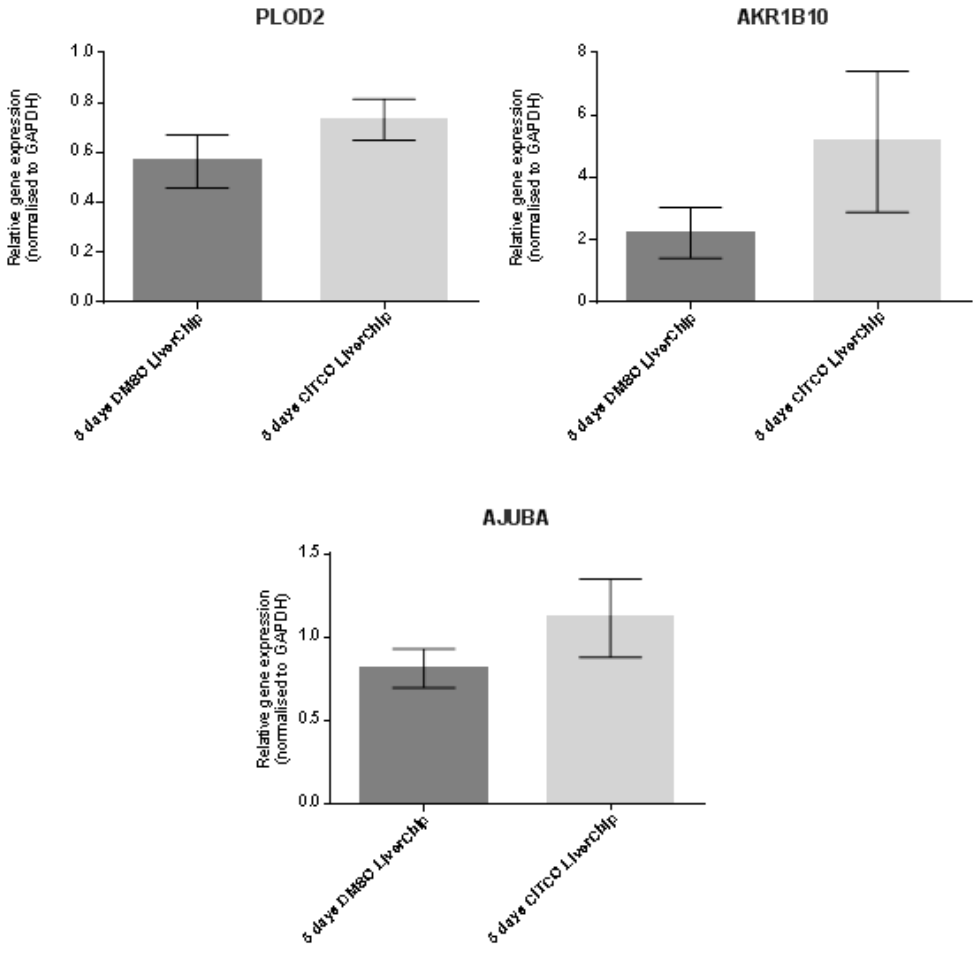

Figure 9-9: Expression pattern of genes shown as up-regulated when studied using microarray in primary human hepatocytes cultured in LiverChip™ after treatment with CITCO over the course of 5 days. Gene expression determined using Taqman qPCR. Data are shown as mean +/- SEM. N = 4 technical repeats.

The expression pattern of genes that were found to be down-regulated in the microarray analysis is consistent when studying the qPCR data (Figure 9-10 and Table 9-8). The trend observed is for the microarray to underestimate the fold change in genes due to CITCO treatment when compared to qPCR.

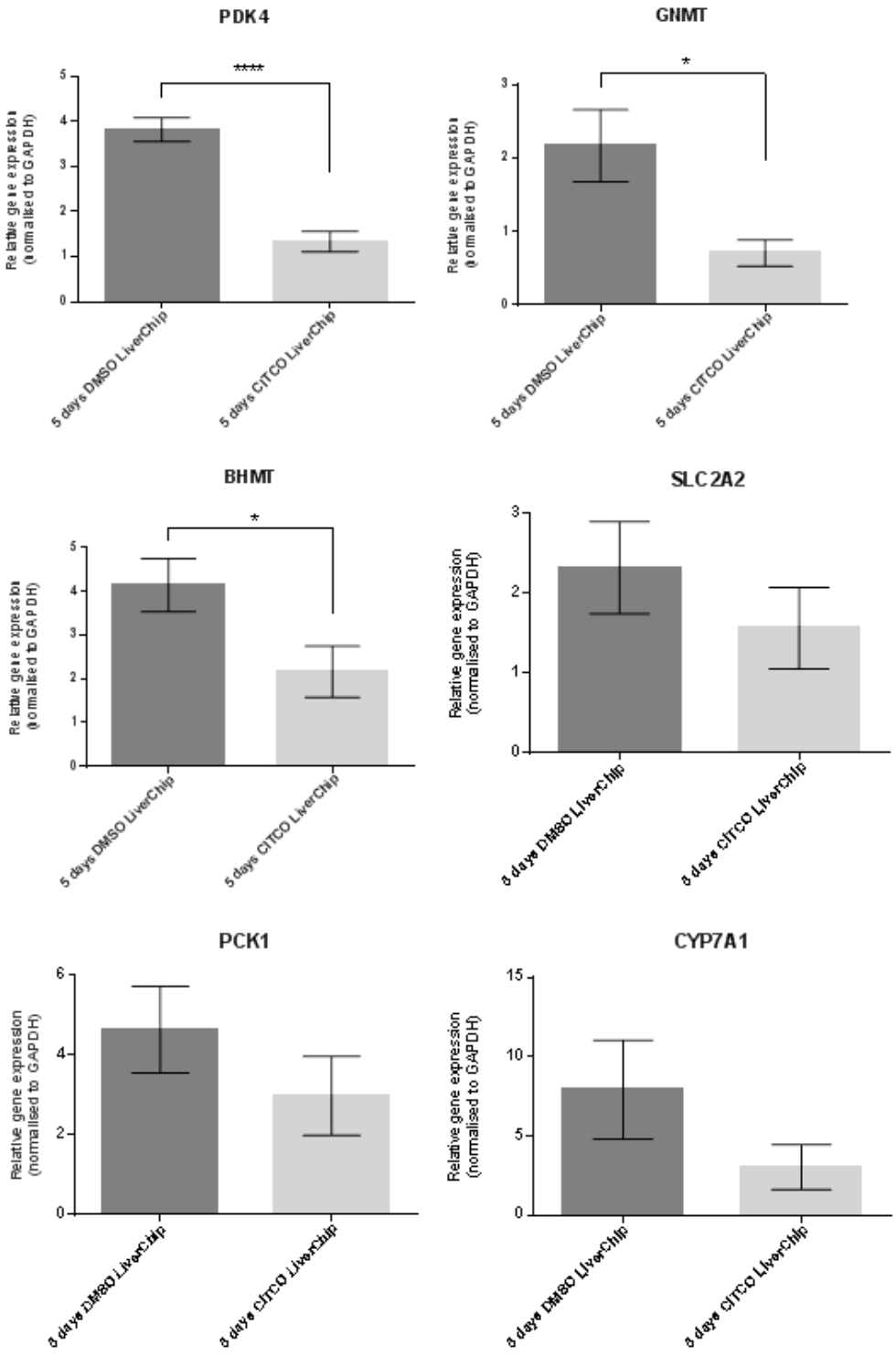

Figure 9-10: Expression pattern of genes shown as down-regulated when studied using microarray in primary human hepatocytes cultured in LiverChip™ after treatment with CITCO over the course of 5 days. Gene expression determined using Taqman qPCR. Data are shown as mean +/- SEM. Unpaired t-test, * = $p<0.05$, **** = $p<0.001$. N = 4 technical repeats.

Gene	Microarray Fold Change	Taqman Fold Change
PLOD2	1.470	1.296
AKR1B10	1.917	2.321
AJUBA	1.447	1.371

Table 9-7: Fold change values associated with genes up-regulated at 5 days in the microarray study. Fold changes are shown as the expression when treated with CITCO compared to control.

Gene	Microarray Fold Change	Taqman Fold Change
PDK4	-2.139	-2.857
GNMT	-2.078	-3.071
BHMT	-1.289 (L238)	-1.742 (L238) -1.914 (Collated)
SLC2A2	-1.380	-1.486
PCK1	-1.411	-1.559
CYP7A1	-1.649 (L228) -2.414 (L238)	-2.403 (L228) -6.501 (L238)

Table 9-8: Fold change values associated with genes down-regulated at 5 days in the microarray study. Fold changes are shown as the expression when treated with CITCO compared to control.

What is important to note in Table 9-8 is the variability of fold change observed between hepatocytes isolated from different patients. This may provide an explanation as to why the changes in gene expression using qPCR do not show as significant. For example, Figure 9-11 shows the up-regulated qPCR data split up by patient and treatment. For all three genes shown it is clear that individual patients show a differing degree of change in response to CITCO treatment.

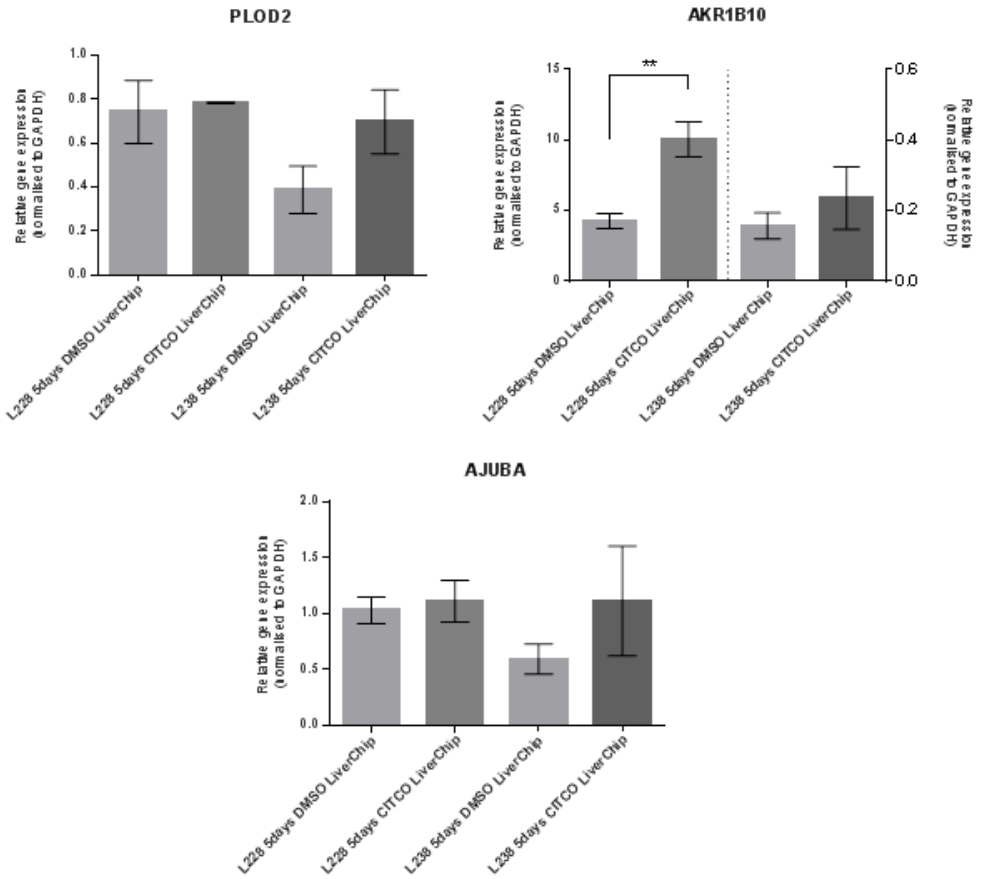

Figure 9-11: Expression pattern of genes shown as up-regulated when studied using microarray in primary human hepatocytes cultured in LiverChip™ after treatment with CITCO over the course of 5 days. Data are divided by patient and treatment. Gene expression determined using Taqman qPCR. Data are shown as mean +/- SEM. Unpaired t-test, ** = $p<0.01$. N = 4 technical repeats.

Figure 9-12 contains gene expression profiles of specific genes that shown as non-significantly down-regulated in response to CITCO treatment in Figure 9-10. The data is split up by patient and treatment to determine whether inter-patient variability is having an effect on the gene expression profiles of those genes. As discussed before inter-patient variability can have a major impact on the expression of a diverse range of genes and this set is no different. Hepatocytes derived from patient L238 have lower expression levels of all the genes shown in Figure 9-10. The expression patterns are broadly the same in both patients though. Upon treatment with CITCO the genes displayed are down-regulated.

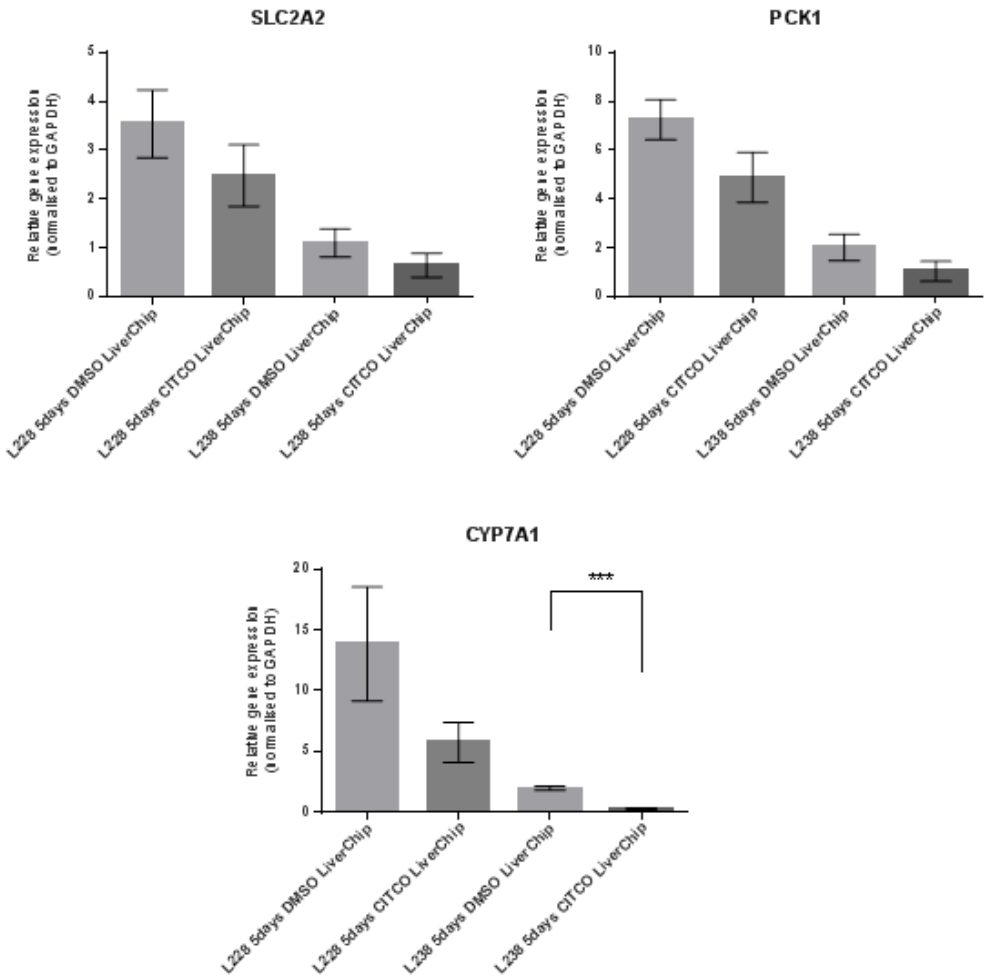

Figure 9-12: Expression pattern of genes shown as down-regulated when studied using microarray in primary human hepatocytes cultured in LiverChip^{TM} after treatment with CITCO over the course of 5 days. Data are divided by patient and treatment. Gene expression determined using Taqman qPCR. Data are shown as mean +/- SEM. Unpaired t-test, *** = $p<0.005$. N = 4 technical repeats.

When assessing whether the microarray data has produced reliable results it is important to note that all but one (ERN1 at 24 hours, Table 9-5) of the gene expression profiles have followed a pattern consistent the microarray data when studied using qPCR. When the data set produced using qPCR is studied as a whole, in terms of number of gene expression profiles that are consistent

with those observed in the microarray data (Table 9-9), it demonstrates that the microarray had a tendency to underestimate the fold change. Using this data we were confident that the results shown by the microarray are genuine changes in the gene expression profile of hepatocytes and were reliable.

Consistent with Microarray	Underestimated by Microarray	Overestimated by Microarray
18	14	4

Table 9-9: Number of gene expression profiles that show a fold change when studied using qPCR that is consistent with that observed in the microarray data (column A). Column B shows the number of gene expression profiles where the fold change was underestimated by the microarray data. Column C shows the number of genes where the fold change was overestimated by microarray data.

9.8 Pathway analysis of differentially expressed genes in hepatocytes isolated from L225 and treated with CITCO over 24 hours

Due to fact that the combined list of differentially regulated genes observed after 24 hours CITCO treatment is so small the decision to further analyse the list of genes differentially regulated in patient L225 (see Appendix I, section 11.1) was made. The list of genes differentially regulated at 24 hours was uploaded into Ingenuity Pathway Analysis (IPA, Qiagen) and a core analysis carried out. A list of cellular functions and disease states that are affected by CITCO treatment over 24 hours in hepatocytes derived from patient L225 is shown in Table 9-10. Despite the small number of differentially regulated

genes there are a number of genes implicated in the alteration of cellular functions and diseases, the majority of which pertain to increased proliferation and cancer.

Diseases or Functions Annotation	Molecules	# Molecules
proliferation of cells	AKR1B10, CCL20, CLIP1, CYP1A1, CYP2A6 (includes others), CYP2B6, GDF15, GLDC, GNMT,mir-197, NTN4, PLOD2, SERPINE1, SLC7A11, TMSB10/TMSB4X, UGT2B15, USP12	17
Cancer	AKR1B10, ALAS1, BHMT, CCL20, CYP1A1, CYP2A6 (includes others), GDF15, GLDC, GNMT, mir-197, NTN4, PLOD2, RDH16, SERPINE1, SLC7A11, TMSB10/TMSB4X, TXNRD1	17
proliferation of tumor cell lines	AKR1B10, CCL20, CLIP1, CYP1A1, CYP2A6 (includes others), CYP2B6, GDF15, GLDC, GNMT, PLOD2, SERPINE1, SLC7A11, TMSB10/TMSB4X, UGT2B15, USP12	15
abdominal cancer	AKR1B10, ALAS1, BHMT, CCL20, CYP1A1, GDF15, GLDC, GNMT, mir-197, PLOD2, RDH16, SERPINE1, SLC7A11, TXNRD1	14
epithelial cancer	AKR1B10, BHMT, CCL20, CYP1A1, GDF15, GLDC, GNMT, PLOD2, SERPINE1, SLC7A11, TMSB10/TMSB4X, TXNRD1	12
digestive system cancer	AKR1B10, ALAS1, BHMT, CCL20, GDF15, GNMT, mir-197, PLOD2, RDH16, SERPINE1, SLC7A11, TXNRD1	12

Table 9-10: Diseases and cellular functions that are predicted to be affected by CITCO treatment over 24 hours.

When the effects on toxicity are studied (Table 9-11) a similar pattern emerges, the categories specific to liver that are altered involve mainly pro-proliferative and hepatocellular carcinoma.

It is important to note however that this analysis is performed on the list of genes differentially regulated in hepatocytes derived from a single patient. As the combined list of genes significantly differentially regulated in both patients was confined to the cytochrome P450 enzymes the only cellular functions noticeably altered according to pathway analysis were involved in xenobiotic metabolism. Another point to note is that the list of genes that

were analysed using IPA is small. It is for these reasons that a more in depth pathway analysis has not been carried out. Despite this it is clear that treatment of primary human hepatocytes isolated from patient L225 with CITCO tends towards a more proliferative phenotype.

Categories	Diseases or Functions Annotation	Molecules	# Molecules
Liver Hyperplasia/Hyperproliferation	liver cancer	AKR1B10, BHMT, CCL20, GNMT, RDH16, SERPINE1, TXNRD1	7
Hepatocellular Carcinoma, Liver Hyperplasia/Hyperproliferation	hepatocellular carcinoma	AKR1B10, BHMT, CCL20, GNMT, SERPINE1, TXNRD1	6
Renal Damage	nephrotoxicity	CYP2A6 (includes others), SLC7A11, TMSB10/TMSB4X, TXNRD1	4
Liver Cholestasis	cholestasis	ABCG8, ADH6, RDH16, UGT2B15	4
Liver Cholestasis	progressive familial intrahepatic cholestasis type 1	ADH6, RDH16, UGT2B15	3
Renal Damage, Renal Tubule Injury	proximal tubular toxicity	CYP2A6 (includes others), TMSB10/TMSB4X, TXNRD1	3
Heart Failure	failure of heart	AVPR1A, SERPINE1, SLC7A11	3
Hepatocellular Carcinoma, Liver Hyperplasia/Hyperproliferation	growth of hepatocellular carcinoma	AKR1B10, GNMT	2
Kidney Failure	chronic renal failure	CYP1A1, SLC7A11	2
Renal Damage	damage of kidney	CYP2C8, SERPINE1	2
Cardiac Hypertrophy	hypertrophy of cardiomyocytes	GDF15, SERPINE1	2
Cardiac Infarction	myocardial infarction	CYP2C8, SERPINE1	2
Cardiac Arteriopathy	coronary artery disease	SERPINE1, SLC7A11	2
Liver Steatosis	hepatic steatosis	GNMT, GPD1	2
Liver Inflammation/Hepatitis	inflammation of liver	GNMT, SERPINE1	2

Table 9-11: Toxicity functions affected by CITCO treatment over the 24 hours in primary human hepatocytes derived from patient L225.

9.9 Pathway analysis of differentially expressed genes at 5 days

The gene expression changes that occur after 5 days repeated CITCO dosing are greater than those present at 24 hours. Appendix II (Section 11.2) contains the full list of differentially regulated genes after 5 days repeated dosing with CITCO that show a fold change above 1.25. When this data is entered into IPA a similar analysis to that carried out for the 24 hour samples was undertaken. Initially the effect that the differentially expressed genes had on cellular processes and the resulting functional change or disease state was explored. In a similar trend to that observed in samples derived from patient L225 the majority of the diseases and functions affected by direct hCAR activation are related to increased proliferation and cell survival (Table 9-12). What becomes immediately clear is that the top diseases and functions, organised by z-score and therefore activation state, that are related to cancer and cell survival. The top disease and functions with an increased predicted activation state are involved in cellular movement, protein synthesis and steatosis. When the functions and diseases with high z-scores are included in this list it is clear that hepatocytes are becoming disposed towards a pro-proliferative and an anti-apoptotic phenotype.

Categories	Diseases or Functions Annotation	p-Value	Predicted Activation State	Activation z-score	# Molecules
Cellular Movement	migration of tumor cell lines	1.17E-06	Increased	2.387	24
Protein Synthesis	metabolism of protein	1.04E-02	Increased	2.296	11
Gastrointestinal Disease, Hepatic System Disease, Metabolic Disease	hepatic steatosis	1.52E-03	Increased	2.158	8
Cellular Movement	migration of cells	1.06E-04	Increased	2.018	37
Cellular Growth and Proliferation	formation of cells	8.26E-03		1.955	15
Cancer, Organismal Injury and Abnormalities	growth of malignant tumor	5.94E-04		1.744	14
Cancer, Organismal Injury and Abnormalities	growth of carcinoma	4.44E-03		1.686	6
Inflammatory Response	inflammation of body region	4.89E-03		1.676	18
Cellular Assembly and Organization, Cellular Development, Cellular Growth and Proliferation, Nervous System Development and Function, Tissue Development	growth of neurites	9.60E-03		1.669	11
Cellular Movement	cell movement	1.88E-04		1.586	39

Table 9-12: Top 10 cellular functions and related disease states that are predicted to increase by direct hCAR activation by CITCO in primary human hepatocytes over 5 days repeated dosing. Z score of a pathway or disease state is used as a measure of predicted activation or suppression of the particular disease or function. Highlighted in red are the diseases and functions with a z-score above 2.

The processes predicted to decrease with direct hCAR activation by CITCO over 5 days is shown in Table 9-13. The predicted outcome when the pathways predicted to decrease are examined reinforces the pro proliferative nature of the gene expression changes shown in the up-regulated pathways of Table 9-12.

Categories	Diseases or Function Annotation	p-Value	Predicted Activation State	Activation z-score	# Molecules
Cell Death and Survival	necrosis	7.74E-04	Decreased	-2.695	44
Carbohydrate Metabolism, Molecular Transport, Small Molecule Biochemistry	uptake of D-glucose	1.16E-05	Decreased	-2.375	11
Cell Death and Survival	cell death of kidney cells	3.99E-03	Decreased	-2.283	10
Cell Death and Survival	cell death of tumor cell lines	2.45E-04	Decreased	-2.253	33
Cell Death and Survival	cell death	6.52E-04	Decreased	-2.150	50
Cell Death and Survival	apoptosis of tumor cell lines	1.57E-04	Decreased	-2.007	29
Cell Morphology, Cellular Assembly and Organization, Cellular Function and Maintenance	formation of lamellipodia	3.68E-04	Decreased	-2.000	7
Carbohydrate Metabolism	gluconeogenesis	4.81E-04	Decreased	-2.000	4
Carbohydrate Metabolism	glycolysis	8.34E-06		-1.980	8
Cell Death and Survival	apoptosis	1.21E-03		-1.950	41
Lipid Metabolism, Molecular Transport, Small Molecule Biochemistry	concentration of phospholipid	1.04E-02		-1.881	6
Carbohydrate Metabolism, Lipid Metabolism, Molecular Transport, Small Molecule Biochemistry	concentration of phosphatidic acid	1.15E-02		-1.710	5
Carbohydrate Metabolism	uptake of monosaccharide	4.72E-06		-1.616	13
Cell Death and Survival	cell death of leukaemia cell lines	3.11E-03		-1.477	10

Table 9-13: Cellular functions and related disease states that are predicted to decrease by direct hCAR activation by CITCO in primary human hepatocytes over 5 days repeated dosing. Z score of a pathway or disease state is used as a measure of predicted activation or suppression of the particular disease or function. Highlighted in blue are the diseases and functions with a z-score below -2.

When looking at the pathway functions predicted to decrease upon direct activation of hCAR with CITCO the pathways predicted to decrease with a z-

score below -2 include necrosis, cell death and apoptosis. This adds to the prediction that direct activation of hCAR by CITCO treatment over 5 days is leading towards a pro-proliferative, anti-apoptotic and hepatocellular carcinoma phenotype. Also of note in Table 9-13 is the finding that gluconeogenesis is predicted to become down-regulated by treatment with CITCO and direct hCAR activation. This is a finding reported previously in rodents in response to indirect activation of CAR by phenobarbital (Ueda et al., 2002, Gao et al., 2009). A reduction in lipid metabolism is also shown in our data set and this has also been shown previously in rodent studies (Roth et al., 2008).

To further analyse the potential toxicological effects that direct hCAR activation may have on primary human hepatocytes an analysis of pathways implicated in an increase in toxicity were examined (Table 9-14). The outcome is similar to that observed when examining the general cellular pathways and diseases. The majority of predicted pathways affected are cell proliferation and decreases in cell death. This supports the analysis carried out in Table 9-12 and Table 9-13.

Categories	Diseases or Functions	p-Value	Molecules	# Molecules
Liver Hyperplasia/Hyperproliferation	liver cancer	4.04E-07	ADH1B,C9,CCL2,CCL20,EGFR,ERBB3,GNMT, GPX2,HABP2,HP,IGFBP2,JUN,LRG1,mir-21,PDK4, SCP2,SERPINE1,SOX4,TNFSF10,TXNRD1	20
Hepatocellular Carcinoma, Liver Hyperplasia/Hyperproliferation	hepatocellular carcinoma	5.63E-05	C9,CCL20,EGFR,ERBB3,GNMT,GPX2,HP,JUN, mir-21,PDK4,SERPINE1,SOX4,TNFSF10,TXNRD1	14
Renal Necrosis/Cell Death	cell death of kidney cells	3.99E-03	CAT,CCNI,EGFR,HSPB1,IL32,ITGAV,mir-21, TNFSF10,TP53INP1,TRPM7	10
Liver Steatosis	hepatic steatosis	1.52E-03	CAT,CCL2,CYP2E1,GNMT,INSIG1,IRS2,mir-21,PLIN2	8
Liver Necrosis/Cell Death	necrosis of liver	1.79E-03	CAT,CYP2E1,EGFR,IGFBP1,ITGAV,JUN,SERPINE1,TNFSF10	8
Renal Necrosis/Cell Death	cell death of kidney cell lines	1.32E-02	CAT,EGFR,HSPB1,IL32,ITGAV,TNFSF10,TP53INP1,TRPM7	8
Liver Damage	damage of liver	2.11E-02	CCL2,CYP2E1,EGR1,JUN,SDC4,SERPINE1,TNFSF10	7
Liver Necrosis/Cell Death	cell death of liver cells	4.33E-03	CAT,CYP2E1,EGFR,IGFBP1,ITGAV,JUN,TNFSF10	7
Liver Proliferation	proliferation of liver cells	1.65E-02	EGFR,IGFBP1,ITGAV,JUN,mir-21,TNFRSF12A	6
Liver Inflammation/Hepatitis	inflammation of liver	3.39E-02	CCL2,CYP2E1,GNMT,HP,SERPINE1,TNFSF10	6
Cardiac Hypertrophy	hypertrophy of heart	8.04E-02	EGFR,GDF15,JUN,mir-21,PFKFB1,SERPINE1	6
Liver Necrosis/Cell Death	apoptosis of liver cells	4.95E-03	CAT,EGFR,IGFBP1,ITGAV,JUN,TNFSF10	6
Liver Necrosis/Cell Death	cell death of hepatocytes	3.02E-03	CAT,CYP2E1,EGFR,IGFBP1,JUN,TNFSF10	6
Cardiac Necrosis/Cell Death	cell death of cardiomyocytes	2.36E-02	ABCC9,CAT,HSPB1,KNG1,MAOA,mir-21	6
Liver Steatosis	nonalcoholic fatty liver disease	2.52E-05	CAT,CCL2,CYP2E1,GNMT,mir-21,PLIN2	6
Liver Cholestasis	cholestasis	4.17E-04	ABCB1,ADH1C,BAAT,GPX2,SCP2,TNFSF10	6

Table 9-14: Cellular functions able to affect toxicity and predicted to be affected by treatment with CITCO in primary human hepatocytes.

As a consequence of this pathway analysis it is clear that direct activation of hCAR in primary human hepatocytes by CITCO leads to a tendency towards a pro-proliferative phenotype. As hepatocarcinoma and pro-carcinogenic cellular functions are most affected by the differentially regulated genes in response to CITCO treatment the upstream analysis of these was performed. This aims to elucidate the potential regulators that are upstream of the genes implicated in the change in cellular function. The results of this analysis are shown in Table 9-15.

Upstream Regulator	Molecule Type	Predicted Activation State	Activation z-score	p-value of overlap	Mechanistic Network
PPARG	ligand-dependent nuclear receptor	Inhibited	-2.261	8.30E-10	65 (16)
NR3C1	ligand-dependent nuclear receptor	Inhibited	-2.099	2.45E-06	36 (7)
ERK1/2	group	Activated	2.074	1.17E-03	43 (13)
Jnk	group	Activated	2.410	5.18E-03	48 (14)
Pdgf (complex)	complex	Activated	2.376	2.33E-04	44 (15)
IGF1	growth factor	Activated	2.062	1.38E-04	53 (14)
MTOR	kinase	Activated	2.000	3.96E-02	
IL3	cytokine	Activated	2.219	1.88E-03	48 (17)
AKT1	kinase	Activated	2.138	8.57E-05	59 (20)
TGFB1	growth factor	Activated	3.854	3.21E-04	50 (16)
F2	peptidase	Activated	2.411	5.64E-05	40 (13)
RELA	transcription regulator	Activated	2.948	5.16E-04	52 (12)
IFNG	cytokine	Activated	2.023	2.87E-06	54 (18)
TNFSF11	cytokine	Activated	2.173	5.41E-02	
OSM	cytokine	Activated	2.437	1.35E-03	58 (19)

Table 9-15: Upstream analysis of the genes differentially regulated in response to CITCO treatment in primary human hepatocytes over 5 days. Coloured blue are the upstream regulators predicted to be inhibited and coloured red are those predicted to be activated (by z-score analysis performed in IPA). Z-score analysis takes into consideration the number of genes differentially regulated and the direction of expression changes in the data set and compares that to literature available. Results that are broadly consistent lead to an activation or inhibition z-score. Mechanistic network highlights the number of genes that have been

found to cause the stated change in activation state and the number of genes (in brackets) in the data set that have been found as consistent with that change.

What becomes clear is that many of the upstream regulators that are activated are prevalent in the causation of carcinoma in a variety of tissues. An example of this is the ERK1/2 kinase; a member of the mitogen activated protein kinase (MAPK) family. ERK1/2 has been shown as a regulator in a variety of cancers in different tissues (Roberts and Der, 2007). Figure 9-13 lays out the control that ERK1/2 can have over a subset of differentially regulated genes from our data set that have all been shown to influence the migration of cells in a tumour cell line.

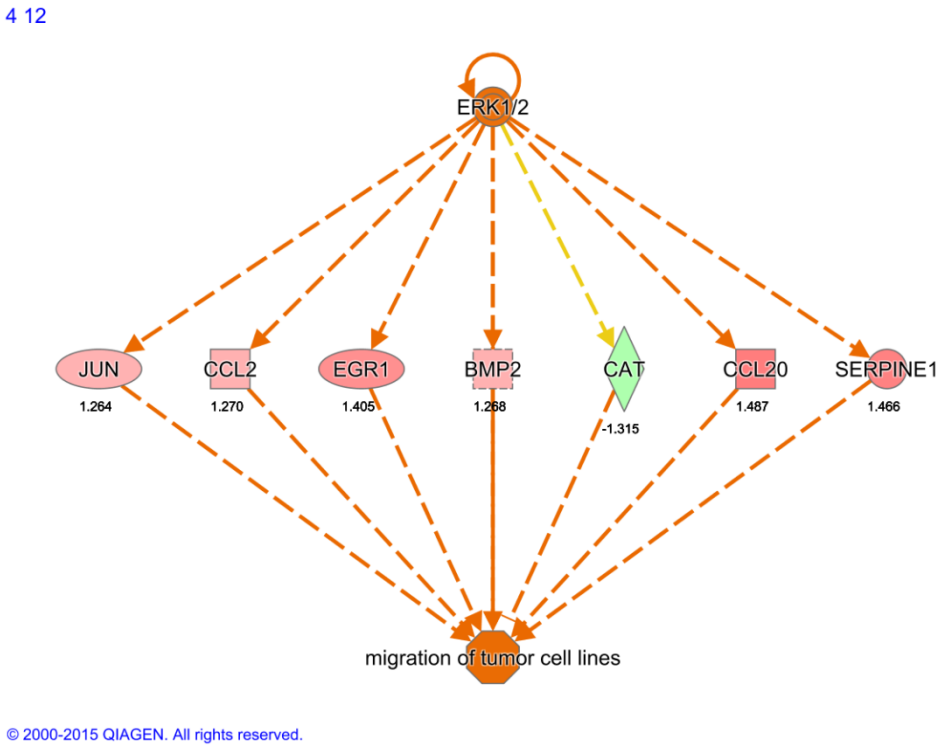

Figure 9-13: Genes differentially regulated (fold change of each gene is presented underneath the corresponding gene) in our data set, under the control of ERK1/2, which have also been shown to cause a migration of cells in tumour cell lines. Orange relationships leading from

ERK1/2 show that the differential expression of the gene connected is consistent with that expected; yellow relationships show it is inconsistent. Orange arrows leading to the cellular outcome from genes differentially expressed indicates that the expression pattern favours an increase in that cellular outcome.

A further example of a pro-proliferative upstream regulator is AKT1. This gene is a critical mediator in many cellular signal transduction pathways, the aberrant control of which has been linked to cancer progression (Altomare and Testa, 2005, Bellacosa et al., 2005). Figure 9-14 highlights the differentially regulated genes in our data set that are implicated in a reduction in cell death and apoptosis and their potential mechanism of control by AKT1.

3 9

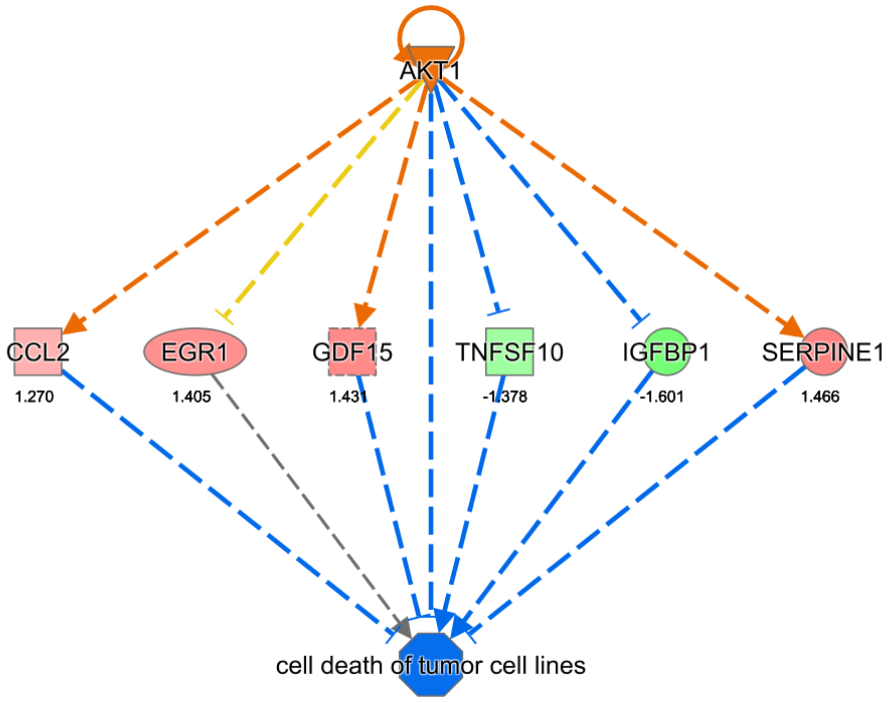

Figure 9-14: Genes differentially regulated in our data set, under the control of ERK1/2, which have also been shown to cause a decrease in cell death. Orange relationships leading from AKT1 show that the differential expression of the gene connected is consistent with that

expected and is upregulated; yellow relationships show it is inconsistent. A blue relationship indicates that the gene expression is consistent with that expected and is down-regulated. Blue relationships leading to the cellular outcome from genes differentially expressed indicates that the expression pattern favours a decrease in that cellular outcome.

These examples illustrate upstream regulators that may be responsible for the pro-proliferative, anti-apoptotic, invasive and pro-carcinogenic phenotype displayed by primary human hepatocytes treated with direct hCAR activator CITCO. Another layer of complexity that has to be considered is the role of miRNA in carcinogenesis. There is emerging evidence to suggest that miRNA expression can play diverse roles in cancer progression, for example the epithelial-mesenchymal transition in cancer stem cells (Hao et al., 2014). Alteration of miRNA expression in human and rodent hepatocellular carcinoma has also been reported. Overexpression of miR-21 has been implicated in the control of PTEN (tumour suppressor gene) in hepatocellular carcinoma (Meng et al., 2007). Phenobarbital mediated tumour progression also elicits changes in the miRNAome. When rats were treated with phenobarbital, expression of the miR-200a/200b/429 cluster was altered (Koufaris et al., 2013). These examples of miRNA dysregulation as a potential marker or cause of hepatocellular carcinoma shows the importance of studying miRNA expression in primary human hepatocytes treated with the direct hCAR activator CITCO.

9.10 miRNA changes associated with direct hCAR activation at 24 hours

Having examined the mRNA expression changes associated with direct hCAR activation by CITCO the miRNA changes caused by direct activation of hCAR were also investigated. Total RNA was loaded onto the miRNA 4.0 array chip from Affymetrix and expression of individual miRNAs measured (described in section 7.15). The same samples as those used in the study of mRNA expression were used to shed light on miRNA expression changes in response to CITCO treatment. The differentially expressed miRNAs in primary human hepatocytes at 24 hours due to treatment with CITCO are shown in Table 9-16 and Table 9-17.

Transcript ID	Fold Change (CITCO vs. DMSO)
hsa-miR-200a-3p	1.97
hsa-miR-550a-5p	1.60
hsa-miR-6836-5p	1.58
hsa-miR-671-5p	1.54
hsa-mir-6804	1.40
hsa-miR-3195	1.39
hsa-miR-4689	1.39
hsa-miR-1470	1.38
hsa-miR-541-5p	1.33
hsa-miR-718	1.33
hsa-miR-564	1.32
hsa-mir-663b	1.32
hsa-miR-6835-3p	1.31

Table 9-16: miRNA transcripts shown as up-regulated upon CITCO treatment in primary human hepatocytes over 24 hours. Fold change > 1.3

Transcript ID	Fold Change (CITCO vs. DMSO)
hsa-miR-335-5p	-1.91
hsa-miR-6735-5p	-1.60
hsa-miR-6741-5p	-1.40
hsa-miR-8075	-1.49
hsa-miR-3945	-1.42
hsa-miR-4445-3p	-1.42
hsa-miR-6741-5p	-1.40
hsa-miR-6738-5p	-1.36
ACA37	-1.31
hsa-miR-501-3p	-1.30

Table 9-17: miRNA transcripts shown as down-regulated upon CITCO treatment in primary human hepatocytes over 24 hours. Fold change > -1.3

The list of differentially regulated miRNAs is small at 24 hours which is in line with previously published literature that suggests it requires repeated activation of CAR to illicit substantial changes in the miRNAome (Koufaris et al., 2013). To confirm that the changes in miRNA expression are accurate a confirmation study using SYBR green qPCR was carried out according to methods described previously in sections 7.12 and 7.14. Briefly, total RNA was reverse transcribed to DNA using polyadenylation and reverse transcription. This was then used in a SYBR green qPCR reaction to quantify expression of the specific miRNAs. Data from this experiment is shown in Figure 9-15 and Table 9-18.

The fold changes associated with each miRNA when the expression profiles are examined using SYBR green qPCR indicates that the differential direction of expression concurs with that observed using the full miRNA array. What is different is the magnitude of fold change associated with each miRNA. Some

are over estimated by miRNA array compared to SYBR green and some are under estimated.

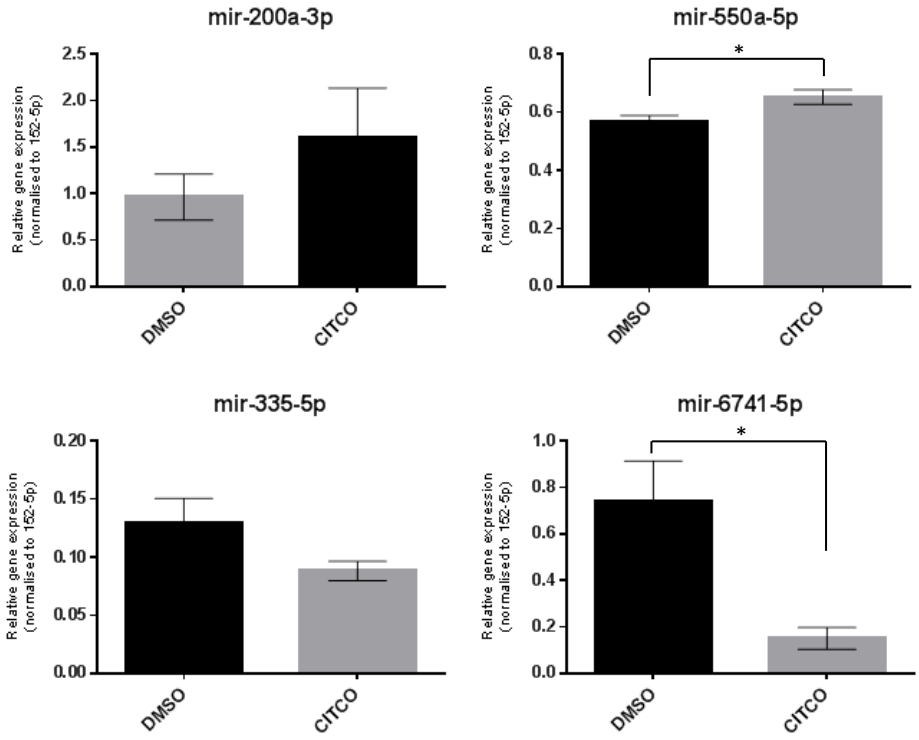

Figure 9-15: Differing expression patterns, generated by SYBR green qPCR, of the top two up and down regulated miRNA transcripts highlighted in the miRNA array performed on samples generated by treating with CITCO for 24 hours. Data are shown as mean +/- SEM. N = 4. Unpaired T-test, * = $P < 0.05$.

Transcript ID	miRNA Array Fold Change	SYBR Green qPCR Fold Change
miR-200a-3p	1.97	1.67
miR-550a-5p	1.60	1.15
miR-335-5p	-1.91	-1.47
miR-6741-5p	-1.60	-4.91

Table 9-18: Fold change values generated by the full miRNA array compared to those generated using SYBR green qPCR.

9.11 miRNA changes associated with direct hCAR activation at 5 days

Having examined the samples presented at 24 hours and found that the changes in gene miRNA expression profile were small the samples from the 5 day study were also examined using the same method as previously described. The differentially expressed miRNA transcripts are shown in Table 9-19 and Table 9-20.

Transcript ID	Fold Change
hsa-miR-3613-5p	2.096
hsa-miR-4668-5p	1.983
hsa-miR-548ac	1.935
hsa-miR-6750-5p	1.898
mmu-miR-7116-5p	1.697
mmu-miR-6906-5p	1.680
hsa-miR-1298-3p	1.679
mmu-miR-6983-5p	1.616
mmu-miR-6949-5p	1.526
hsa-miR-16-2-3p	1.470
mmu-miR-7001-5p	1.464
mmu-mir-465c-1	1.435
mmu-mir-465c-2	1.435
hsa-mir-6080	1.394
hsa-mir-4530	1.388
hsa-mir-548ab	1.367
hsa-miR-340-5p	1.358
hsa-miR-668-5p	1.352
hsa-miR-4446-3p	1.347
mmu-miR-3113-3p	1.345
hsa-miR-6728-5p	1.310
hsa-mir-548ab	1.302

Table 9-19: miRNA transcripts shown as up-regulated upon CITCO treatment in primary human hepatocytes over 5 days. Fold change > 1.3

Transcript ID	Fold Change
mmu-miR-7047-3p	-2.352
hsa-miR-642a-3p	-2.032
hsa-miR-642b-3p	-1.978
hsa-miR-1281	-1.730
mmu-miR-7033-5p	-1.721
hsa-miR-188-5p	-1.680
hsa-miR-1238-3p	-1.652
hsa-miR-6780b-5p	-1.651
hsa-miR-1973	-1.630
hsa-miR-5739	-1.623
mmu-miR-7018-5p	-1.570
hsa-miR-4433-3p	-1.505
hsa-miR-6069	-1.502
mmu-miR-7088-5p	-1.462
hsa-miR-7150	-1.460
mmu-miR-7040-5p	-1.451
hsa-miR-6124	-1.451
hsa-miR-4534	-1.427
hsa-miR-4290	-1.413
hsa-miR-4485	-1.408
hsa-miR-6891-5p	-1.396
hsa-miR-7107-5p	-1.394
hsa-mir-3123	-1.375
hsa-mir-663b	-1.371
hsa-mir-663b	-1.347
mmu-miR-194-2-3p	-1.345
mmu-miR-6240	-1.343
hsa-miR-194-3p	-1.339
mmu-miR-6973a-5p	-1.315

Table 9-20: miRNA transcripts shown as down-regulated upon CITCO treatment in primary human hepatocytes over 5 days. Fold change > -1.3

Comparing these lists to those produced after 24 hours CITCO treatment it is clear to see that there are more differentially expressed miRNA transcripts.

A follow up confirmation study using SYBR green qPCR was undertaken to confirm that the differential gene expression pattern observed using the miRNA array was consistent with qPCR. Figure 9-16 presents data gained

when miRNA transcript expression is investigated by SYBR green qPCR and Table 9-21 is a summary of the fold changes observed in both miRNA array and SYBR green qPCR.

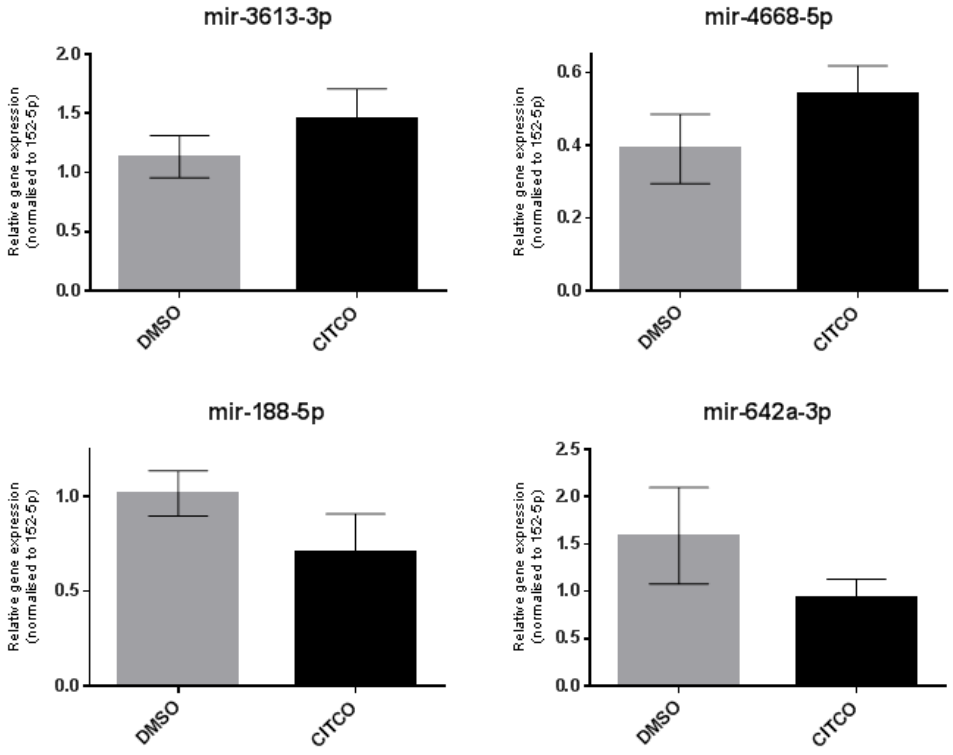

Figure 9-16: Differing expression patterns, generated by SYBR green qPCR, of two up and down regulated miRNA transcripts highlighted in the miRNA array performed on samples generated by treating with CITCO over 5 days. Data are shown as mean +/- SEM.

Transcript ID	miRNA Array Fold Change	SYBR Green qPCR Fold Change
miR-3613-3p	2.096	1.275
miR-4668-5p	1.983	1.389
miR-188-5p	-2.032	-1.450
miR-642a-3p	-1.680	-1.702

Table 9-21: Fold change values generated by the miRNA array compared to those generated using SYBR green qPCR for transcripts differentially regulated after 5 days treatment with CITCO.

From examining the data produced it is clear that there are discrepancies between the fold changes produced by the miRNA array and those produced using SYBR green qPCR. However the direction of expression is consistent for all miRNA transcripts investigated. This follows the pattern observed when looking at the 24 hours samples; despite the differences in fold change the miRNA expression pattern as a whole is accurate when assessing the transcripts with the highest fold change.

9.11.1 miR-21 up-regulation in response to CITCO treatment

The design of miRNA 4.0 array chip allows the simultaneous measurement of human and rodent miRNA transcripts in addition to miRNA transcripts across all species. For the previous analysis only the human and rodent transcripts have been included but when all transcripts of all species are included one miRNA that is particularly implicated in a wide variety of cancers (Calin and Croce, 2006) become clearly up-regulated, miR-21. The miR-21 transcript was consistently shown as being up-regulated in response to CITCO treatment in primary human hepatocytes with fold changes ranging from +3.145 to +1.550. As a consequence of this the expression of human miR-21-5p was also studied using SYBR green qPCR Figure 9-17. What became clear was that expression of

the human version of miR-21 was also up-regulated upon treatment of primary human hepatocytes with CITCO for 5 days.

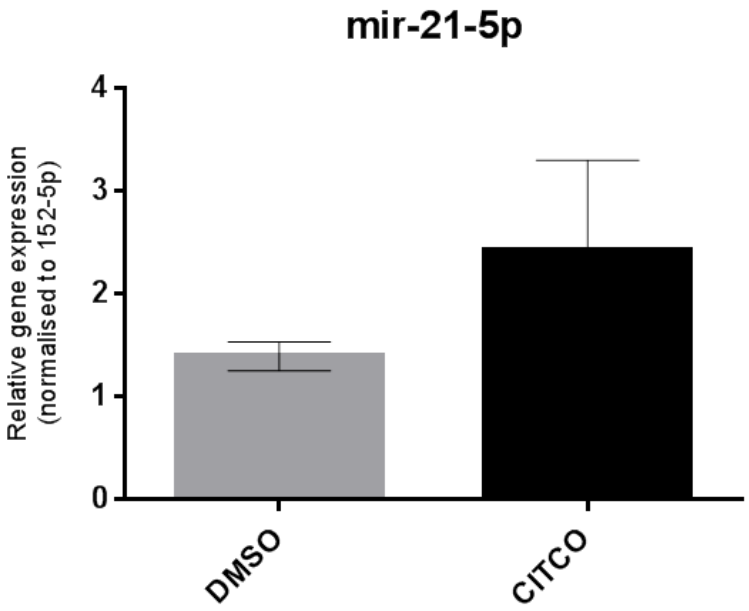

Figure 9-17: Expression profile of human miR-21-5p in primary human hepatocytes treated with CITCO for 5 days. Fold change observed is +1.746. Data are shown as mean +/- SEM.

9.12 Expression changes compared to previous rodent data

When comparing the changes in gene and miRNA expression observed in our human *in vitro* study to the data available in rodent *in vivo* experiments similarities and differences become clear. The number and magnitude of the gene expression changes at 24 hours was small but when more in depth analysis was carried out the gene expression changes pointed towards a pro-proliferative phenotype and increased risk of eventual hepatocarcinoma (section 9.9). This is in line with previous rodent data produced looking at indirect activation of rCAR by phenobarbital (Whysner et al., 1996). Also

consistent with rodent data produced *in vivo* was the up-regulation of miR-200 (Koufaris et al., 2013). The difference between this rodent data and our human *in vitro* data is the time period during which miR-200 is up-regulated and the length of miR-200 up-regulation. Rodent miR-200 is only up-regulated after a period of 14 days phenobarbital dosing and then remains up regulated over the course of exposure and during the entire proliferative response. This led to changes in global cell methylation state via zinc finger enhancer binding proteins (zeb1/zeb2). These zinc finger proteins are thought to aid the epithelial to mesenchymal transition; a fundamental process in development and disease, specifically cancer (Brabletz and Brabletz, 2010). When primary human hepatocytes *in* vitro are treated with CITCO miR-200 becomes up-regulated during the first 24 hours dosing. By 5 days repeated dosing miR-200 is no longer up-regulated according to our data. What this means for a pro-proliferative phenotype is unclear at this stage. Proliferation in response to direct activation of hCAR is not guaranteed despite the pathway analysis highlighting many pro-proliferative pathways. To investigate whether primary hepatocytes proliferate in response to CITCO treatment the assessment of BrdU incorporation was carried out.

9.13 Lack of proliferation in response to CITCO treatment in primary human hepatocytes

Having analysed both the mRNA and miRNA expression in response to CITCO treatment the conclusion that a more proliferative phenotype was observed when hepatocytes were treated with CITCO. To determine whether this caused proliferation of primary human hepatocytes *in vitro* a proliferation assay was carried out. Primary human hepatocytes were isolated and cultured as previously described in sections 7.2 and 7.4 and treated with CITCO for a period of 5 days. Proliferation was measured using the rate of BrdU incorporation during the final 24 hours in culture as described in section 7.6. Analysis of CYP2B6 expression was also undertaken to ensure that the hepatocytes were isolated from a patient who showed a robust response to direct hCAR activation. CYP2B6 induction is shown in Figure 9-18.

Figure 9-18 demonstrates that CITCO treatment of primary human hepatocytes isolated from patient L252 has caused a significant induction of CYP2B6 expression. This suggests that direct activation of hCAR in these primary hepatocytes is occurring as per those studied during the microarray. When the data from the proliferation assay is examined Figure 9-19 it becomes clear that there is no proliferation occurring in response to CITCO treatment.

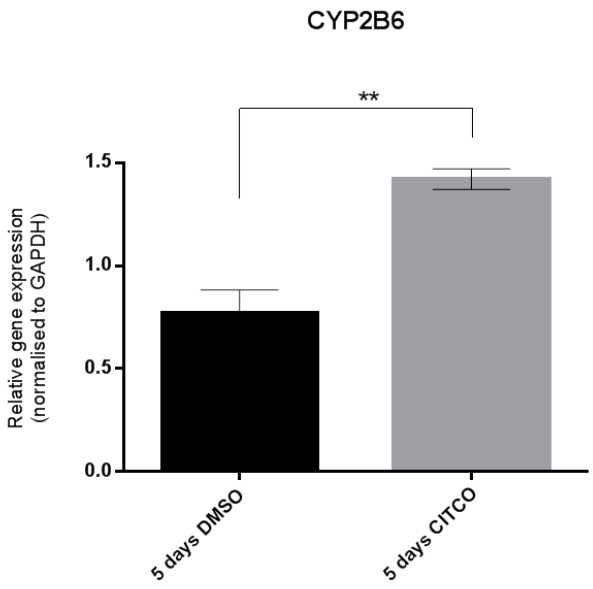

Figure 9-18: CYP2B6 gene expression in primary human hepatocytes isolated from patient L252 in response to CITCO treatment over 5 days. Fold change observed = +1.844. ** = $p < 0.01$, unpaired t-test, N= 4. Data are shown as mean +/- SEM.

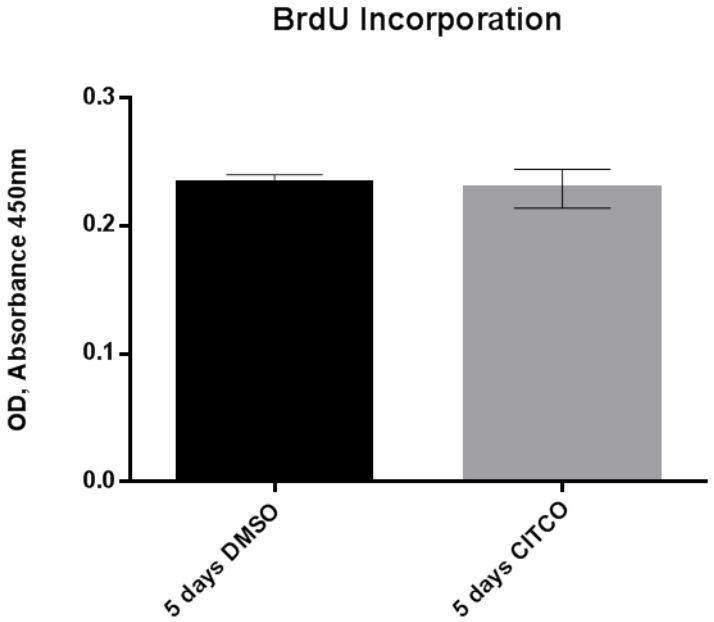

Figure 9-19: BrdU incorporation assay as a measure of proliferation in primary human hepatocytes isolated from patient L252 and treated with CITCO over 5 days. Data are presented as mean +/- SEM. N = 4.

10 Discussion

The mechanism of indirect CAR activation in rodents and the outcome of repeated dosing of rodents with known CAR activators has been reported previously (see section 5.3.2.2). Upon exposure to phenobarbital, an indirect activator of rodent CAR, rodent liver shows signs of hepatomegaly, proliferation and eventual hepatocarcinoma (Huang et al., 2005a); however the effect in human hepatic cells is less clear. There is a pressing need to investigate the effect of direct hCAR activation in human hepatic cells. This need comes from the potential for human exposure to direct hCAR activators that are present in many pharmaceuticals, industrial chemicals and crop protection agents (Stanley et al., 2006, di Masi et al., 2009, Zhang et al., 2006).

Primary human hepatocytes represent the gold standard when it comes to studying human hepatocyte function *in vitro*. The phenotype displayed by primary human hepatocytes is as similar to that *in vivo* as it is currently possible to be. The maintenance of *in vivo* hepatic phenotype is beneficial when studying cellular functions specific to human hepatocytes. The most significant problem arising when primary hepatocytes are cultured *in vitro* is the dedifferentiation and cell death shown during the first few days in culture (Bissell et al., 1987b, Clayton and Darnell, 1983b, Godoy et al., 2009b, Koide et al., 1989b, Tong et al., 1994). To prevent the dedifferentiation of primary human hepatocytes *in vitro* three dimensional dynamic culture is often employed in an attempt to mimic *in vivo* conditions. By culturing primary

human hepatocytes in a dynamic three dimensional system *in* vitro we were able to maintain hepatic phenotype for longer than traditional static culture (section 8.4). Primary human hepatocytes also showed improved metabolic function and energy production when compared to static conditions. The study of direct hCAR activation by CITCO was possible due to the maintenance of hepatic phenotype. Despite the success of this dynamic three dimensional culture system, there remain some limitations to using primary human hepatocytes. one of which is that experiments were still reliant on the availability of suitable tissue donated via hepatic resections. Due to a good relationship and network between our lab, the Nottingham University Hospitals Trust BioBank and surgeons carrying out operations the availability of tissue was maximised. However there were still periods where tissue demand exceeded supply. There is no easy fix to this limitation of using primary human hepatocytes. We carried out steps aimed at maximising supply; we are located in the same building as major centre of liver surgery, have maintained good links with surgeons and are able to isolate primary human hepatocytes routinely and repeatedly from tissue arriving at any time. Other strategies that may help improve the availability of representative and good quality cells rely on the improvement of differentiation protocols used to differentiate liver stem cells into mature differentiated hepatocytes with an *in vivo* like phenotype. Earlier in 2015 a method describing the long term expansion and differentiation into functional hepatocytes was published (Huch et al., 2015). This paper sets out a promising set of protocols that

enable the isolation of liver stem cells, the subsequent expansion of these cells and finally the differentiation into functional human hepatocytes. This method could lead to a solution that removes the current limitation of a lack of human tissue available for primary hepatocyte isolation.

Having established that hepatic phenotype and metabolic function were maintained over the course of 5 days post hepatocyte isolation the direct activation of hCAR was studied. Using primary human hepatocytes isolated in our lab we found that 5 days was the time period at which hCAR dependant cytochrome P450 (CYP2B6) induction was highest (section 8.6). When gene expression changes associated with direct hCAR activation at 24 hours were studied few gene expression changes were observed. This is not entirely unexpected as *in vivo* rodent data suggests that the larger scale gene expression changes are not seen until later in the dosing regimen (Koufaris et al., 2013). The 24 hour gene expression data observed when the hepatocytes isolated from two patients are used highlights a further complication that has to be taken into consideration, inter-patient variability. In one of these patients changes in gene expression in response to CITCO treatment were low (L233) and there were few genes that were found to be differentially regulated. In the second patient (L225) however, more substantial changes were observed. There was greater consensus between patients when treated with CITCO for 5 days.

When an in depth analysis of the list of genes differentially expressed after 5 days treatment with CITCO was analysed in depth a similar but more pronounced pattern emerged. The gene expression changes suggested a pro-proliferative and anti-apoptotic phenotype (section 9.9). An important aspect of the data produced is that there was no proliferation seen in primary human hepatocytes *in vitro* in response to direct hCAR activation despite the pathway analysis predicting this may be the case.

What does this mean for human toxicity and cancer progression in response to direct hCAR activation? There could be a number of explanations for the lack of proliferation seen *in vitro* despite the indication that gene expression changes would have elicited a proliferative response. An obvious explanation would be that the changes in gene expression were insufficient to cause a proliferative response on their own. This doesn't necessarily indicate that exposure to direct hCAR activators is safe. An additive effect of a second or even third hepatic insult combining with the pro-proliferative phenotype associated with direct hCAR activation could then cause proliferation and liver hyperplasia. A further possibility is that gene expression changes and proliferation are being held in check and the response shown is nothing more than a physiological response aiding the body with the metabolism of compounds responsible for direct hCAR activation.

An extra layer of complexity is the probability that changes in miRNA expression is having an effect on the toxicological outcome of direct hCAR

activation. For example miR-200 which is up-regulated in response to phenobarbital treatment in rodent studies (Koufaris et al., 2012) is up-regulated during the first 24 hours in primary human hepatocytes but subsequently drops away over the next 4 days. The explanation for this could be that the initial response to direct hCAR activation does not reach a critical threshold above which proliferation would occur so there is a subsequent reduction in miR-200 expression. Whether miR-200 is causal or a consequence remains to be investigated.

Further investigation into the mechanisms underlying direct hCAR activation and the subsequent response of the human liver will help to shed light on the potential toxicity associated with direct hCAR activators. An initial step to help with this is the issue of donor patient variability. Gene expression changes associated with nuclear receptor activation are likely to be in the order of tens and hundreds at most whereas the changes in gene expression between two patients are likely to be in the order of thousands of genes. The removal of inter-patient variability can be achieved in a number of ways. The obvious is to limit samples to those produced using the same donor patient. This is a robust way to limit variability however is not always the most useful or practical approach. A wide cross section of the population will be exposed to hCAR activating compounds so multiple donors are important. A data and mathematical approach is a further way to help remove patient variability. What was clear in the PCA plots shown in section 9.4 is that the principle

component of variation is patient identity and not CITCO treatment. Projection score analysis is a mathematical analysis that enables the removal of known unwanted variables such as inter-patient variability (Fontes and Soneson, 2011). This can be applied to data sets already collected so a logical first step would be a re-analysis of the current data using projection score analysis to remove patient variability.

Further work to identify other direct hCAR activators other than CITCO that are selective towards hCAR rather than PXR will help to determine whether the gene expression changes shown here are specific to treatment with CITCO or are common to all direct activators of hCAR. Following on from this, if the gene expression changes are ligand specific what is causing these changes? A possibility is the creation of secondary metabolites caused by the initial induction of cytochrome P450 enzymes that are able to metabolise ligands and form potentially reactive species that are the cause of the proliferative phenotype. Ultimately the goal is to understand the effect that gene expression and miRNA changes as a result of hCAR activation have in human hepatic cells and whether activation of hCAR in humans is a risk factor in the progression of hepatocellular carcinoma and wider toxicity. To achieve this a better understanding of the mechanisms underpinning and controlling the gene expression changes, and the interplay of miRNA in this process, is required.

11 Appendix

"Log Ratio" values in all subsequent tables are taken directly from GeneSpring GX13 without any changes or manipulation. The software presents the log ratios as a positive or negative number to enable easier interpretation of the results.

11.1 Appendix I (Differentially Regulated Genes in Patient L225 after 24 hours CITCO Dosing)

Fold Change	Log Ratio	Symbol	Entrez Gene Name	Location	Type(s)
1.937	0.954	SCARNA3	small Cajal body-specific RNA 3	Other	other
1.780	0.832	CYP2A6 (includes others)	cytochrome P450, family 2, subfamily A, polypeptide 6	Cytoplasm	enzyme
1.729	0.790	CYP2B7P	cytochrome P450, family 2, subfamily B, polypeptide 7, pseudogene	Other	enzyme
1.613	0.690	CYP2B6	cytochrome P450, family 2, subfamily B, polypeptide 6	Cytoplasm	enzyme
1.601	0.679	SNORA2A	small nucleolar RNA, H/ACA box 2A	Other	other
1.557	0.639	CYP2A6 (includes others)	cytochrome P450, family 2, subfamily A, polypeptide 6	Cytoplasm	enzyme
1.418	0.504	CYP2C8	cytochrome P450, family 2, subfamily C, polypeptide 8	Cytoplasm	enzyme
1.383	0.468	CYP2A7P1	cytochrome P450, family 2, subfamily A, polypeptide 7 pseudogene 1	Other	other
1.351	0.434	LINC01564	long intergenic non-protein coding RNA 1564	Other	other
1.344	0.427	PLOD2	procollagen-lysine, 2-oxoglutarate 5-	Cytoplasm	enzyme

			dioxygenase 2		
1.343	0.426	EID3	EP300 interacting inhibitor of differentiation 3	Cytoplasm	other
1.333	0.414	CLIP1	CAP-GLY domain containing linker protein 1	Cytoplasm	other
1.326	0.407	AKR1B10	aldo-keto reductase family 1, member B10 (aldose reductase)	Cytoplasm	enzyme
1.322	0.402	SNORA14A	small nucleolar RNA, H/ACA box 14A	Other	other
1.303	0.382	GCLM	glutamate-cysteine ligase, modifier subunit	Cytoplasm	enzyme
1.299	0.378	SLC7A11	solute carrier family 7 (anionic amino acid transporter light chain, xc- system), member 11	Plasma Membrane	transporter
1.293	0.371	ERN1	endoplasmic reticulum to nucleus signalling 1	Cytoplasm	kinase
1.290	0.368	F2RL2	coagulation factor II (thrombin) receptor-like 2	Plasma Membrane	G-protein coupled receptor
1.280	0.356	RNU6-21P	RNA, U6 small nuclear 21, pseudogene	Other	other
1.278	0.354	TXNRD1	thioredoxin reductase 1	Cytoplasm	enzyme
1.276	0.351	ALAS1	5'-aminolevulinate synthase 1	Cytoplasm	enzyme
1.275	0.351	TULP3	tubby like protein 3	Extracellular Space	other
1.270	0.345	NTN4	netrin 4	Extracellular Space	other
1.266	0.341	PKD1P6	polycystic kidney disease 1 (autosomal dominant) pseudogene 6	Other	other
1.265	0.339	LUCAT1	lung cancer associated transcript 1 (non-protein coding)	Other	other
1.264	0.338	LOC101927136	uncharacterized LOC101927136	Other	other
1.263	0.337	USP12	ubiquitin specific peptidase 12	Cytoplasm	peptidase
1.262	0.335	FAT1	FAT atypical cadherin 1	Plasma Membrane	other
1.259	0.332	SERPINE1	serpin peptidase inhibitor, clade E	Extracellular Space	other

			(nexin, plasminogen activator inhibitor type 1), member 1		
1.257	0.330	mir-548	microRNA 548c	Cytoplasm	microRNA
1.257	0.329	GDF15	growth differentiation factor 15	Extracellular Space	growth factor
1.256	0.328	DLGAP1-AS2	DLGAP1 antisense RNA 2	Other	other
1.254	0.327	TMSB10/TMSB4X	thymosin beta 10	Cytoplasm	other
1.254	0.327	CCL20	chemokine (C-C motif) ligand 20	Extracellular Space	cytokine
1.252	0.324	NPIPA8 (includes others)	nuclear pore complex interacting protein family, member A1	Nucleus	other
1.251	0.323	PKD1P1	polycystic kidney disease 1 (autosomal dominant) pseudogene 1	Other	other
-1.254	-0.327	ABCG8	ATP-binding cassette, sub-family G (WHITE), member 8	Plasma Membrane	transporter
-1.255	-0.328	LOC728040	hCG1813624	Other	other
-1.258	-0.331	AVPR1A	arginine vasopressin receptor 1A	Plasma Membrane	G-protein coupled receptor
-1.266	-0.341	RDH16	retinol dehydrogenase 16 (all-trans)	Cytoplasm	enzyme
-1.277	-0.353	FBP1	fructose-1,6-bisphosphatase 1	Cytoplasm	phosphatase
-1.281	-0.358	DHODH	dihydroorotate dehydrogenase (quinone)	Cytoplasm	enzyme
-1.283	-0.359	GPD1	glycerol-3-phosphate dehydrogenase 1 (soluble)	Cytoplasm	enzyme
-1.288	-0.365	MIR4757	microRNA 4757	Cytoplasm	microRNA
-1.293	-0.371	mir-197	microRNA 197	Cytoplasm	microRNA
-1.296	-0.374	GNMT	glycine N-methyltransferase	Cytoplasm	enzyme
-1.298	-0.377	MFSD2A	major facilitator superfamily domain containing 2A	Plasma Membrane	transporter
-1.300	-0.379	GLDC	glycine dehydrogenase (decarboxylating)	Cytoplasm	enzyme
-1.303	-0.381	MIR4646	microRNA 4646	Cytoplasm	microRNA
-1.311	-0.390	ADH6	alcohol dehydrogenase 6 (class V)	Cytoplasm	enzyme

-1.323	-0.403	COL7A1	collagen, type VII, alpha 1	Extracellular Space	other
-1.325	-0.406	PCK1	phosphoenolpyruvate carboxykinase 1 (soluble)	Cytoplasm	kinase
-1.338	-0.420	MIR1470	microRNA 1470	Cytoplasm	microRNA
-1.350	-0.433	CPS1	carbamoyl-phosphate synthase 1, mitochondrial	Cytoplasm	enzyme
-1.379	-0.463	CPS1-IT1	CPS1 intronic transcript 1	Other	other
-1.384	-0.469	MIR4740	microRNA 4740	Cytoplasm	microRNA
-1.394	-0.479	BHMT	betaine--homocysteine S-methyltransferase	Cytoplasm	enzyme
-1.419	-0.505	SLC38A4	solute carrier family 38, member 4	Plasma Membrane	transporter
-1.436	-0.522	SLC2A2	solute carrier family 2 (facilitated glucose transporter), member 2	Plasma Membrane	transporter
-1.702	-0.767	CYP1A1	cytochrome P450, family 1, subfamily A, polypeptide 1	Cytoplasm	enzyme
-1.722	-0.784	CYP1A2	cytochrome P450, family 1, subfamily A, polypeptide 2	Cytoplasm	enzyme

11.2 Appendix II (Differentially Regulated Genes After 5 Days Repeated CITCO Dosing)

Fold Change	Log Ratio	Symbol	Entrez Gene Name	Location	Type(s)
1.870	0.903	EGOT	eosinophil granule ontogeny transcript (non-protein coding)	Other	other
1.684	0.752	METTL7B	methyltransferase like 7B	Other	enzyme
1.681	0.749	CYP2B7P	cytochrome P450, family 2, subfamily B, polypeptide 7, pseudogene	Other	enzyme
1.614	0.691	ANKRD1	ankyrin repeat domain 1 (cardiac muscle)	Cytoplasm	transcription regulator
1.595	0.674	CCAT1	colon cancer	Other	other

			associated transcript 1 (non-protein coding)		
1.595	0.674	CYP2B6	cytochrome P450, family 2, subfamily B, polypeptide 6	Cytoplasm	enzyme
1.531	0.614	EMP3	epithelial membrane protein 3	Plasma Membrane	other
1.528	0.612	MSN	moesin	Plasma Membrane	other
1.492	0.577	RAB3B	RAB3B, member RAS oncogene family	Cytoplasm	enzyme
1.487	0.572	CCL20	chemokine (C-C motif) ligand 20	Extracellular Space	cytokine
1.470	0.556	PLOD2	procollagen-lysine, 2-oxoglutarate 5-dioxygenase 2	Cytoplasm	enzyme
1.466	0.552	SERPINE1	serpin peptidase inhibitor, clade E (nexin, plasminogen activator inhibitor type 1), member 1	Extracellular Space	other
1.458	0.544	C14orf105	chromosome 14 open reading frame 105	Other	other
1.457	0.543	GBE1	glucan (1,4-alpha-), branching enzyme 1	Cytoplasm	enzyme
1.447	0.533	AJUBA	ajuba LIM protein	Nucleus	transcription regulator
1.440	0.526	TPRG1-AS1	TPRG1 antisense RNA 1	Other	other
1.439	0.525	GPX2	glutathione peroxidase 2	Cytoplasm	enzyme
1.433	0.519	NTN4	netrin 4	Extracellular Space	other
1.431	0.517	GDF15	growth differentiation factor 15	Extracellular Space	growth factor
1.423	0.509	APOBEC3B	apolipoprotein B mRNA editing enzyme, catalytic polypeptide-like 3B	Cytoplasm	enzyme
1.418	0.504	GLIPR1	GLI pathogenesis-related 1	Extracellular Space	other
1.417	0.502	FAT1	FAT atypical cadherin 1	Plasma Membrane	other
1.405	0.491	EGR1	early growth response 1	Nucleus	transcription regulator
1.403	0.488	ABCB1	ATP-binding cassette, sub-family B (MDR/TAP), member 1	Plasma Membrane	transporter
1.385	0.470	GUCA2B	guanylate cyclase	Extracellular	other

			activator 2B (uroguanylin)	Space	
1.376	0.460	PLP2	proteolipid protein 2 (colonic epithelium-enriched)	Cytoplasm	transporter
1.374	0.459	LUCAT1	lung cancer associated transcript 1 (non-protein coding)	Other	other
1.361	0.444	TAAR3	trace amine associated receptor 3 (gene/pseudogene)	Plasma Membrane	G-protein coupled receptor
1.357	0.441	ITGAV	integrin, alpha V	Plasma Membrane	ion channel
1.353	0.437	FLRT3	fibronectin leucine rich transmembrane protein 3	Plasma Membrane	other
1.349	0.432	PIK3AP1	phosphoinositide-3-kinase adaptor protein 1	Cytoplasm	other
1.343	0.425	INHBC	inhibin, beta C	Extracellular Space	growth factor
1.334	0.416	HABP2	hyaluronan binding protein 2	Extracellular Space	peptidase
1.326	0.408	MT1F	metallothionein 1F	Other	other
1.325	0.406	HSPB1	heat shock 27kDa protein 1	Cytoplasm	other
1.321	0.401	SOX4	SRY (sex determining region Y)-box 4	Nucleus	transcription regulator
1.320	0.401	KYNU	kynureninase	Cytoplasm	enzyme
1.309	0.388	VIL1	villin 1	Cytoplasm	other
1.305	0.384	KPNA2	karyopherin alpha 2 (RAG cohort 1, importin alpha 1)	Nucleus	transporter
1.305	0.384	IL32	interleukin 32	Extracellular Space	cytokine
1.304	0.383	MPZL2	myelin protein zero-like 2	Plasma Membrane	other
1.296	0.374	SERPINB9	serpin peptidase inhibitor, clade B (ovalbumin), member 9	Cytoplasm	other
1.294	0.371	DIO1	deiodinase, iodothyronine, type I	Cytoplasm	enzyme
1.290	0.367	DNM1P46	dynamin 1 pseudogene 46	Other	other
1.287	0.364	SDCBP2	syndecan binding protein (syntenin) 2	Cytoplasm	other
1.283	0.359	TES	testin LIM domain protein	Plasma Membrane	other
1.282	0.358	LRG1	leucine-rich alpha-2-glycoprotein 1	Extracellular Space	other

1.272	0.347	TXNRD1	thioredoxin reductase 1	Cytoplasm	enzyme
1.272	0.347	mir-21	microRNA 21	Cytoplasm	microRNA
1.270	0.345	CCL2	chemokine (C-C motif) ligand 2	Extracellular Space	cytokine
1.268	0.343	BMP2	bone morphogenetic protein 2	Extracellular Space	growth factor
1.268	0.343	CCNI	cyclin I	Other	other
1.264	0.338	JUN	jun proto-oncogene	Nucleus	transcription regulator
1.263	0.337	TNFRSF12A	tumor necrosis factor receptor superfamily, member 12A	Plasma Membrane	transmembrane receptor
1.262	0.336	PLIN2	perilipin 2	Plasma Membrane	other
1.261	0.335	LASP1	LIM and SH3 protein 1	Cytoplasm	transporter
1.260	0.333	mir-4796	microRNA 4796	Cytoplasm	microRNA
1.259	0.332	VLDLR	very low density lipoprotein receptor	Plasma Membrane	transporter
1.256	0.328	ACTN1	actinin, alpha 1	Cytoplasm	transcription regulator
1.255	0.327	TSKU	tsukushi, small leucine rich proteoglycan	Extracellular Space	other
1.254	0.327	SDC4	syndecan 4	Plasma Membrane	other
1.252	0.324	RAB8B	RAB8B, member RAS oncogene family	Cytoplasm	enzyme
1.251	0.323	mir-622	microRNA 622	Cytoplasm	microRNA
1.250	0.322	HS1BP3-IT1	HS1BP3 intronic transcript 1	Other	other
-1.251	-0.323	MPC1	mitochondrial pyruvate carrier 1	Cytoplasm	other
-1.251	-0.323	TRPM7	transient receptor potential cation channel, subfamily M, member 7	Plasma Membrane	kinase
-1.254	-0.326	ARHGEF26	Rho guanine nucleotide exchange factor (GEF) 26	Plasma Membrane	other
-1.255	-0.328	DNAAF2	dynein, axonemal, assembly factor 2	Cytoplasm	other
-1.257	-0.330	TP53INP1	tumor protein p53 inducible nuclear protein 1	Nucleus	other
-1.257	-0.330	KNG1	kininogen 1	Extracellular Space	other
-1.261	-0.335	SLC25A30	solute carrier family 25, member 30	Cytoplasm	other
-1.262	-0.335	ALDH7A1	aldehyde dehydrogenase 7	Cytoplasm	enzyme

			family, member A1		
-1.263	-0.337	LOC101927269	uncharacterized LOC101927269	Other	other
-1.266	-0.340	UPB1	ureidopropionase, beta	Cytoplasm	enzyme
-1.266	-0.340	SLC23A2	solute carrier family 23 (ascorbic acid transporter), member 2	Plasma Membrane	transporter
-1.266	-0.340	AGL	amylo-alpha-1, 6-glucosidase, 4-alpha-glucanotransferase	Cytoplasm	enzyme
-1.267	-0.341	SC5D	sterol-C5-desaturase	Cytoplasm	enzyme
-1.269	-0.344	AGXT	alanine-glyoxylate aminotransferase	Cytoplasm	enzyme
-1.270	-0.345	ADGRA3	adhesion G protein-coupled receptor A3	Plasma Membrane	G-protein coupled receptor
-1.270	-0.345	RNU6-31P	RNA, U6 small nuclear 31, pseudogene	Other	other
-1.272	-0.347	OAF	OAF homolog (Drosophila)	Cytoplasm	other
-1.272	-0.347	ETNK2	ethanolamine kinase 2	Cytoplasm	kinase
-1.272	-0.347	SLC22A25	solute carrier family 22, member 25	Other	other
-1.272	-0.347	LRIG3	leucine-rich repeats and immunoglobulin-like domains 3	Extracellular Space	other
-1.273	-0.348	FAM35DP	family with sequence similarity 35, member A pseudogene	Other	other
-1.274	-0.350	SIK2	salt-inducible kinase 2	Cytoplasm	kinase
-1.275	-0.351	REPS1	RALBP1 associated Eps domain containing 1	Plasma Membrane	other
-1.276	-0.352	CYP2E1	cytochrome P450, family 2, subfamily E, polypeptide 1	Cytoplasm	enzyme
-1.276	-0.352	LOC100287497	uncharacterized LOC100287497	Other	other
-1.278	-0.354	CTH	cystathionine gamma-lyase	Cytoplasm	enzyme
-1.279	-0.355	ARG1	arginase 1	Cytoplasm	enzyme
-1.281	-0.357	ECHDC2	enoyl CoA hydratase domain containing 2	Other	other
-1.281	-0.357	ERBB3	erb-b2 receptor tyrosine kinase 3	Plasma Membrane	kinase
-1.281	-0.357	SNORD58C	small nucleolar RNA, C/D box 58C	Other	other

-1.282	-0.358	MLXIPL	MLX interacting protein-like	Nucleus	transcription regulator
-1.282	-0.359	ABCA9	ATP-binding cassette, sub-family A (ABC1), member 9	Cytoplasm	transporter
-1.286	-0.363	KCNK5	potassium channel, two pore domain subfamily K, member 5	Plasma Membrane	ion channel
-1.288	-0.365	MAOA	monoamine oxidase A	Cytoplasm	enzyme
-1.291	-0.369	EGFR	epidermal growth factor receptor	Plasma Membrane	kinase
-1.292	-0.370	TMEM56	transmembrane protein 56	Other	other
-1.293	-0.371	BAAT	bile acid CoA:amino acid N-acyltransferase	Cytoplasm	enzyme
-1.297	-0.376	CFHR2	complement factor H-related 2	Extracellular Space	other
-1.299	-0.377	DHX35	DEAH (Asp-Glu-Ala-His) box polypeptide 35	Other	enzyme
-1.299	-0.377	ADH1B	alcohol dehydrogenase 1B (class I), beta polypeptide	Cytoplasm	enzyme
-1.301	-0.380	PPM1L	protein phosphatase, Mg2+/Mn2+ dependent, 1L	Cytoplasm	phosphatase
-1.304	-0.383	ADAM20P1	ADAM metallopeptidase domain 20 pseudogene 1	Other	other
-1.306	-0.385	AADAT	aminoadipate aminotransferase	Cytoplasm	enzyme
-1.306	-0.385	PFKFB1	6-phosphofructo-2-kinase/fructose-2,6-biphosphatase 1	Cytoplasm	kinase
-1.309	-0.388	CDKN2AIP	CDKN2A interacting protein	Nucleus	transcription regulator
-1.311	-0.390	PON3	paraoxonase 3	Extracellular Space	enzyme
-1.312	-0.392	HSD11B1	hydroxysteroid (11-beta) dehydrogenase 1	Cytoplasm	enzyme
-1.315	-0.396	CAT	catalase	Cytoplasm	enzyme
-1.316	-0.396	GANC	glucosidase, alpha; neutral C	Extracellular Space	enzyme
-1.316	-0.396	SNORD63	small nucleolar RNA, C/D box 63	Other	other
-1.322	-0.403	HRSP12	heat-responsive	Cytoplasm	enzyme

			protein 12		
-1.324	-0.405	CAPN7	calpain 7	Cytoplasm	peptidase
-1.325	-0.406	KIAA1551	KIAA1551	Other	other
-1.327	-0.408	SEC14L2	SEC14-like 2 (S. cerevisiae)	Cytoplasm	transporter
-1.327	-0.408	GPT2	glutamic pyruvate transaminase (alanine aminotransferase) 2	Cytoplasm	enzyme
-1.328	-0.409	FAM83D	family with sequence similarity 83, member D	Other	other
-1.328	-0.410	PRKAB2	protein kinase, AMP-activated, beta 2 non-catalytic subunit	Cytoplasm	kinase
-1.335	-0.417	KLKB1	kallikrein B, plasma (Fletcher factor) 1	Extracellular Space	peptidase
-1.336	-0.418	FAM76B	family with sequence similarity 76, member B	Nucleus	other
-1.337	-0.419	HMGN3	high mobility group nucleosomal binding domain 3	Nucleus	other
-1.342	-0.424	MME	membrane metallo-endopeptidase	Plasma Membrane	peptidase
-1.343	-0.426	HP	haptoglobin	Extracellular Space	peptidase
-1.347	-0.429	TTPA	tocopherol (alpha) transfer protein	Cytoplasm	transporter
-1.356	-0.439	CIART	circadian associated repressor of transcription	Nucleus	other
-1.362	-0.445	RNU11	RNA, U11 small nuclear	Nucleus	other
-1.363	-0.447	AFM	afamin	Extracellular Space	transporter
-1.364	-0.448	ALDH1L1	aldehyde dehydrogenase 1 family, member L1	Cytoplasm	enzyme
-1.367	-0.451	PER3	period circadian clock 3	Nucleus	other
-1.367	-0.451	IGFBP2	insulin-like growth factor binding protein 2, 36kDa	Extracellular Space	other
-1.377	-0.462	C6	complement component 6	Extracellular Space	other
-1.378	-0.463	ADH1C	alcohol dehydrogenase 1C (class I), gamma polypeptide	Cytoplasm	enzyme
-1.378	-0.463	TNFSF10	tumor necrosis factor (ligand) superfamily,	Extracellular Space	cytokine

			member 10		
-1.380	-0.464	SLC2A2	solute carrier family 2 (facilitated glucose transporter), member 2	Plasma Membrane	transporter
-1.384	-0.469	HPR	haptoglobin-related protein	Extracellular Space	peptidase
-1.384	-0.469	HSD17B14	hydroxysteroid (17-beta) dehydrogenase 14	Cytoplasm	enzyme
-1.384	-0.469	LINC01018	long intergenic non-protein coding RNA 1018	Other	other
-1.394	-0.479	HSD17B7P2	hydroxysteroid (17-beta) dehydrogenase 7 pseudogene 2	Other	other
-1.397	-0.482	MIR3646	microRNA 3646	Cytoplasm	microRNA
-1.403	-0.488	SLC38A4	solute carrier family 38, member 4	Plasma Membrane	transporter
-1.406	-0.492	FBP1	fructose-1,6-bisphosphatase 1	Cytoplasm	phosphatase
-1.407	-0.493	HAO2-IT1	HAO2 intronic transcript 1	Other	other
-1.408	-0.493	TBC1D2B	TBC1 domain family, member 2B	Other	other
-1.411	-0.497	SAT2	spermidine/spermine N1-acetyltransferase family member 2	Plasma Membrane	enzyme
-1.411	-0.497	PCK1	phosphoenolpyruvate carboxykinase 1 (soluble)	Cytoplasm	kinase
-1.420	-0.506	HSD17B7	hydroxysteroid (17-beta) dehydrogenase 7	Cytoplasm	enzyme
-1.420	-0.506	GPAM	glycerol-3-phosphate acyltransferase, mitochondrial	Cytoplasm	enzyme
-1.429	-0.515	C9	complement component 9	Extracellular Space	other
-1.431	-0.517	FKBP5	FK506 binding protein 5	Nucleus	enzyme
-1.431	-0.517	ACSM3	acyl-CoA synthetase medium-chain family member 3	Cytoplasm	enzyme
-1.433	-0.519	HMGCS2	3-hydroxy-3-methylglutaryl-CoA synthase 2 (mitochondrial)	Cytoplasm	enzyme
-1.437	-0.524	AKR1C6P	aldo-keto reductase family 1, member C6, pseudogene	Other	enzyme
-1.450	-0.536	ACADSB	acyl-CoA	Cytoplasm	enzyme

			dehydrogenase, short/branched chain		
-1.456	-0.542	ABCC9	ATP-binding cassette, sub-family C (CFTR/MRP), member 9	Plasma Membrane	ion channel
-1.457	-0.543	SCP2	sterol carrier protein 2	Cytoplasm	transporter
-1.457	-0.543	ADH1A	alcohol dehydrogenase 1A (class I), alpha polypeptide	Cytoplasm	enzyme
-1.460	-0.546	LOC102723766	uncharacterized LOC102723766	Other	other
-1.462	-0.548	ARRDC3	arrestin domain containing 3	Plasma Membrane	other
-1.464	-0.550	UAP1	UDP-N-acetylglucosamine pyrophosphorylase 1	Nucleus	enzyme
-1.468	-0.554	AASS	aminoadipate-semialdehyde synthase	Cytoplasm	enzyme
-1.480	-0.566	mir-548	microRNA 548c	Cytoplasm	microRNA
-1.499	-0.584	GYS2	glycogen synthase 2 (liver)	Cytoplasm	enzyme
-1.502	-0.586	GLS2	glutaminase 2 (liver, mitochondrial)	Cytoplasm	enzyme
-1.502	-0.587	MDN1	MDN1, midasin homolog (yeast)	Nucleus	other
-1.509	-0.594	LINC00844	long intergenic non-protein coding RNA 844	Other	other
-1.518	-0.602	ANKRD28	ankyrin repeat domain 28	Cytoplasm	other
-1.519	-0.603	INSIG1	insulin induced gene 1	Cytoplasm	other
-1.523	-0.607	SAMHD1	SAM domain and HD domain 1	Nucleus	enzyme
-1.601	-0.679	IGFBP1	insulin-like growth factor binding protein 1	Extracellular Space	other
-1.655	-0.726	HOMER2	homer scaffolding protein 2	Plasma Membrane	other
-1.675	-0.744	IRS2	insulin receptor substrate 2	Cytoplasm	enzyme
-1.689	-0.756	HAO2	hydroxyacid oxidase 2 (long chain)	Cytoplasm	enzyme
-2.078	-1.055	GNMT	glycine N-methyltransferase	Cytoplasm	enzyme
-2.139	-1.097	PDK4	pyruvate dehydrogenase kinase, isozyme 4	Cytoplasm	kinase

12 References

ALAVANJA, M. C. & BONNER, M. R. 2005. Pesticides and human cancers. *Cancer investigation,* 23**,** 700-11.

ALTOMARE, D. A. & TESTA, J. R. 2005. Perturbations of the AKT signaling pathway in human cancer. *Oncogene,* 24**,** 7455-64.

BAEK, D., VILLEN, J., SHIN, C., CAMARGO, F. D., GYGI, S. P. & BARTEL, D. P. 2008. The impact of microRNAs on protein output. *Nature,* 455**,** 64-71.

BAIN, D. L., HENEGHAN, A. F., CONNAGHAN-JONES, K. D. & MIURA, M. T. 2007. Nuclear receptor structure: implications for function. *Annual review of physiology,* 69**,** 201-20.

BAKER, T. K., CARFAGNA, M. A., GAO, H., DOW, E. R., LI, Q. Q., SEARFOSS, G. H. & RYAN, T. P. 2001. Temporal gene expression analysis of monolayer cultured rat hepatocytes. *Chemical research in toxicology,* 14**,** 1218-1231.

BARTEL, D. P. 2004. MicroRNAs: genomics, biogenesis, mechanism, and function. *Cell,* 116**,** 281-97.

BAUER, D., WOLFRAM, N., KAHL, G. F. & HIRSCH-ERNST, K. I. 2004. Transcriptional regulation of CYP2B1 induction in primary rat hepatocyte cultures: repression by epidermal growth factor is mediated via a distal enhancer region. *Molecular pharmacology,* 65**,** 172-80.

BEIGEL, J., FELLA, K., KRAMER, P. J., KROEGER, M. & HEWITT, P. 2008. Genomics and proteomics analysis of cultured primary rat hepatocytes. *Toxicology in Vitro,* 22**,** 171-181.

BELLACOSA, A., KUMAR, C. C., DI CRISTOFANO, A. & TESTA, J. R. 2005. Activation of AKT kinases in cancer: implications for therapeutic targeting. *Advances in cancer research,* 94**,** 29-86.

BERTHIAUME, F., MOGHE, P. V., TONER, M. & YARMUSH, M. L. 1996. Effect of extracellular matrix topology on cell structure, function, and physiological responsiveness: hepatocytes cultured in a sandwich configuration. *FASEB journal : official publication of the Federation of American Societies for Experimental Biology,* 10**,** 1471-84.

BISSELL, D. M., ARENSON, D. M., MAHER, J. J. & ROLL, F. J. 1987a. Support of Cultured-Hepatocytes by a Laminin-Rich Gel - Evidence for a Functionally Significant Subendothelial Matrix in Normal Rat-Liver. *Journal of Clinical Investigation,* 79**,** 801-812.

BISSELL, D. M., ARENSON, D. M., MAHER, J. J. & ROLL, F. J. 1987b. Support of cultured hepatocytes by a laminin-rich gel. Evidence for a functionally significant subendothelial matrix in normal rat liver. *The Journal of clinical investigation,* 79**,** 801-12.

BLUMBERG, B., SABBAGH, W., JR., JUGUILON, H., BOLADO, J., JR., VAN METER, C. M., ONG, E. S. & EVANS, R. M. 1998. SXR, a novel steroid and xenobiotic-sensing nuclear receptor. *Genes & development,* 12**,** 3195-205.

BRABLETZ, S. & BRABLETZ, T. 2010. The ZEB/miR-200 feedback loop--a motor of cellular plasticity in development and cancer? *EMBO reports,* 11**,** 670-7.

BURK, O., ARNOLD, K. A., GEICK, A., TEGUDE, H. & EICHELBAUM, M. 2005. A role for constitutive androstane receptor in the regulation of human intestinal MDR1 expression. *Biological chemistry,* 386**,** 503-13.

CALIN, G. A. & CROCE, C. M. 2006. MicroRNA signatures in human cancers. *Nature reviews. Cancer,* 6**,** 857-66.

CHANG, T. T. & HUGHES-FULFORD, M. 2009. Monolayer and spheroid culture of human liver hepatocellular carcinoma cell line cells demonstrate distinct global gene expression patterns and functional phenotypes. *Tissue engineering. Part A,* 15**,** 559-67.

CHO, C. H., PARK, J., NAGRATH, D., TILLES, A. W., BERTHIAUME, F., TONER, M. & YARMUSH, M. L. 2007. Oxygen uptake rates and liver-specific functions of hepatocyte and 3T3 fibroblast co-cultures. *Biotechnology and bioengineering,* 97**,** 188-99.

CLAYTON, D. F. & DARNELL, J. E. 1983a. Changes in Liver-Specific Compared to Common Gene-Transcription during Primary Culture of Mouse Hepatocytes. *Molecular and Cellular Biology,* 3**,** 1552-1561.

CLAYTON, D. F. & DARNELL, J. E., JR. 1983b. Changes in liver-specific compared to common gene transcription during primary culture of mouse hepatocytes. *Molecular and Cellular Biology,* 3**,** 1552-61.

CLAYTON, D. F., HARRELSON, A. L. & DARNELL, J. E. 1985. Dependence of Liver-Specific Transcription on Tissue Organization. *Molecular and Cellular Biology,* 5**,** 2623-2632.

DASH, A., INMAN, W., HOFFMASTER, K., SEVIDAL, S., KELLY, J., OBACH, R. S., GRIFFITH, L. G. & TANNENBAUM, S. R. 2009. Liver tissue engineering in the evaluation of drug safety. *Expert opinion on drug metabolism & toxicology,* 5**,** 1159-74.

DI MASI, A., DE MARINIS, E., ASCENZI, P. & MARINO, M. 2009. Nuclear receptors CAR and PXR: Molecular, functional, and biomedical aspects. *Molecular aspects of medicine,* 30**,** 297-343.

DOMANSKY, K., INMAN, W., SERDY, J., DASH, A., LIM, M. H. & GRIFFITH, L. G. 2010. Perfused multiwell plate for 3D liver tissue engineering. *Lab on a chip,* 10**,** 51-8.

DONATO, M. T., LAHOZ, A., CASTELL, J. V. & GOMEZ-LECHON, M. J. 2008. Cell lines: a tool for in vitro drug metabolism studies. *Current drug metabolism,* 9**,** 1-11.

DUNN, J. C., TOMPKINS, R. G. & YARMUSH, M. L. 1991. Long-term in vitro function of adult hepatocytes in a collagen sandwich configuration. *Biotechnology progress,* 7**,** 237-45.

DUSSAULT, I., LIN, M., HOLLISTER, K., FAN, M., TERMINI, J., SHERMAN, M. A. & FORMAN, B. M. 2002. A structural model of the constitutive androstane receptor defines novel interactions that mediate ligand-independent activity. *Molecular and Cellular Biology,* 22**,** 5270-80.

ELAUT, G., HENKENS, T., PAPELEU, P., SNYKERS, S., VINKEN, M., VANHAECKE, T. & ROGIERS, V. 2006. Molecular mechanisms underlying the dedifferentiation process of isolated hepatocytes and their cultures. *Current drug metabolism,* 7**,** 629-660.

ELORANTA, J. J., MEIER, P. J. & KULLAK-UBLICK, G. A. 2005. Coordinate transcriptional regulation of transport and metabolism. *Phase Ii Conjugation Enzymes and Transport Systems,* 400**,** 511-+.

EULALIO, A., HUNTZINGER, E. & IZAURRALDE, E. 2008. Getting to the root of miRNA-mediated gene silencing. *Cell,* 132**,** 9-14.

FAUCETTE, S. R., SUEYOSHI, T., SMITH, C. M., NEGISHI, M., LECLUYSE, E. L. & WANG, H. 2006. Differential regulation of hepatic CYP2B6 and CYP3A4 genes by constitutive androstane receptor but not pregnane X receptor. *The Journal of pharmacology and experimental therapeutics,* 317**,** 1200-9.

FILIPOWICZ, W., BHATTACHARYYA, S. N. & SONENBERG, N. 2008. Mechanisms of post-transcriptional regulation by microRNAs: are the answers in sight? *Nature reviews. Genetics,* 9**,** 102-14.

FONTES, M. & SONESON, C. 2011. The projection score--an evaluation criterion for variable subset selection in PCA visualization. *BMC bioinformatics,* 12**,** 307.

FORMAN, B. M., TZAMELI, I., CHOI, H. S., CHEN, J., SIMHA, D., SEOL, W., EVANS, R. M. & MOORE, D. D. 1998. Androstane metabolites bind to and deactivate the nuclear receptor CAR-beta. *Nature,* 395**,** 612-5.

FUNATSU, K., IJIMA, H., NAKAZAWA, K., YAMASHITA, Y., SHIMADA, M. & SUGIMACHI, K. 2001. Hybrid artificial liver using hepatocyte organoid culture. *Artificial organs,* 25**,** 194-200.

GAO, J., HE, J., ZHAI, Y., WADA, T. & XIE, W. 2009. The constitutive androstane receptor is an anti-obesity nuclear receptor that improves insulin sensitivity. *The Journal of biological chemistry,* 284**,** 25984-92.

GERBAL-CHALOIN, S., PASCUSSI, J. M., PICHARD-GARCIA, L., DAUJAT, M., WAECHTER, F., FABRE, J. M., CARRERE, N. & MAUREL, P. 2001. Induction of CYP2C genes in human hepatocytes in primary culture. *Drug metabolism and disposition: the biological fate of chemicals,* 29**,** 242-51.

GIGUERE, V. 1999. Orphan nuclear receptors: from gene to function. *Endocrine reviews,* 20**,** 689-725.

GODOY, P., HENGSTLER, J. G., ILKAVETS, I., MEYER, C., BACHMANN, A., MULLER, A., TUSCHL, G., MUELLER, S. O. & DOOLEY, S. 2009a. Extracellular Matrix Modulates Sensitivity of Hepatocytes to Fibroblastoid Dedifferentiation and Transforming Growth Factor beta-induced Apoptosis. *Hepatology,* 49**,** 2031-2043.

GODOY, P., HENGSTLER, J. G., ILKAVETS, I., MEYER, C., BACHMANN, A., MULLER, A., TUSCHL, G., MUELLER, S. O. & DOOLEY, S. 2009b. Extracellular matrix modulates sensitivity of hepatocytes to fibroblastoid dedifferentiation and transforming growth factor beta-induced apoptosis. *Hepatology,* 49**,** 2031-43.

GOODWIN, B., HODGSON, E. & LIDDLE, C. 1999. The orphan human pregnane X receptor mediates the transcriptional activation of CYP3A4 by rifampicin through a distal enhancer module. *Molecular pharmacology,* 56**,** 1329-39.

GOODWIN, B., MOORE, L. B., STOLTZ, C. M., MCKEE, D. D. & KLIEWER, S. A. 2001. Regulation of the human CYP2B6 gene by the nuclear pregnane X receptor. *Molecular pharmacology,* 60**,** 427-31.

GRIFFITH, L. G. & SWARTZ, M. A. 2006. Capturing complex 3D tissue physiology in vitro. *Nature reviews. Molecular cell biology,* 7**,** 211-24.

HANDSCHIN, C. & MEYER, U. A. 2003. Induction of drug metabolism: the role of nuclear receptors. *Pharmacological reviews,* 55**,** 649-73.

HAO, J., ZHANG, Y., DENG, M., YE, R., ZHAO, S., WANG, Y., LI, J. & ZHAO, Z. 2014. MicroRNA control of epithelial-mesenchymal transition in cancer stem cells. *International journal of cancer. Journal international du cancer,* 135**,** 1019-27.

HE, L., HE, X., LIM, L. P., DE STANCHINA, E., XUAN, Z., LIANG, Y., XUE, W., ZENDER, L., MAGNUS, J., RIDZON, D., JACKSON, A. L., LINSLEY, P. S., CHEN, C., LOWE, S. W., CLEARY, M. A. & HANNON, G. J. 2007. A microRNA component of the p53 tumour suppressor network. *Nature,* 447**,** 1130-4.

HERNANDEZ, J. P., MOTA, L. C. & BALDWIN, W. S. 2009. Activation of CAR and PXR by Dietary, Environmental and Occupational Chemicals Alters Drug Metabolism, Intermediary Metabolism, and Cell Proliferation. *Current pharmacogenomics and personalized medicine,* 7**,** 81-105.

HONKAKOSKI, P., ZELKO, I., SUEYOSHI, T. & NEGISHI, M. 1998. The nuclear orphan receptor CAR-retinoid X receptor heterodimer activates the phenobarbital-responsive enhancer module of the CYP2B gene. *Molecular and Cellular Biology,* 18**,** 5652-8.

HUANG, W., ZHANG, J., WASHINGTON, M., LIU, J., PARANT, J. M., LOZANO, G. & MOORE, D. D. 2005a. Xenobiotic stress induces hepatomegaly and liver tumors via the nuclear receptor constitutive androstane receptor. *Molecular Endocrinology,* 19**,** 1646-53.

HUANG, W. D., ZHANG, J., WASHINGTON, M., LIU, J., PARANT, J. M., LOZANO, G. & MOORE, D. D. 2005b. Xenobiotic stress induces hepatomegaly and liver tumors via the nuclear receptor constitutive androstane receptor. *Molecular Endocrinology,* 19**,** 1646-1653.

HUCH, M., GEHART, H., VAN BOXTEL, R., HAMER, K., BLOKZIJL, F., VERSTEGEN, M. M., ELLIS, E., VAN WENUM, M., FUCHS, S. A., DE LIGT, J., VAN DE WETERING, M., SASAKI, N., BOERS, S. J., KEMPERMAN, H., DE JONGE, J., IJZERMANS, J. N., NIEUWENHUIS, E. E., HOEKSTRA, R., STROM, S., VRIES, R. R., VAN DER LAAN, L. J., CUPPEN, E. & CLEVERS, H. 2015. Long-term culture of genome-stable bipotent stem cells from adult human liver. *Cell,* 160**,** 299-312.

HUTVAGNER, G. & ZAMORE, P. D. 2002. A microRNA in a multiple-turnover RNAi enzyme complex. *Science,* 297**,** 2056-60.

JEYARATNAM, J. 1990. Acute pesticide poisoning: a major global health problem. *World health statistics quarterly. Rapport trimestriel de statistiques sanitaires mondiales,* 43**,** 139-44.

JOANNARD, F., RISSEL, M., GILOT, D., ANDERSON, A., ORFILA-LEFEUVRE, L., GUILLOUZO, A., ATFI, A. & LAGADIC-GOSSMANN, D. 2006. Role for mitogen-activated protein kinases in phenobarbital-induced expression of cytochrome P450 2B in primary cultures of rat hepatocytes. *Toxicology Letters,* 161**,** 61-72.

JOHNSON, S. M., GROSSHANS, H., SHINGARA, J., BYROM, M., JARVIS, R., CHENG, A., LABOURIER, E., REINERT, K. L., BROWN, D. & SLACK, F. J. 2005. RAS is regulated by the let-7 microRNA family. *Cell,* 120**,** 635-47.

KANEBRATT, K. P. & ANDERSSON, T. B. 2008. Evaluation of HepaRG cells as an in vitro model for human drug metabolism studies. *Drug metabolism and disposition: the biological fate of chemicals,* 36**,** 1444-52.

KANNO, Y., SUZUKI, M., NAKAHAMA, T. & INOUYE, Y. 2005. Characterization of nuclear localization signals and cytoplasmic retention region in the nuclear receptor CAR. *Biochimica et biophysica acta,* 1745**,** 215-22.

KAST, H. R., GOODWIN, B., TARR, P. T., JONES, S. A., ANISFELD, A. M., STOLTZ, C. M., TONTONOZ, P., KLIEWER, S., WILLSON, T. M. & EDWARDS, P. A. 2002. Regulation of multidrug resistance-associated protein 2 (ABCC2) by the nuclear receptors pregnane X receptor, farnesoid X-activated receptor, and constitutive androstane receptor. *The Journal of biological chemistry,* 277**,** 2908-15.

KAWAMOTO, T., SUEYOSHI, T., ZELKO, I., MOORE, R., WASHBURN, K. & NEGISHI, M. 1999. Phenobarbital-responsive nuclear translocation of the receptor CAR in induction of the CYP2B gene. *Molecular and Cellular Biology,* 19**,** 6318-22.

KELM, J. M., DJONOV, V., ITTNER, L. M., FLURI, D., BORN, W., HOERSTRUP, S. P. & FUSSENEGGER, M. 2006. Design of custom-shaped vascularized tissues using microtissue spheroids as minimal building units. *Tissue engineering,* 12**,** 2151-60.

KELM, J. M. & FUSSENEGGER, M. 2004. Microscale tissue engineering using gravity-enforced cell assembly. *Trends in biotechnology,* 22**,** 195-202.

KELM, J. M., TIMMINS, N. E., BROWN, C. J., FUSSENEGGER, M. & NIELSEN, L. K. 2003. Method for generation of homogeneous multicellular tumor spheroids applicable to a wide variety of cell types. *Biotechnology and bioengineering,* 83**,** 173-80.

KIENHUIS, A. S., WORTELBOER, H. M., MAAS, W. J., VAN HERWIJNEN, M., KLEINJANS, J. C., VAN DELFT, J. H. & STIERUM, R. H. 2007. A sandwich-cultured rat hepatocyte system with increased metabolic competence evaluated by gene expression profiling. *Toxicology in vitro : an international journal published in association with BIBRA,* 21**,** 892-901.

KIM, Y., LASHER, C. D., MILFORD, L. M., MURALI, T. M. & RAJAGOPALAN, P. 2010. A comparative study of genome-wide transcriptional profiles of primary hepatocytes in collagen sandwich and monolayer cultures. *Tissue engineering. Part C, Methods,* 16**,** 1449-60.

KLIEWER, S. A., GOODWIN, B. & WILLSON, T. M. 2002. The nuclear pregnane X receptor: a key regulator of xenobiotic metabolism. *Endocrine reviews,* 23**,** 687-702.

KOBAYASHI, K., SUEYOSHI, T., INOUE, K., MOORE, R. & NEGISHI, M. 2003. Cytoplasmic accumulation of the nuclear receptor CAR by a tetratricopeptide repeat protein in HepG2 cells. *Molecular pharmacology,* 64**,** 1069-75.

KOEBE, H. G., PAHERNIK, S., EYER, P. & SCHILDBERG, F. W. 1994. Collagen gel immobilization: a useful cell culture technique for long-term metabolic studies on human hepatocytes. *Xenobiotica; the fate of foreign compounds in biological systems,* 24**,** 95-107.

KOIDE, N., SHINJI, T., TANABE, T., ASANO, K., KAWAGUCHI, M., SAKAGUCHI, K., KOIDE, Y., MORI, M. & TSUJI, T. 1989a. Continued High Albumin Production by Multicellular Spheroids of Adult-Rat Hepatocytes Formed in the Presence of Liver-Derived Proteoglycans. *Biochemical and Biophysical Research Communications,* 161**,** 385-391.

KOIDE, N., SHINJI, T., TANABE, T., ASANO, K., KAWAGUCHI, M., SAKAGUCHI, K., KOIDE, Y., MORI, M. & TSUJI, T. 1989b. Continued high albumin production by multicellular spheroids of adult rat hepatocytes formed in the presence of liver-derived proteoglycans. *Biochemical and Biophysical Research Communications,* 161**,** 385-91.

KOIKE, C., MOORE, R. & NEGISHI, M. 2007a. Extracellular signal-regulated kinase is an endogenous signal retaining the nuclear constitutive active/androstane receptor (CAR) in the cytoplasm of mouse primary hepatocytes. *Molecular Pharmacology,* 71**,** 1217-1221.

KOIKE, C., MOORE, R. & NEGISHI, M. 2007b. Extracellular signal-regulated kinase is an endogenous signal retaining the nuclear constitutive active/androstane receptor (CAR) in the cytoplasm of mouse primary hepatocytes. *Molecular pharmacology,* 71**,** 1217-21.

KOUFARIS, C., WRIGHT, J., CURRIE, R. A. & GOODERHAM, N. J. 2012. Hepatic microRNA profiles offer predictive and mechanistic insights after exposure to genotoxic and epigenetic hepatocarcinogens. *Toxicological sciences : an official journal of the Society of Toxicology,* 128**,** 532-43.

KOUFARIS, C., WRIGHT, J., OSBORNE, M., CURRIE, R. A. & GOODERHAM, N. J. 2013. Time and dose-dependent effects of phenobarbital on the rat liver miRNAome. *Toxicology,* 314**,** 247-53.

KRIEGER, R. I. 2001. *Handbook of pesticide toxicology,* San Diego, Calif. ; London, Academic.

KUMAR, R. & THOMPSON, E. B. 1999. The structure of the nuclear hormone receptors. *Steroids,* 64**,** 310-9.

LEE, P. J., HUNG, P. J. & LEE, L. P. 2007. An artificial liver sinusoid with a microfluidic endothelial-like barrier for primary hepatocyte culture. *Biotechnology and bioengineering,* 97**,** 1340-6.

LI, A. P., KAMINSKI, D. L. & RASMUSSEN, A. 1995. Substrates of human hepatic cytochrome P450 3A4. *Toxicology,* 104**,** 1-8.

LI, H., CHEN, T., COTTRELL, J. & WANG, H. 2009. Nuclear translocation of adenoviral-enhanced yellow fluorescent protein-tagged-human constitutive androstane receptor (hCAR): a novel tool for screening hCAR activators in human primary hepatocytes. *Drug metabolism and disposition: the biological fate of chemicals,* 37**,** 1098-106.

LI, L., CHEN, T., STANTON, J. D., SUEYOSHI, T., NEGISHI, M. & WANG, H. 2008. The peripheral benzodiazepine receptor ligand 1-(2-chlorophenyl-methylpropyl)-3-isoquinoline-carboxamide is a novel antagonist of human constitutive androstane receptor. *Molecular pharmacology,* 74**,** 443-53.

LILLEGARD, J. B., FISHER, J. E., NEDREDAL, G., LUEBKE-WHEELER, J., BAO, J., WANG, W., AMOIT, B. & NYBERG, S. L. 2011. Normal atmospheric oxygen tension and the use of antioxidants improve hepatocyte spheroid viability and function. *Journal of cellular physiology,* 226**,** 2987-96.

LU, J., GETZ, G., MISKA, E. A., ALVAREZ-SAAVEDRA, E., LAMB, J., PECK, D., SWEET-CORDERO, A., EBERT, B. L., MAK, R. H., FERRANDO, A. A., DOWNING, J. R., JACKS, T., HORVITZ, H. R. & GOLUB, T. R. 2005. MicroRNA expression profiles classify human cancers. *Nature,* 435**,** 834-8.

LUBBERSTEDT, M., MULLER-VIEIRA, U., MAYER, M., BIEMEL, K. M., KNOSPEL, F., KNOBELOCH, D., NUSSLER, A. K., GERLACH, J. C. & ZEILINGER, K. 2011. HepaRG human hepatic cell line utility as a surrogate for primary human hepatocytes in drug metabolism assessment in vitro. *Journal of pharmacological and toxicological methods,* 63**,** 59-68.

MACDOUGALL, J. D. & MCCABE, M. 1967. Diffusion coefficient of oxygen through tissues. *Nature,* 215**,** 1173-4.

MAGLICH, J. M., PARKS, D. J., MOORE, L. B., COLLINS, J. L., GOODWIN, B., BILLIN, A. N., STOLTZ, C. A., KLIEWER, S. A., LAMBERT, M. H., WILLSON, T. M. & MOORE, J. T. 2003. Identification of a novel human constitutive androstane receptor (CAR) agonist and its use in the identification of CAR target genes. *The Journal of biological chemistry,* 278**,** 17277-83.

MAGLICH, J. M., STOLTZ, C. M., GOODWIN, B., HAWKINS-BROWN, D., MOORE, J. T. & KLIEWER, S. A. 2002. Nuclear pregnane x receptor and constitutive androstane receptor regulate overlapping but distinct sets of genes involved in xenobiotic detoxification. *Molecular pharmacology,* 62**,** 638-46.

MAKINEN, J., FRANK, C., JYRKKARINNE, J., GYNTHER, J., CARLBERG, C. & HONKAKOSKI, P. 2002. Modulation of mouse and human phenobarbital-responsive enhancer module by nuclear receptors. *Molecular pharmacology,* 62**,** 366-78.

MATSUSHITA, T., IJIMA, H., KOIDE, N. & FUNATSU, K. 1991. High Albumin Production by Multicellular Spheroids of Adult-Rat Hepatocytes Formed in the Pores of Polyurethane Foam. *Applied Microbiology and Biotechnology,* 36**,** 324-326.

MENG, F., HENSON, R., WEHBE-JANEK, H., GHOSHAL, K., JACOB, S. T. & PATEL, T. 2007. MicroRNA-21 regulates expression of the PTEN tumor suppressor gene in human hepatocellular cancer. *Gastroenterology,* 133**,** 647-58.

MOGHE, P. V., COGER, R. N., TONER, M. & YARMUSH, M. L. 1997. Cell-cell interactions are essential for maintenance of hepatocyte function in collagen gel but not on matrigel. *Biotechnology and bioengineering,* 56**,** 706-11.

MOLNAR, F., KUBLBECK, J., JYRKKARINNE, J., PRANTNER, V. & HONKAKOSKI, P. 2013. An update on the constitutive androstane receptor (CAR). *Drug metabolism and drug interactions,* 28**,** 79-93.

MOORE, L. B., PARKS, D. J., JONES, S. A., BLEDSOE, R. K., CONSLER, T. G., STIMMEL, J. B., GOODWIN, B., LIDDLE, C., BLANCHARD, S. G., WILLSON, T. M., COLLINS, J. L. & KLIEWER, S. A. 2000. Orphan nuclear receptors constitutive androstane receptor and pregnane X receptor share xenobiotic and steroid ligands. *The Journal of biological chemistry,* 275**,** 15122-7.

MULUKUTLA, B. C., KHAN, S., LANGE, A. & HU, W. S. 2010. Glucose metabolism in mammalian cell culture: new insights for tweaking vintage pathways. *Trends in biotechnology,* 28**,** 476-84.

MUTOH, S., OSABE, M., INOUE, K., MOORE, R., PEDERSEN, L., PERERA, L., REBOLLOSO, Y., SUEYOSHI, T. & NEGISHI, M. 2009. Dephosphorylation of threonine 38 is required for nuclear translocation and activation of human xenobiotic receptor CAR (NR1I3). *The Journal of biological chemistry,* 284**,** 34785-92.

MUTOH, S., SOBHANY, M., MOORE, R., PERERA, L., PEDERSEN, L., SUEYOSHI, T. & NEGISHI, M. 2013. Phenobarbital indirectly activates the constitutive active androstane receptor (CAR) by inhibition of epidermal growth factor receptor signaling. *Science signaling,* 6**,** ra31.

NEVEROVA, I., SCAMAN, C. H., SRIVASTAVA, O. P., SZWEDA, R., VIJAY, I. K. & PALCIC, M. M. 1994. A spectrophotometric assay for glucosidase I. *Analytical biochemistry,* 222**,** 190-5.

OSABE, M. & NEGISHI, M. 2011. Active ERK1/2 protein interacts with the phosphorylated nuclear constitutive active/androstane receptor (CAR; NR1I3), repressing dephosphorylation and sequestering CAR in the cytoplasm. *The Journal of biological chemistry,* 286**,** 35763-9.

PASCUSSI, J. M., GERBAL-CHALOIN, S., DROCOURT, L., ASSENAT, E., LARREY, D., PICHARD-GARCIA, L., VILAREM, M. J. & MAUREL, P. 2004. Cross-talk between xenobiotic detoxication and other signalling pathways: clinical and toxicological consequences. *Xenobiotica; the fate of foreign compounds in biological systems,* 34**,** 633-64.

PASCUSSI, J. M., GERBAL-CHALOIN, S., DURET, C., DAUJAT-CHAVANIEU, M., VILAREM, M. J. & MAUREL, P. 2008. The tangle of nuclear receptors that controls xenobiotic metabolism and transport: crosstalk and consequences. *Annual review of pharmacology and toxicology,* 48**,** 1-32.

PELKONEN, O., TURPEINEN, M., HAKKOLA, J., HONKAKOSKI, P., HUKKANEN, J. & RAUNIO, H. 2008. Inhibition and induction of human cytochrome P450 enzymes: current status. *Archives of toxicology,* 82**,** 667-715.

PESHWA, M. V., WU, F. J., SHARP, H. L., CERRA, F. B. & HU, W. S. 1996. Mechanistics of formation and ultrastructural evaluation of hepatocyte spheroids. *In vitro cellular & developmental biology. Animal,* 32**,** 197-203.

PRESTWICH, G. D., LIU, Y., YU, B., SHU, X. Z. & SCOTT, A. 2007. 3-D culture in synthetic extracellular matrices: new tissue models for drug toxicology and cancer drug discovery. *Advances in enzyme regulation,* 47**,** 196-207.

QATANANI, M. & MOORE, D. D. 2005. CAR, the continuously advancing receptor, in drug metabolism and disease. *Current drug metabolism,* 6**,** 329-39.

RANUCCI, C. S., KUMAR, A., BATRA, S. P. & MOGHE, P. V. 2000. Control of hepatocyte function on collagen foams: sizing matrix pores toward selective induction of 2-D and 3-D cellular morphogenesis. *Biomaterials,* 21**,** 783-93.

RESCHLY, E. J. & KRASOWSKI, M. D. 2006. Evolution and function of the NR1I nuclear hormone receptor subfamily (VDR, PXR, and CAR) with respect to metabolism of xenobiotics and endogenous compounds. *Current drug metabolism,* 7**,** 349-65.

RINGEL, M., VON MACH, M. A., SANTOS, R., FEILEN, P. J., BRULPORT, M., HERMES, M., BAUER, A. W., SCHORMANN, W., TANNER, B., SCHON, M. R., OESCH, F. & HENGSTLER, J. G. 2005. Hepatocytes cultured in alginate microspheres: an optimized technique to study enzyme induction. *Toxicology,* 206**,** 153-67.

ROBERTS, P. J. & DER, C. J. 2007. Targeting the Raf-MEK-ERK mitogen-activated protein kinase cascade for the treatment of cancer. *Oncogene,* 26**,** 3291-310.

RODRIGUEZ-ANTONA, C., DONATO, M. T., BOOBIS, A., EDWARDS, R. J., WATTS, P. S., CASTELL, J. V. & GOMEZ-LECHON, M. J. 2002. Cytochrome P450 expression in human hepatocytes and hepatoma cell lines: molecular mechanisms that determine lower expression in cultured cells. *Xenobiotica; the fate of foreign compounds in biological systems,* 32**,** 505-20.

ROTH, A., LOOSER, R., KAUFMANN, M., BLATTLER, S. M., RENCUREL, F., HUANG, W., MOORE, D. D. & MEYER, U. A. 2008. Regulatory cross-talk between drug metabolism and lipid homeostasis: constitutive androstane receptor and pregnane X receptor increase Insig-1 expression. *Molecular pharmacology,* 73**,** 1282-9.

ROWE, C., GOLDRING, C. E., KITTERINGHAM, N. R., JENKINS, R. E., LANE, B. S., SANDERSON, C., ELLIOTT, V., PLATT, V., METCALFE, P. & PARK, B. K. 2010. Network analysis of primary hepatocyte dedifferentiation using a shotgun proteomics approach. *Journal of proteome research,* 9**,** 2658-68.

ROWLEY, J. A., MADLAMBAYAN, G. & MOONEY, D. J. 1999. Alginate hydrogels as synthetic extracellular matrix materials. *Biomaterials,* 20**,** 45-53.

RUSYN, I. & CORTON, J. C. 2012. Mechanistic considerations for human relevance of cancer hazard of di(2-ethylhexyl) phthalate. *Mutation research,* 750**,** 141-58.

SCAMAN, C. H., LIPARI, F. & HERSCOVICS, A. 1996. A spectrophotometric assay for alpha-mannosidase activity. *Glycobiology,* 6**,** 265-70.

SEGLEN, P. O. 1976. Preparation of isolated rat liver cells. *Methods in cell biology,* 13**,** 29-83.

SELBACH, M., SCHWANHAUSSER, B., THIERFELDER, N., FANG, Z., KHANIN, R. & RAJEWSKY, N. 2008. Widespread changes in protein synthesis induced by microRNAs. *Nature,* 455**,** 58-63.

SHAN, L., VINCENT, J., BRUNZELLE, J. S., DUSSAULT, I., LIN, M., IANCULESCU, I., SHERMAN, M. A., FORMAN, B. M. & FERNANDEZ, E. J. 2004. Structure of the murine constitutive androstane receptor complexed to androstenol: a molecular basis for inverse agonism. *Molecular Cell,* 16**,** 907-17.

SIVARAMAN, A., LEACH, J. K., TOWNSEND, S., IIDA, T., HOGAN, B. J., STOLZ, D. B., FRY, R., SAMSON, L. D., TANNENBAUM, S. R. & GRIFFITH, L. G. 2005. A microscale in vitro

physiological model of the liver: predictive screens for drug metabolism and enzyme induction. *Current drug metabolism,* 6**,** 569-91.

SIVERTSSON, L., EK, M., DARNELL, M., EDEBERT, I., INGELMAN-SUNDBERG, M. & NEVE, E. P. 2010. CYP3A4 catalytic activity is induced in confluent Huh7 hepatoma cells. *Drug metabolism and disposition: the biological fate of chemicals,* 38**,** 995-1002.

STANLEY, L. A., HORSBURGH, B. C., ROSS, J., SCHEER, N. & WOLF, C. R. 2006. PXR and CAR: nuclear receptors which play a pivotal role in drug disposition and chemical toxicity. *Drug metabolism reviews,* 38**,** 515-97.

SUEYOSHI, T., KAWAMOTO, T., ZELKO, I., HONKAKOSKI, P. & NEGISHI, M. 1999a. The repressed nuclear receptor CAR responds to phenobarbital in activating the human CYP2B6 gene. *The Journal of biological chemistry,* 274**,** 6043-6.

SUEYOSHI, T., KAWAMOTO, T., ZELKO, I., HONKAKOSKI, P. & NEGISHI, M. 1999b. The repressed nuclear receptor CAR responds to phenobarbital in activating the human CYP2B6 gene. *Journal of Biological Chemistry,* 274**,** 6043-6046.

SUEYOSHI, T., MOORE, R., SUGATANI, J., MATSUMURA, Y. & NEGISHI, M. 2008. PPP1R16A, the membrane subunit of protein phosphatase 1beta, signals nuclear translocation of the nuclear receptor constitutive active/androstane receptor. *Molecular pharmacology,* 73**,** 1113-21.

SUEYOSHI, T. & NEGISHI, M. 2001. Phenobarbital response elements of cytochrome P450 genes and nuclear receptors. *Annual review of pharmacology and toxicology,* 41**,** 123-43.

SUGATANI, J., KOJIMA, H., UEDA, A., KAKIZAKI, S., YOSHINARI, K., GONG, Q. H., OWENS, I. S., NEGISHI, M. & SUEYOSHI, T. 2001. The phenobarbital response enhancer module in the human bilirubin UDP-glucuronosyltransferase UGT1A1 gene and regulation by the nuclear receptor CAR. *Hepatology,* 33**,** 1232-8.

SUINO, K., PENG, L., REYNOLDS, R., LI, Y., CHA, J. Y., REPA, J. J., KLIEWER, S. A. & XU, H. E. 2004. The nuclear xenobiotic receptor CAR: structural determinants of constitutive activation and heterodimerization. *Molecular Cell,* 16**,** 893-905.

SYNOLD, T. W., DUSSAULT, I. & FORMAN, B. M. 2001. The orphan nuclear receptor SXR coordinately regulates drug metabolism and efflux. *Nature medicine,* 7**,** 584-90.

TIRONA, R. G. & KIM, R. B. 2005. Nuclear receptors and drug disposition gene regulation. *Journal of Pharmaceutical Sciences,* 94**,** 1169-1186.

TONG, J. Z., DELAGAUSIE, P., FURLAN, V., CRESTEIL, T., BERNARD, O. & ALVAREZ, F. 1992. Long-Term Culture of Adult-Rat Hepatocyte Spheroids. *Experimental Cell Research,* 200**,** 326-332.

TONG, J. Z., SARRAZIN, S., CASSIO, D., GAUTHIER, F. & ALVAREZ, F. 1994. Application of spheroid culture to human hepatocytes and maintenance of their differentiation. *Biology of the cell / under the auspices of the European Cell Biology Organization,* 81**,** 77-81.

TROTTIER, E., BELZIL, A., STOLTZ, C. & ANDERSON, A. 1995. Localization of a phenobarbital-responsive element (PBRE) in the 5'-flanking region of the rat CYP2B2 gene. *Gene,* 158**,** 263-8.

TZAMELI, I. & MOORE, D. D. 2001. Role reversal: new insights from new ligands for the xenobiotic receptor CAR. *Trends in endocrinology and metabolism: TEM,* 12**,** 7-10.

TZAMELI, I., PISSIOS, P., SCHUETZ, E. G. & MOORE, D. D. 2000. The xenobiotic compound 1,4-bis[2-(3,5-dichloropyridyloxy)]benzene is an agonist ligand for the nuclear receptor CAR. *Molecular and Cellular Biology,* 20**,** 2951-8.

TZANAKAKIS, E. S., HANSEN, L. K. & HU, W. S. 2001. The role of actin filaments and microtubules in hepatocyte spheroid self-assembly. *Cell motility and the cytoskeleton,* 48**,** 175-89.

UEDA, A., HAMADEH, H. K., WEBB, H. K., YAMAMOTO, Y., SUEYOSHI, T., AFSHARI, C. A., LEHMANN, J. M. & NEGISHI, M. 2002. Diverse roles of the nuclear orphan receptor CAR in regulating hepatic genes in response to phenobarbital. *Molecular pharmacology,* 61**,** 1-6.

VAZQUEZ, A., LIU, J., ZHOU, Y. & OLTVAI, Z. N. 2010. Catabolic efficiency of aerobic glycolysis: the Warburg effect revisited. *BMC systems biology,* 4**,** 58.

WATKINS, R. E., WISELY, G. B., MOORE, L. B., COLLINS, J. L., LAMBERT, M. H., WILLIAMS, S. P., WILLSON, T. M., KLIEWER, S. A. & REDINBO, M. R. 2001. The human nuclear xenobiotic receptor PXR: structural determinants of directed promiscuity. *Science,* 292**,** 2329-33.

WHYSNER, J., ROSS, P. M. & WILLIAMS, G. M. 1996. Phenobarbital mechanistic data and risk assessment: enzyme induction, enhanced cell proliferation, and tumor promotion. *Pharmacology & therapeutics,* 71**,** 153-91.

WILLSON, T. M. & KLIEWER, S. A. 2002. PXR, CAR and drug metabolism. *Nature reviews. Drug discovery,* 1**,** 259-66.

WINTER, J., JUNG, S., KELLER, S., GREGORY, R. I. & DIEDERICHS, S. 2009. Many roads to maturity: microRNA biogenesis pathways and their regulation. *Nature cell biology,* 11**,** 228-34.

WRIGHTON, S. A., SCHUETZ, E. G., THUMMEL, K. E., SHEN, D. D., KORZEKWA, K. R. & WATKINS, P. B. 2000. The human CYP3A subfamily: practical considerations. *Drug metabolism reviews,* 32**,** 339-61.

WU, B., LI, S. & DONG, D. 2013. 3D structures and ligand specificities of nuclear xenobiotic receptors CAR, PXR and VDR. *Drug discovery today,* 18**,** 574-81.

XIE, W., BARWICK, J. L., SIMON, C. M., PIERCE, A. M., SAFE, S., BLUMBERG, B., GUZELIAN, P. S. & EVANS, R. M. 2000. Reciprocal activation of xenobiotic response genes by nuclear receptors SXR/PXR and CAR. *Genes & development,* 14**,** 3014-23.

XIE, W., YEUH, M. F., RADOMINSKA-PANDYA, A., SAINI, S. P., NEGISHI, Y., BOTTROFF, B. S., CABRERA, G. Y., TUKEY, R. H. & EVANS, R. M. 2003. Control of steroid, heme, and carcinogen metabolism by nuclear pregnane X receptor and constitutive androstane

receptor. *Proceedings of the National Academy of Sciences of the United States of America,* 100**,** 4150-5.

XU, R. X., LAMBERT, M. H., WISELY, B. B., WARREN, E. N., WEINERT, E. E., WAITT, G. M., WILLIAMS, J. D., COLLINS, J. L., MOORE, L. B., WILLSON, T. M. & MOORE, J. T. 2004. A structural basis for constitutive activity in the human CAR/RXRalpha heterodimer. *Molecular Cell,* 16**,** 919-28.

YAMADA, H., ISHII, Y., YAMAMOTO, M. & OGURI, K. 2006. Induction of the hepatic cytochrome P450 2B subfamily by xenobiotics: research history, evolutionary aspect, relation to tumorigenesis, and mechanism. *Current drug metabolism,* 7**,** 397-409.

YAMAMOTO, Y., MOORE, R., GOLDSWORTHY, T. L., NEGISHI, M. & MARONPOT, R. R. 2004a. The orphan nuclear receptor constitutive active/androstane receptor is essential for liver tumor promotion by phenobarbital in mice. *Cancer Research,* 64**,** 7197-200.

YAMAMOTO, Y., MOORE, R., GOLDSWORTHY, T. L., NEGISHI, M. & MARONPOT, R. R. 2004b. The orphan nuclear receptor constitutive active/androstane receptor is essential for liver tumor promotion by phenobarbital in mice. *Cancer Research,* 64**,** 7197-7200.

YANG, H., GARZEL, B., HEYWARD, S., MOELLER, T., SHAPIRO, P. & WANG, H. 2014. Metformin represses drug-induced expression of CYP2B6 by modulating the constitutive androstane receptor signaling. *Molecular pharmacology,* 85**,** 249-60.

YANG, H. & WANG, H. 2014. Signaling control of the constitutive androstane receptor (CAR). *Protein & cell,* 5**,** 113-23.

YOSHINARI, K., KOBAYASHI, K., MOORE, R., KAWAMOTO, T. & NEGISHI, M. 2003. Identification of the nuclear receptor CAR:HSP90 complex in mouse liver and recruitment of protein phosphatase 2A in response to phenobarbital. *FEBS letters,* 548**,** 17-20.

ZELKO, I., SUEYOSHI, T., KAWAMOTO, T., MOORE, R. & NEGISHI, M. 2001. The peptide near the C terminus regulates receptor CAR nuclear translocation induced by xenochemicals in mouse liver. *Molecular and Cellular Biology,* 21**,** 2838-46.

ZHANG, Q., BAE, Y., KEMPER, J. K. & KEMPER, B. 2006. Analysis of multiple nuclear receptor binding sites for CAR/RXR in the phenobarbital responsive unit of CYP2B2. *Archives of biochemistry and biophysics,* 451**,** 119-27.